Analysis Status of the SBS Neutron Two-Photon Exchange Experiment

Ezekiel Wertz
(On Behalf of the SBS GMn/nTPE collaboration)
January 22, 2026

WILLIAM & MARY
School of Computing, Data Sciences & Physics

SUPER BIGBITE SPECTROMETER

NATIONAL SCIENCE FOUNDATION

Jefferson Lab

Nucleon Elastic Electromagnetic Form Factors

- Differential Cross-Section represented by a point-like factor and a factor for the internal structure.
- $\boldsymbol{G_E}(Q^2) = F_1(Q^2) - \tau F_2(Q^2)$ is the **Sachs Electric Form Factor**
- $\boldsymbol{G_M}(Q^2) = F_1(Q^2) + F_2(Q^2)$is the **Sachs Magnetic Form Factor**
- In a particular reference frame, the Breit frame, G_E and G_M are related to the Fourier Transform of the internal charge and magnetization distributions.

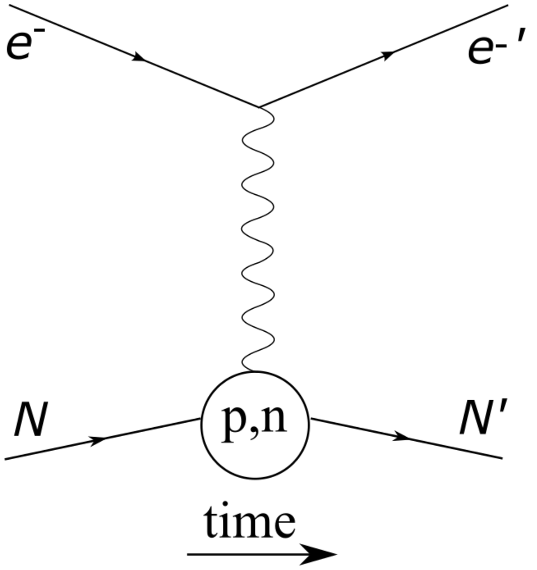

$$\frac{d\sigma}{d\Omega} = \frac{\tau\sigma_{\mathrm{Mott}}}{\epsilon(1+\tau)}\left(\frac{\epsilon}{\tau}G_E^2(Q^2) + G_M^2(Q^2)\right)$$

$$= \frac{\tau\sigma_{\mathrm{Mott}}}{\epsilon(1+\tau)}(\epsilon\sigma_L + \sigma_T)$$

$$\epsilon = (1 + 2(1+\tau)\tan^2(\theta/2))^{-1}$$

Rosenbluth Separation

- Fixed Q^2-value
- Vary electron beam energy and scattering angle, to make measurements at different ϵ values

$$\sigma_R = \frac{\epsilon}{\tau}G_E^2(Q^2) + G_M^2(Q^2)$$

$$= (\epsilon\sigma_L + \sigma_T)$$

Rosenbluth Slope

$$S = \sigma_L/\sigma_T = G_E^2(Q^2)/\tau G_M^2(Q^2)$$

Two-Photon Exchange

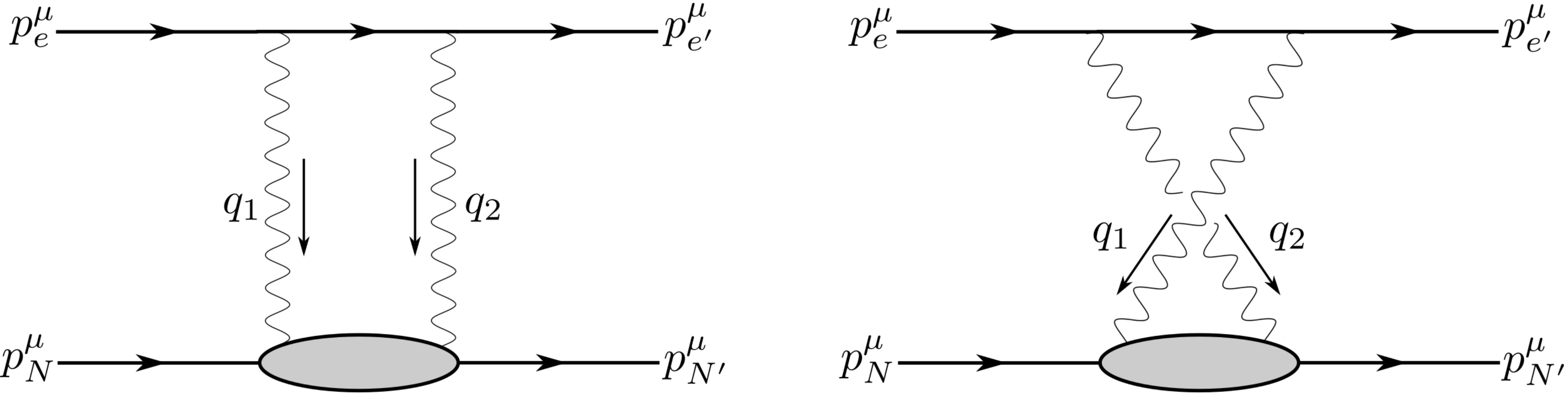

- Higher order diagrams, Two-Photon Exchange (TPE), contribute to the cross-section
- TPE diagrams are difficult to calculate
- Studying TPE effects provides insights into nucleon excitation

Proton Form Factor Ratio World Data Discrepancy

Proton:

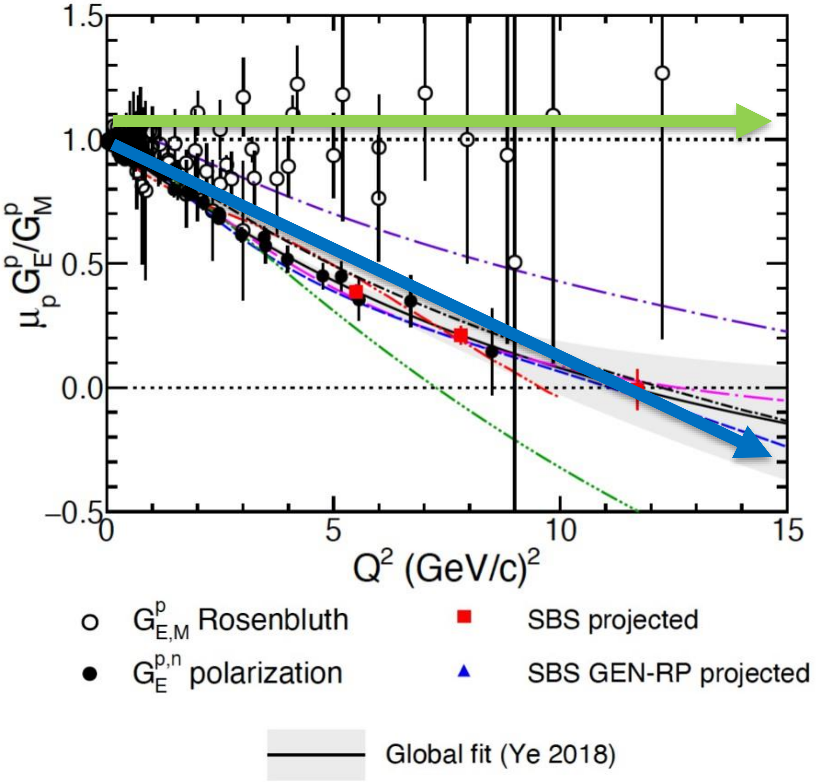

- Primary Methods
  1. Rosenbluth Separation (RS)
  2. Polarization Transfer (PT)
- G_E^p/G_M^p from RS consistent with 1.0
- G_E^p/G_M^p from PT disagrees by 3-4 sigma
- Possible Solution: TPE effects

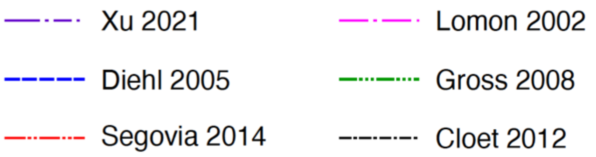

Plots: Franz Gross *et al.*, *50 Years of Quantum Chromodynamics*

Neutron Form Factor Ratio World Data

Neutron:

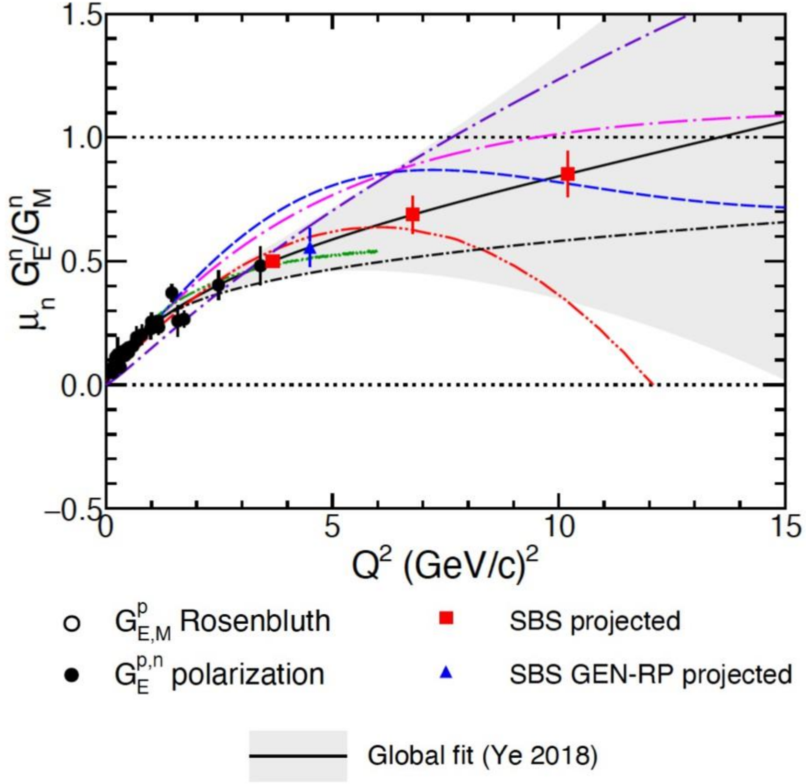

- G_E^n/G_M^n only from PT data
- TPE Effects on the neutron not yet experimentally established
- The nTPE experiment is first extraction of G_E^n/G_M^n from RS

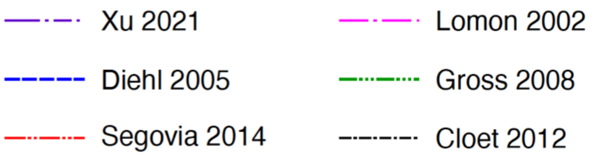

Plots: Franz Gross *et al.*, *50 Years of Quantum Chromodynamics*

Super BigBite Spectrometer (SBS) Apparatus in Hall A

- Liquid Deuterium target - source for protons and neutrons
- BigBite Spectrometer – electron arm
- SBS Magnet + HCal – hadron arm

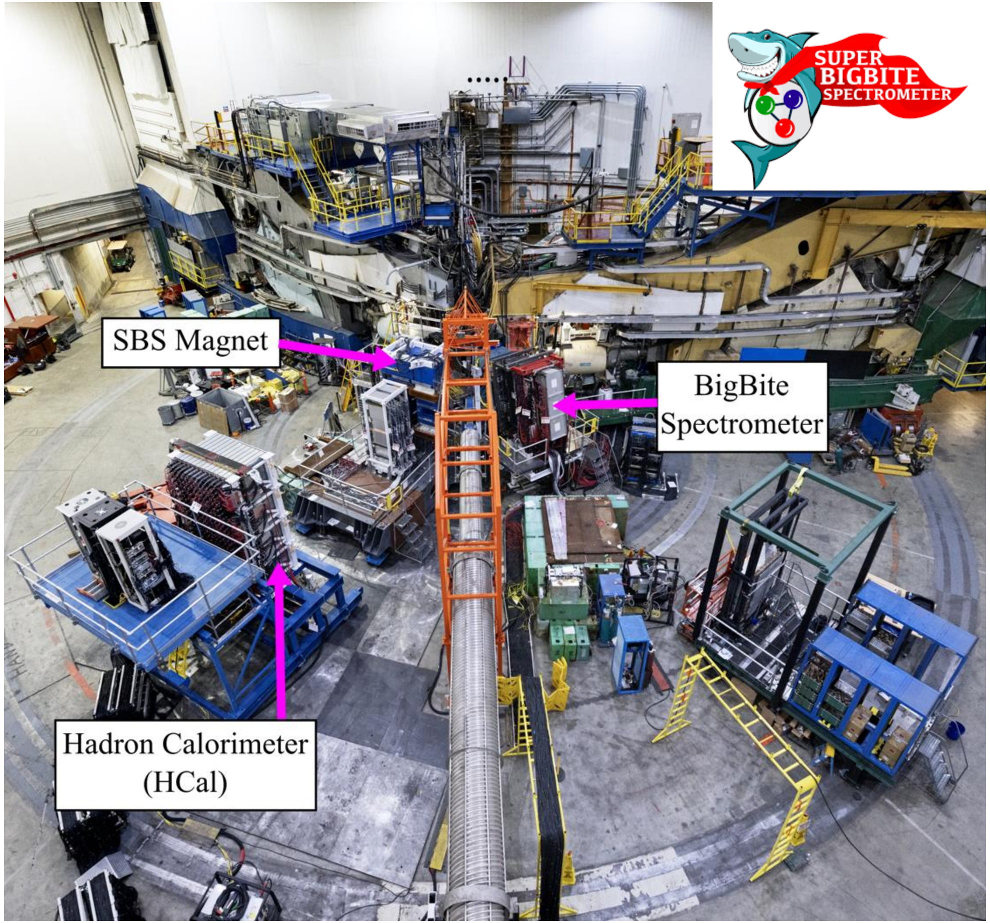

SBS nTPE and GMn experiments

- neutron Two-Photon Exchange (nTPE) Goal: First measurement of the neutron Rosenbluth slope, extract the neutron electromagnetic form factor ratio. Seeks to quantify TPE effects.
- GMn Goal: Precision measurement of neutron magnetic form factor at high Q^2.
- GMn and nTPE took data from October 2021 to February 2022.
- SBS-8 and SBS-9 are kinematics for nTPE.

SBS Config.	Q^2 $(GeV/c)^2$	ϵ	E_{beam} (GeV)	$\theta_{e'}$ (deg)	θ_N (deg)	HCal distance (m)	Electron p (GeV)	Nucleon p (GeV)
SBS-4	3.0	0.72	3.728	36.0	31.9	11.0	2.12	2.4
SBS-7	9.8	0.50	7.906	40.0	16.0	14.0	2.66	6.1
SBS-11	13.5	0.41	9.86	42.0	13.3	14.5	2.67	8.1
SBS-14	7.4	0.46	5.965	46.5	17.3	14.0	2.00	4.81
SBS-8	4.5	0.80	5.965	26.5	29.4	11.0	3.58	3.2
SBS-9	4.5	0.51	4.015	49.0	22.0	11.0	1.6	3.2

The Ratio Method

Measured Observable:

- Simultaneous measurement of both $D(e,e'n)$ and $D(e,e'p)$ reactions for quasi-elastic electron-deuteron scattering.
- Cross-section ratio cancels many systematic effects

$$R = \frac{\left(\frac{d\sigma}{d\Omega}\right)\Big|_{D(e,e'n)}}{\left(\frac{d\sigma}{d\Omega}\right)\Big|_{D(e,e'p)}} = \frac{\left(\frac{d\sigma}{d\Omega}\right)\Big|_{n(e,e')}}{\left(\frac{d\sigma}{d\Omega}\right)\Big|_{p(e,e')}} \cdot f_{nuc} f_{RC} f_{det}$$

Corrections for Effects:

$$R' = \frac{\left(\frac{d\sigma}{d\Omega}\right)\Big|_{n(e,e')}}{\left(\frac{d\sigma}{d\Omega}\right)\Big|_{p(e,e')}} = R \cdot f_{nuc}^{-1} f_{RC}^{-1} f_{Det}^{-1} = \frac{\frac{\tau \sigma_{\text{Mott}}}{\epsilon(1+\tau)}\left(\frac{\epsilon}{\tau}(G_E^n)^2 + (G_M^n)^2\right)}{\left(\frac{d\sigma}{d\Omega}\right)\Big|_{p(e,e')}}$$

Neutron Rosenbluth Slope Technique

Goal: Extract neutron Rosenbluth Slope, $S^n = (G_E^n)^2/\tau_n(G_M^n)^2$

- Consider 2 kinematics with same Q^2-value and with different values of ϵ.
- Consider 2 elastic neutron-to-proton cross-section ratios as described from the Ratio Method.

Physics Result:

- Consider 'super-ratio' of R' for two different values of ϵ.
- Define $S^{n(p)} = \left(G_E^{n(p)}\right)^2/\tau_{n(p)}\left(G_M^{n(p)}\right)^2$ and $\Delta\epsilon = \epsilon_{1,n} - \epsilon_{2,n}$.

Physics Result!

$$S^n = \frac{\left(\frac{R'_{\epsilon_1}}{R'_{\epsilon_2}} - B\right)}{\Delta\epsilon \cdot B} \simeq \frac{(G_E^n)^2}{\tau_n(G_M^n)^2}$$

From Data Extraction

From Kinematic Information

$$B = \frac{\frac{\tau_{\epsilon_{1,n}}}{\epsilon_{1,n}(1+\tau_{\epsilon_{1,n}})}\frac{\tau_{\epsilon_{2,p}}}{\epsilon_{2,p}(1+\tau_{\epsilon_{2,p}})}}{\frac{\tau_{\epsilon_{1,p}}}{\epsilon_{1,p}(1+\tau_{\epsilon_{1,p}})}\frac{\tau_{\epsilon_{2,n}}}{\epsilon_{2,n}(1+\tau_{\epsilon_{2,n}})}} \frac{(G_M^n)^2_{\epsilon_1}}{\left(G_M^p\right)^2_{\epsilon_1}} \frac{\left(G_M^p\right)^2_{\epsilon_2}}{(G_M^n)^2_{\epsilon_2}} \frac{1+\epsilon_{2,p}S^p_{\epsilon_2}}{1+\epsilon_{1,p}S^p_{\epsilon_1}}$$

From Global Form Factor Analysis.

Analysis Overview

- Monte Carlo (MC) Event generator SIMC applies nuclear effects and radiative corrections.
- Geant4 MC Simulation G4SBS
  - MC transports particles through SBS geometry
  - Accounts for detector layout and material properties
- Simulated events are digitized and processed with the same software as the experimental data.
- Experimental observables are extracted by comparing simulation to data.

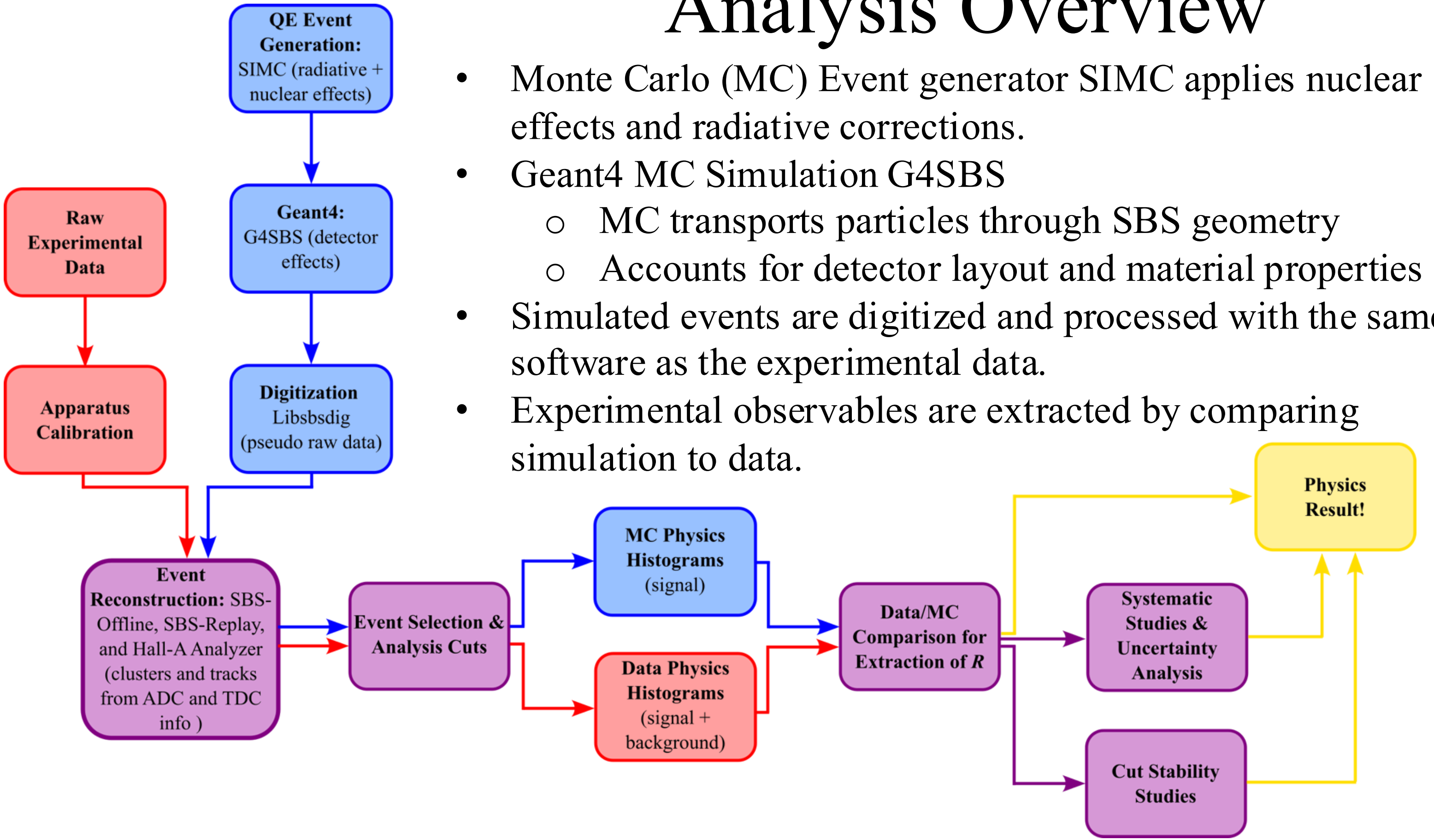

Analysis Methods – Introducing HCal Δx and Δy

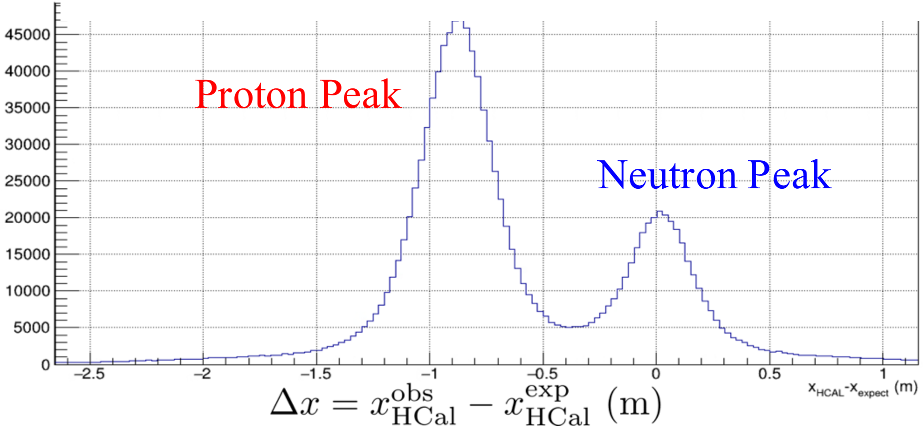

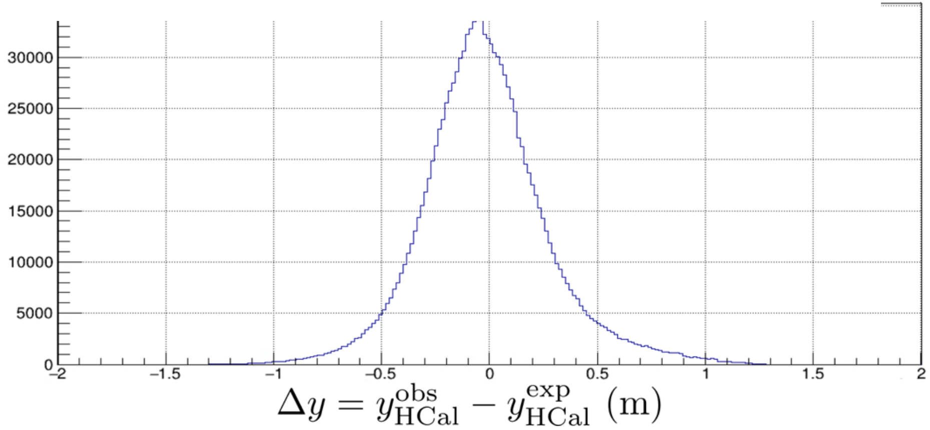

$Q^2 = 4.5\ (\text{GeV/c})^2$

- **Goal:** Separate protons and neutrons in HCal that came from quasi-elastic scattering events.
- **Reconstruct** the four-vector of e' using data from the electron arm.

- Calculate the four-vector for a neutron that underwent quasi-elastic scattering with e' and **project** to HCal.
- Plot the **difference** between the **observed** event in HCal and the projected **expected** location.

$Q^2 = 4.5\ (\mathrm{GeV}/c)^2$

Data-Monte Carlo Comparison

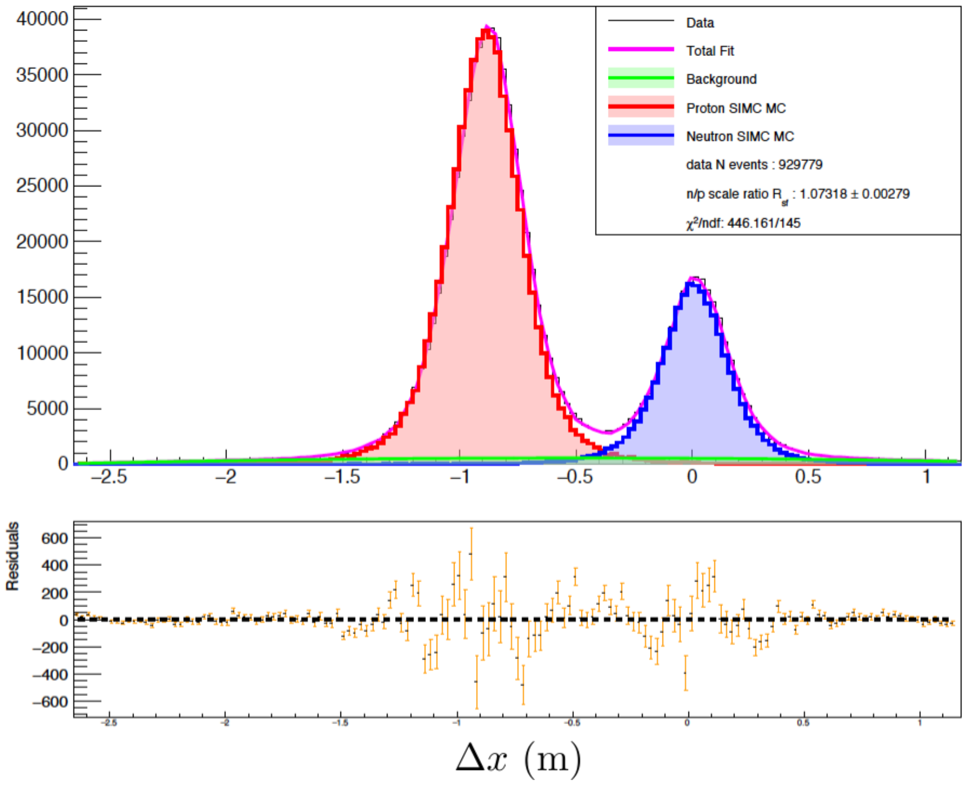

- Fit Equation:

$$f_{total}(x_i) = f_{sf}^{p}\left(R_{sf}^{n/p} h^{n}(x_i - \delta_n) + h^{p}(x_i - \delta_p)\right) + f_{bkgd}(x_i)$$

- Fit Parameters:
  1. f_{sf}^{p} - proton scale factor
  2. $R_{sf}^{n/p}$ - ratio of neutron to proton scale factors
  3. $\delta_{n(p)}$ - neutron (proton) centroid shift parameters
  4. f_{bkgd} - parameters associated with the background
- Interpretation: $R_{sf}^{n/p}$ quantifies the relative scaling of the neutron to proton quasi-elastic scattering cross-section as modeled by the simulation and as observed in data.

$Q^2 = 4.5\ (\mathrm{GeV/c})^2$

Data-Monte Carlo Comparison

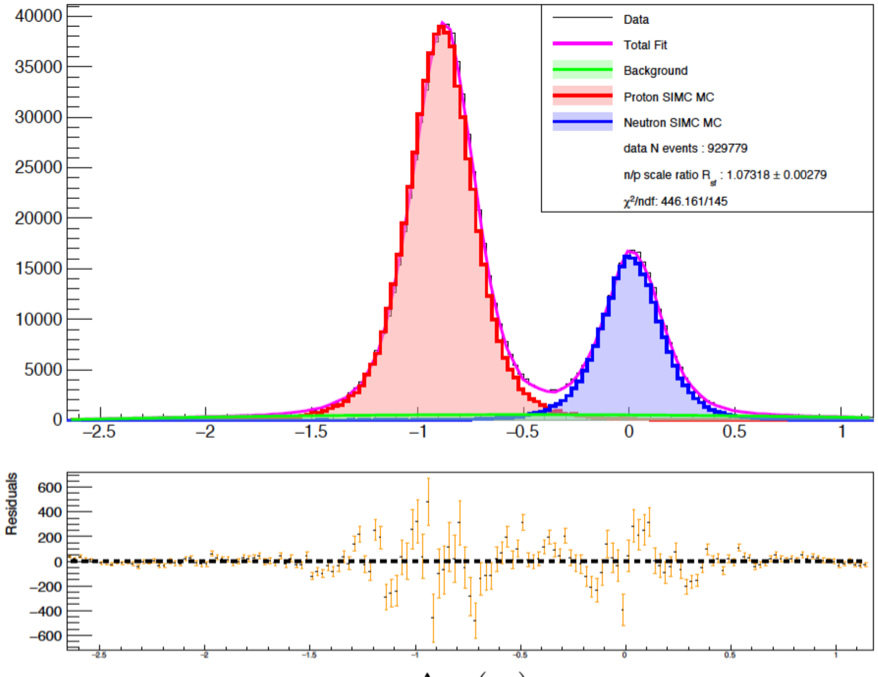

Simulation:

$$R'_{sim} = \frac{\left(\frac{d\sigma}{d\Omega}\right)\Big|_{n(e,e'),sim}}{\left(\frac{d\sigma}{d\Omega}\right)\Big|_{p(e,e'),sim}} = R_{sim} \cdot f_{nuc,sim}^{-1} f_{RC,sim}^{-1} f_{Det,sim}^{-1}$$

Extraction:

$$R = R' \cdot f_{nuc} f_{RC} f_{det} = R_{sf}^{n/p} \cdot R'_{sim} \cdot f_{nuc,sim} f_{RC,sim} f_{det,sim}$$

Claim:

- Simulation consistently replicates nuclear, radiative, and detector effects that are present in the experimental data.

Implication:

$$\frac{f_{nuc}}{f_{nuc,sim}} \sim 1 \qquad \frac{f_{RC}}{f_{RC,sim}} \sim 1 \qquad \frac{f_{det}}{f_{det,sim}} \sim 1$$

$$R' = \frac{\left(\frac{d\sigma}{d\Omega}\right)\Big|_{n(e,e')}}{\left(\frac{d\sigma}{d\Omega}\right)\Big|_{p(e,e')}} = R_{sf}^{n/p} \cdot R'_{sim}$$

Sources of Systematic Uncertainty:

- Cut Stability
- HCal Nucleon Detection Efficiency
- Inelastic Background

HCal Non-Uniformity in Real Data

- Liquid Hydrogen data
- Clear non-uniformities (dips) in the x-direction
- Highly-likely caused by issues with HCal hardware
- Position-dependent non-uniformities in HCal nucleon detection efficiency could introduce bias to $R_{sf}^{n/p}$ extractions.
- Reweight MC events based on data map using a relative efficiency correction factor.

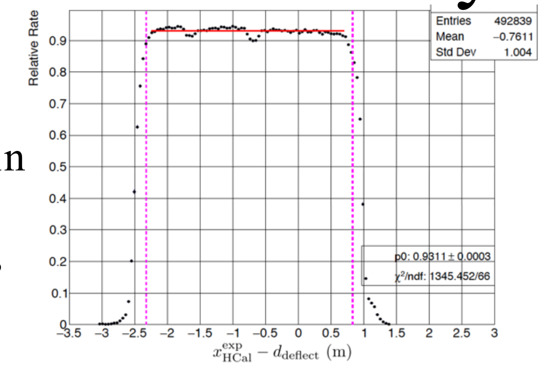

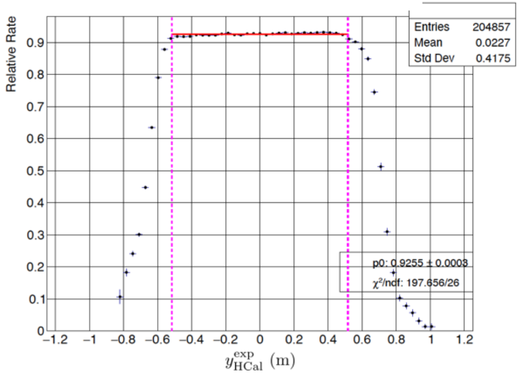

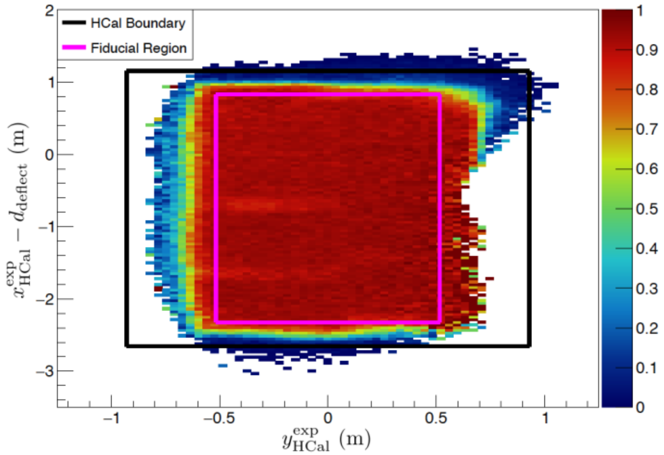

SBS-8, $Q^2 = 4.5\ (GeV/c)^2$

Inelastic Background

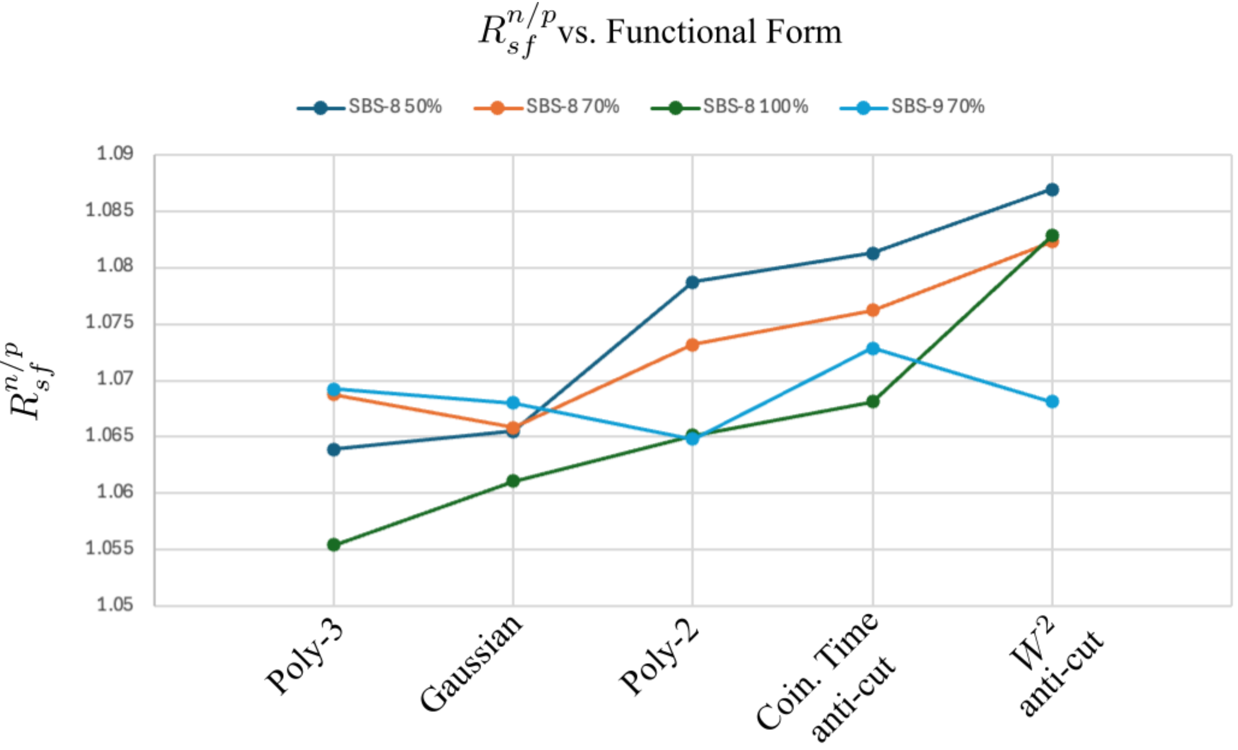

- Five different functional forms for the background
- The 3 parameterizations provide smooth forms for the background shape
- The 2 anti-cuts are data motivated and attempt to capture events corresponding to background
- Systematic effects on $R_{sf}^{n/p}$ due to background shape were quantified

Neutron Rosenbluth Slope Preliminary Result

R'_{ϵ_1} is SBS-8 (Weighted Mean), R'_{ϵ_2} is SBS-9 For $Q^2 = 4.48$ (GeV/c)^2

Quantity	Value	Uncertainty	Uncertainty (%)
R'_{ϵ_1}	0.3908	0.0038	0.97%
R'_{ϵ_2}	0.3875	0.0032	0.83%

Quantity	Value	Uncertainty	Uncertainty (%)
$\frac{R'_{\epsilon_1}}{R'_{\epsilon_2}}$	1.0085	0.0129	1.28%
B	0.98315	0.00281	0.286%
$\Delta\epsilon$	0.281		
$S^n = \frac{\left(\frac{R'_{\epsilon_1}}{R'_{\epsilon_2}} - B\right)}{\Delta\epsilon \cdot B}$	0.0916	0.0476	52%

Neutron Form Factor Ratio Preliminary Result

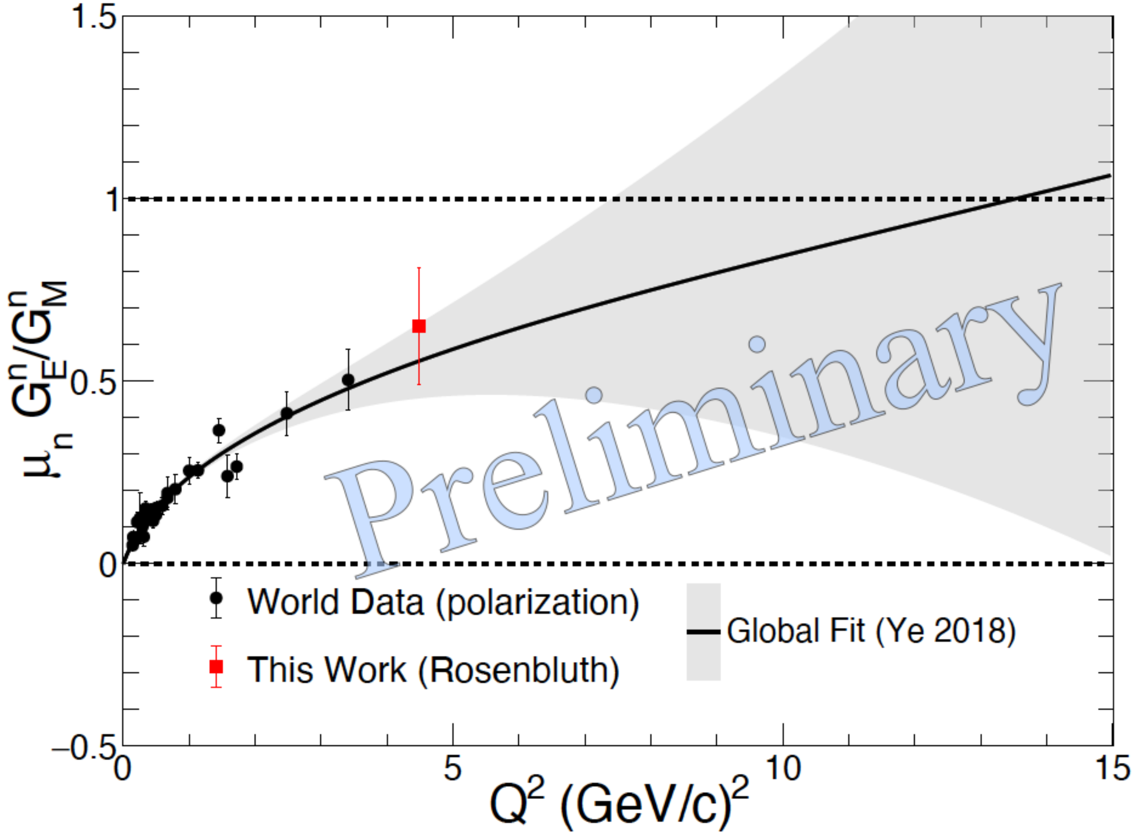

For $Q^2 = 4.48$ (GeV/c)^2

$$\mu_n \frac{G_E^n}{G_M^n} \simeq \mu_n \sqrt{S^n \tau_n}$$
$$= 0.652 \pm 0.160$$

- Does not account for TPE effects

Conclusions:

- S^n result is consistent with the extrapolation of the global parameterization.
- S^n result suggests an absence of large TPE corrections for the neutron
- S^n result is not precise enough to experimentally expose neutron TPE effects

Summary

- Nucleon Structure & Electromagnetic Form Factors
- SBS nTPE experiment and observable extraction
- Overview of Data Analysis Methods
- Physics Extraction from Data/MC Comparison
- Preliminary neutron Rosenbluth Slope, first of a kind measurement

Outlook

Remaining Tasks

- Potentially improve Radiative Correction models in MC
- Quantifying systematic effects due to Radiative Corrections for nTPE results: (Implemented for GMn Analysis by P. Datta)
- Updated (Pass-3) data and MC files with improved detector calibrations
- Study effects due to final-state interactions
- Quantify effects due to absolute HCal nucleon detection efficiency
- Reevaluate Inelastic Background systematic uncertainty with improved method (MC Inelastic and Out-Of-Time): (Implemented for GMn Analysis by P. Datta)
- Reevaluate systematic uncertainty associated with Event Selection Cuts

Thank You!

Special thanks:

PhD advisor: David Armstrong. SBS graduate students John Boyd, Provakar Datta, Anu Rathnayake, Sebastian Seeds, Maria Satnik, Ralph Marinaro, Nathaniel Lashley, Sean Jeffas, Hunter Presley. Hall A/C Staff Arun Tadepalli, Bogdan Wojtsekhowski, Jack Segal, Mark Jones, Jessie Butler, Dave Mack. W&M Folks: Todd Averett, Kate Evans, Jack Jackson, Eric Fuchey. GEM Folks: Nilanga Liyanage, Kondo Gnanvo, Holly Szumila-Vance, Evaristo Cisbani, Roberto Perrino. Andrew Puckett. GMn/nTPE Analysis Working Groups. The SBS Collaboration. NSF for supporting this work.

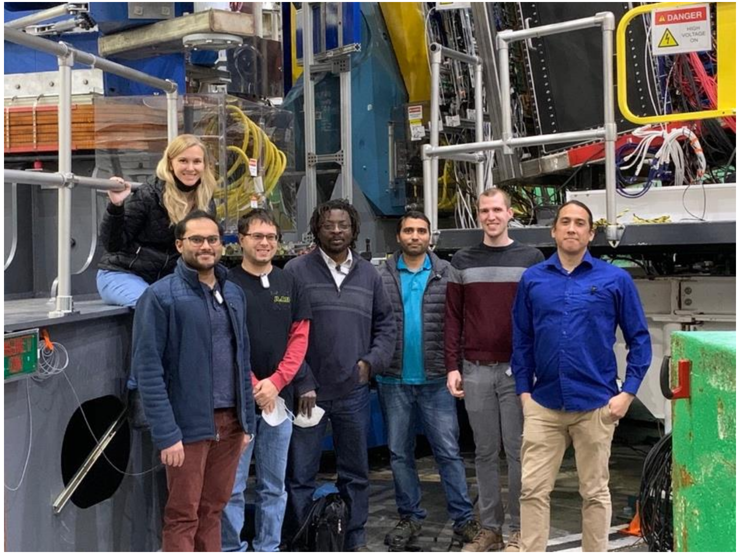

GEM Folks, February 2022. Left to right: Holly Szumila-Vance, Anu Rathnayake, Zeke Wertz, Kondo Gnanvo, Thir Gautam , Sean Jeffas, John Boyd.

DNP Hawaii, November 2023. Left to right: John Boyd, Vimukthi Gamage, Eric Fuchey, Provakar Datta, Zeke Wertz, Sean Jeffas, Hunter Presley, Anu Rathnayake, Sebastian Seeds, Maria Satnik, Andrew Puckett.

Backup

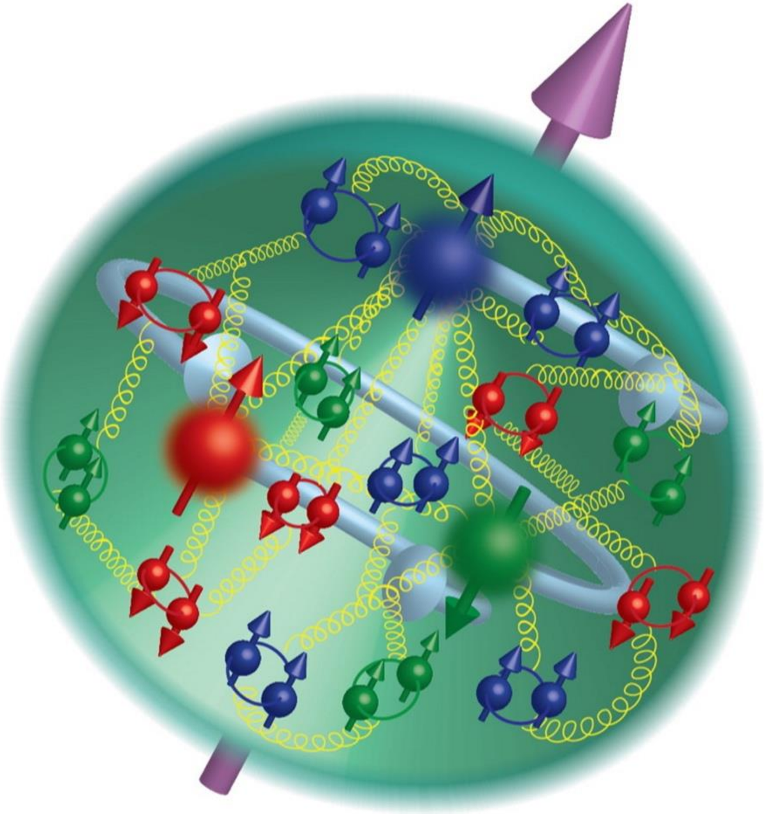

Nucleon Electromagnetic Form Factor World Data

Proton:

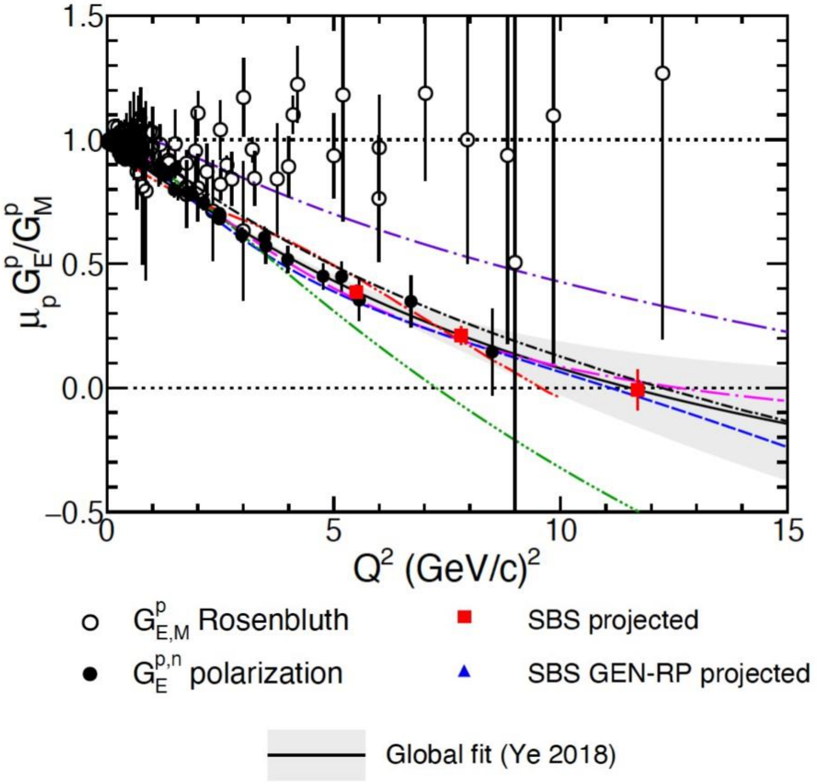

Neutron:

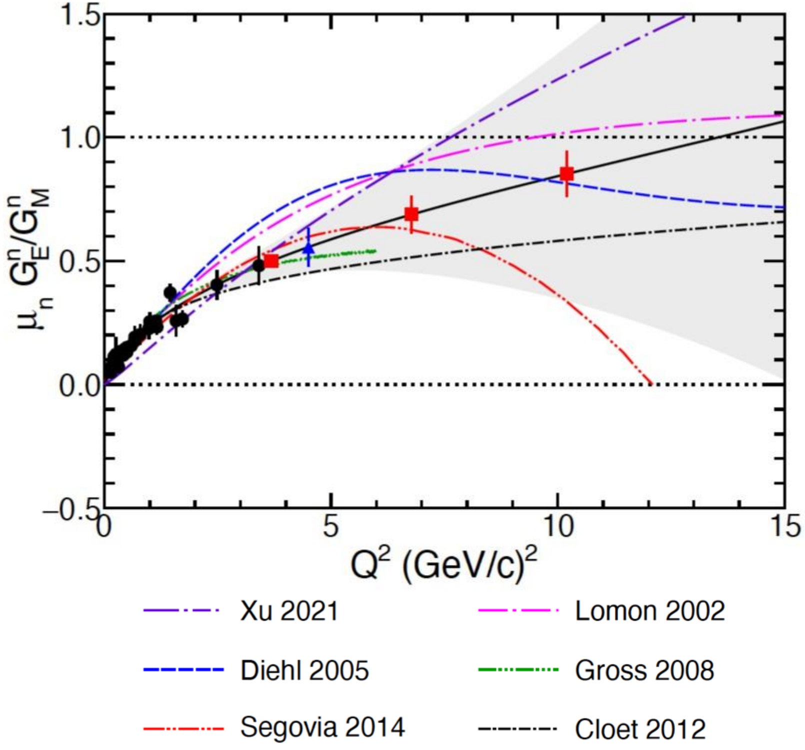

Plots: Franz Gross *et al.*, *50 Years of Quantum Chromodynamics*

Super-Ratio A

	Kine	$\langle Q^2 \rangle$ $(\mathrm{GeV/c})^2$	$\langle \epsilon \rangle$	R'	$\Delta(R')_{\mathrm{total}}$
R'_{ϵ_1}	SBS-8	4.48	0.799	0.3908	0.0038
R'_{ϵ_2}	SBS-9	4.476	0.518	0.3875	0.0032

$$A \equiv \frac{R'_{\epsilon_1}}{R'_{\epsilon_2}}$$

$$\Delta A = |A| \sqrt{\left(\frac{\Delta(R'_{\epsilon_1})}{R'_{\epsilon_1}}\right)^2 + \left(\frac{\Delta(R'_{\epsilon_2})}{R'_{\epsilon_2}}\right)^2}.$$

$$A = 1.0085 \pm 0.0129.$$

B term

Quantity	Value	Total Uncertainty
$\dfrac{\frac{\tau_{n,\epsilon_1}}{\epsilon_{1,n}(1+\tau_{n,\epsilon_1})}\ \frac{\tau_{p,\epsilon_2}}{\epsilon_{2,p}(1+\tau_{p,\epsilon_2})}}{\frac{\tau_{p,\epsilon_1}}{\epsilon_{1,p}(1+\tau_{p,\epsilon_1})}\ \frac{\tau_{n,\epsilon_2}}{\epsilon_{2,n}(1+\tau_{n,\epsilon_2})}}$	1.00044	———
$\frac{\sigma^n_{T,\epsilon_1}}{\sigma^p_{T,\epsilon_1}}\ \frac{\sigma^p_{T,\epsilon_2}}{\sigma^n_{T,\epsilon_2}}$	0.99927	0.00017
$\frac{1+\epsilon_{2,p}S^p_{\epsilon_2}}{1+\epsilon_{1,p}S^p_{\epsilon_1}}$	0.98344	0.0028
B	0.98315	0.00281

- Transverse cross-section term is based on Ye et al. 2018 article
- Proton Rosenbluth Slope term is based on Christ et al. 2022 article

1. Z. Ye, J. Arrington, R. J. Hill, and G. Lee, Proton and neutron electromagnetic formfactors and uncertainties, Physics Letters B 777, 8 (2018).
2. M. E. Christy et al., Form Factors and Two-Photon Exchange in High-Energy Elastic Electron-Proton Scattering, Phys. Rev. Lett. 128, 102002 (2022).

Determination Proton Rosenbluth Slope for B

$S^p_{\epsilon_1/\epsilon_2}$ is determined from Christy et al. (2022) article and supplemental material, which provides most recent parameterization for RS from only e-p cross-section data.

$RS = 1 + c_1\tau + c_2\tau^2$, where $c_1 = -0.456299 \pm 0.124409$, $c_2 = 0.121065 \pm 0.10032$, and $\tau = Q^2/4M_p^2$

$$\Delta RS = \sqrt{\left(\frac{\partial RS}{\partial c_1}\Delta c_1\right)^2 + \left(\frac{\partial RS}{\partial c_2}\Delta c_2\right)^2 + 2\frac{\partial RS}{\partial c_1}\frac{\partial RS}{\partial c_2}cov(c_1, c_2)}$$

$\frac{\partial RS}{\partial c_1} = \tau$, $\frac{\partial RS}{\partial c_2} = \tau^2$, $cov(c_1, c_2) = -0.778\Delta c_1 \Delta c_2$

	Value	Uncertainty	Uncertainty (%)
$RS_{\epsilon_1} = \frac{(\mu_p G_E^p)^2}{(G_M^p)^2}$	0.6151	0.10722	17.4%
$S^p_{\epsilon_1} = \frac{(G_E^p)^2}{\tau_{p,\epsilon_1}(G_M^p)^2}$	0.06186	0.01078	17.4%

	Value	Uncertainty	Uncertainty (%)
$RS_{\epsilon_2} = \frac{(\mu_p G_E^p)^2}{(G_M^p)^2}$	0.6156	0.10674	17.3%
$S^p_{\epsilon_2} = \frac{(G_E^p)^2}{\tau_{p,\epsilon_1}(G_M^p)^2}$	0.06191	0.01074	17.3%

Neutron Rosenbluth Slope Uncertainty

$$S^n = \frac{(A - B)}{B\Delta\epsilon_n}$$

$$\Delta S^n = \sqrt{\left(\frac{\partial S^n}{\partial A}\Delta A\right)^2 + \left(\frac{\partial S^n}{\partial B}\Delta B\right)^2}$$

$$\Delta S^n = \sqrt{\left(\frac{1}{B\Delta\epsilon_n}\Delta A\right)^2 + \left(\frac{-A}{B^2\Delta\epsilon_n}\Delta B\right)^2}$$

Neutron Rosenbluth Slope Preliminary Result

Quantity	Uncertainty Value	Percentage
$\Delta\left(S^n\right)_{\text{Exp}}$	0.0465	50.8%
$\Delta\left(S^n\right)_{\text{Param}}$	0.0104	11.4%
$\Delta\left(S^n\right)_{\text{Total}}$	0.0476	52%

Quantity	Uncertainty Value	Percentage
$\Delta\left(S^n\right)_{\text{Stat}}$	0.0144	15.8%
$\Delta\left(S^n\right)_{\text{HCDENU}}$	0.0182	19.9%
$\Delta\left(S^n\right)_{\text{Cut}}$	0.0227	24.8%
$\Delta\left(S^n\right)_{\text{Ine}}$	0.0317	34.7%
$\Delta\left(S^n\right)_{\text{Exp}}$	0.0465	50.8%

Neutron TPE from Theory

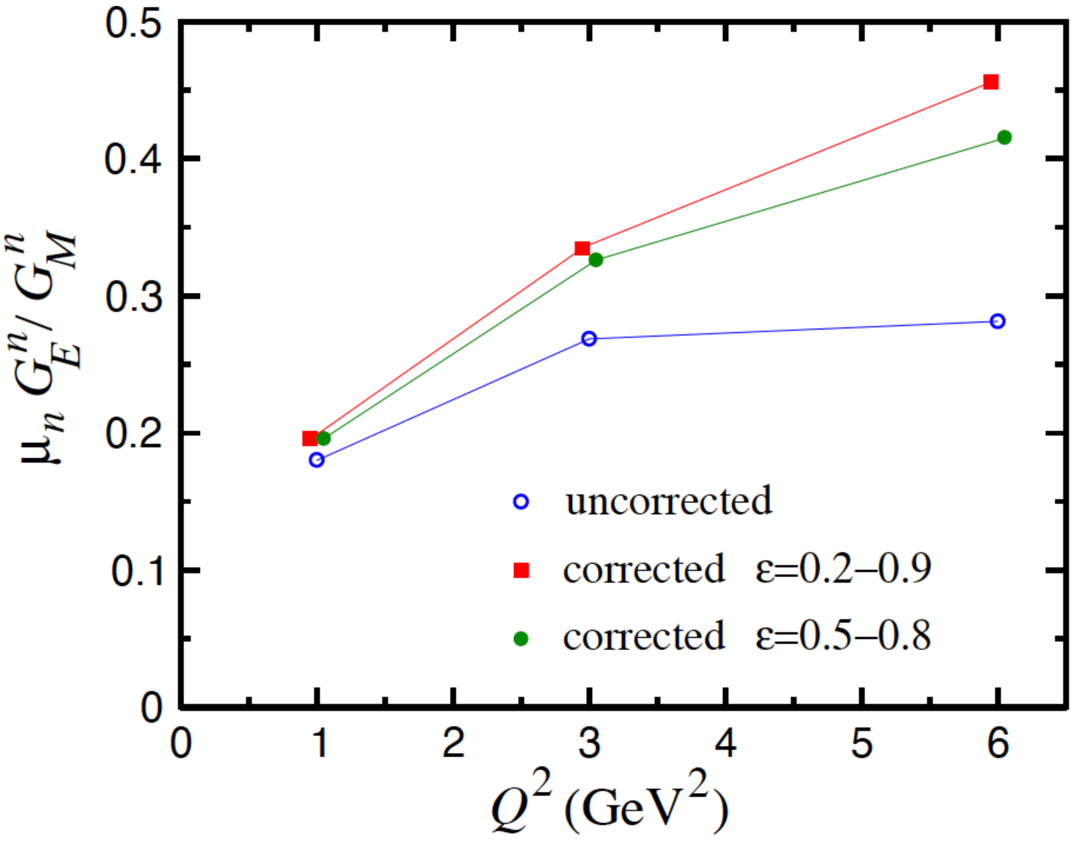

- Calculates TPE contributions to the unpolarized cross-section by computing scattering amplitude for TPE diagrams.
- For Q^2 = 4.5 (GeV/c)^2, TPE correcting a Rosenbluth measurement could increase the neutron form factor ratio by 30%

Ref: P. Blunden *et al*, *Two-photon exchange in elastic electron nucleon scattering*

Neutron Form Factor Ratio Preliminary Result

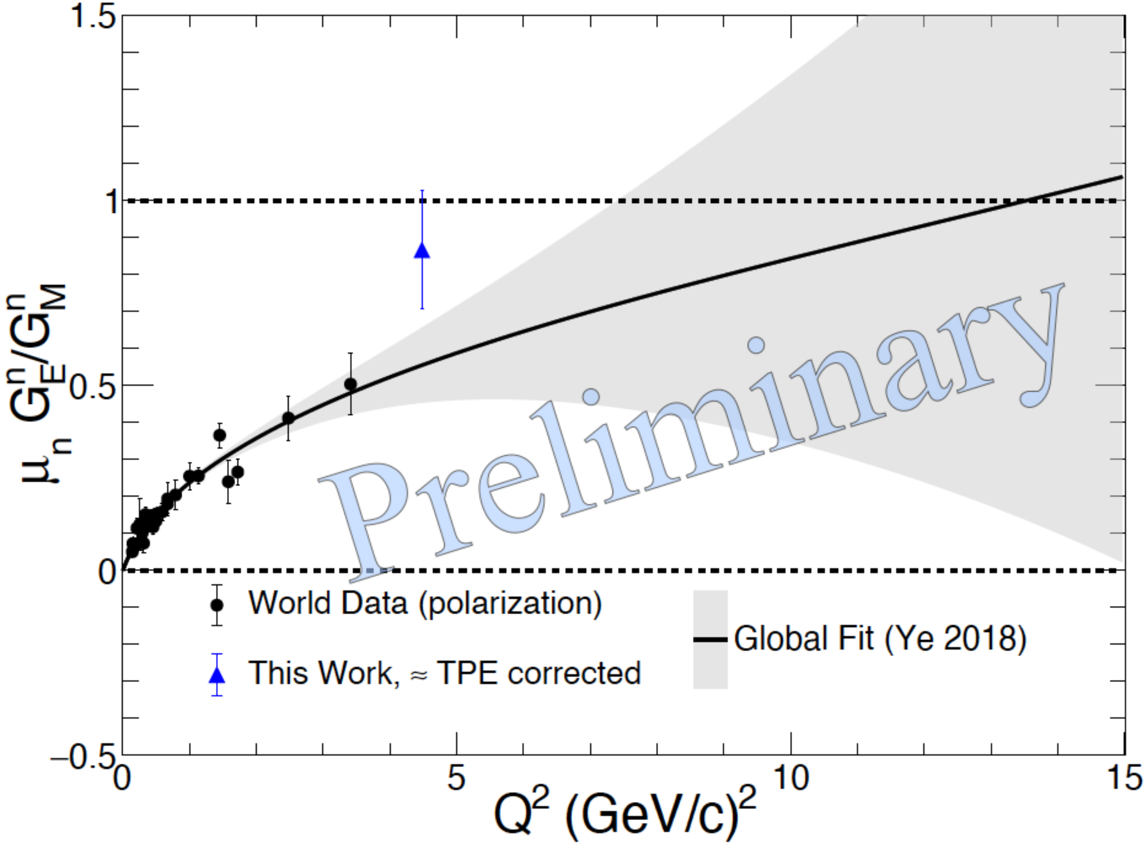

For $Q^2 = 4.48$ (GeV/c)^2

- Approximately TPE corrected based on Blunden et. al.

$$\mu_n \frac{G_E^n}{G_M^n} + TPE \simeq 0.867 \pm 0.160$$

Neutron TPE from Theory Expanded

$$\delta^{2\gamma} \rightarrow \frac{2\mathcal{R}e\left\{\mathcal{M}_0^\dagger \mathcal{M}^{2\gamma}\right\}}{|\mathcal{M}_0|^2}.$$

TPE modification to the CS. Here M_0 and $M_{2\gamma}$ are OPE and TPE amplitudes

$$\mathcal{M}^{2\gamma} = e^4 \int \frac{d^4k}{(2\pi)^4} \frac{N_{\rm box}(k)}{D_{\rm box}(k)} + e^4 \int \frac{d^4k}{(2\pi)^4} \frac{N_{\rm x-box}(k)}{D_{\rm x-box}(k)}$$

Here N_{box}, N_{x-box}, D_{box}, D_{x-box} are matrix elements and propagators, respectively. For TPE diagrams on slide 7

- The TPE amplitude contains finite and IR divergent terms, as well as FFs at the γNN vertices

- The finite terms can be computed analytically
- There are no IR divergent terms for the neutron

Ref: P. Blunden *et al*, *Two-photon exchange in elastic electron nucleon scattering*

Neutron TPE from Theory Expanded

$$F_{1,2}(Q^2) = \sum_{i=1}^{N} \frac{n_i}{d_i + Q^2} ,$$

FF functional form taken from older world data parameterization available when article published

$$n_N = d_N(F_{1,2}(0) - \Sigma_{i=1}^{N-1} n_i/d_i).$$

$$F_1^p(0) = 1 \;\; F_2^p(0) = \kappa_p$$

$$F_1^n(0) = 0 \text{ and } F_2^n(0) = \kappa_n$$

Normalization condition

	F_1^p	F_2^p	F_1^n	F_2^n
N	3	3	3	2
n_1	0.38676	1.01650	24.8109	5.37640
n_2	0.53222	–19.0246	–99.8420	
d_1	3.29899	0.40886	1.98524	0.76533
d_2	0.45614	2.94311	1.72105	0.59289
d_3	3.32682	3.12550	1.64902	—

Ref: P. Blunden *et al*, *Two-photon exchange in elastic electron nucleon scattering*

Neutron TPE from Theory Expanded

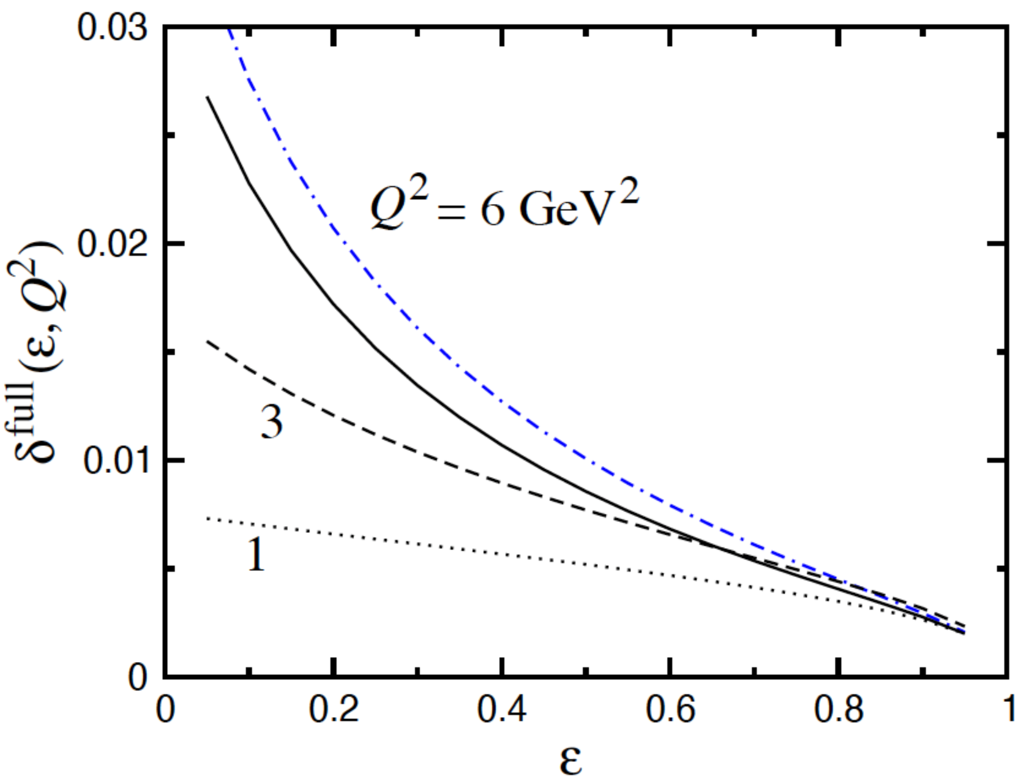

- TPE contribution to the unpolarized electron-neutron elastic scattering cross-section
- The dot-dashed curve for $Q^2 = 6$ GeV^2 comes from a particular older world data parameterization
- The other curves come from a different older world data parameterization
- Magnitude of TPE contribution is approx. 3 times smaller than proton
- Sign change is due to negative neutron anomalous magnetic moment

Ref: P. Blunden *et al*, *Two-photon exchange in elastic electron nucleon scattering*

Neutron TPE from Theory Expanded

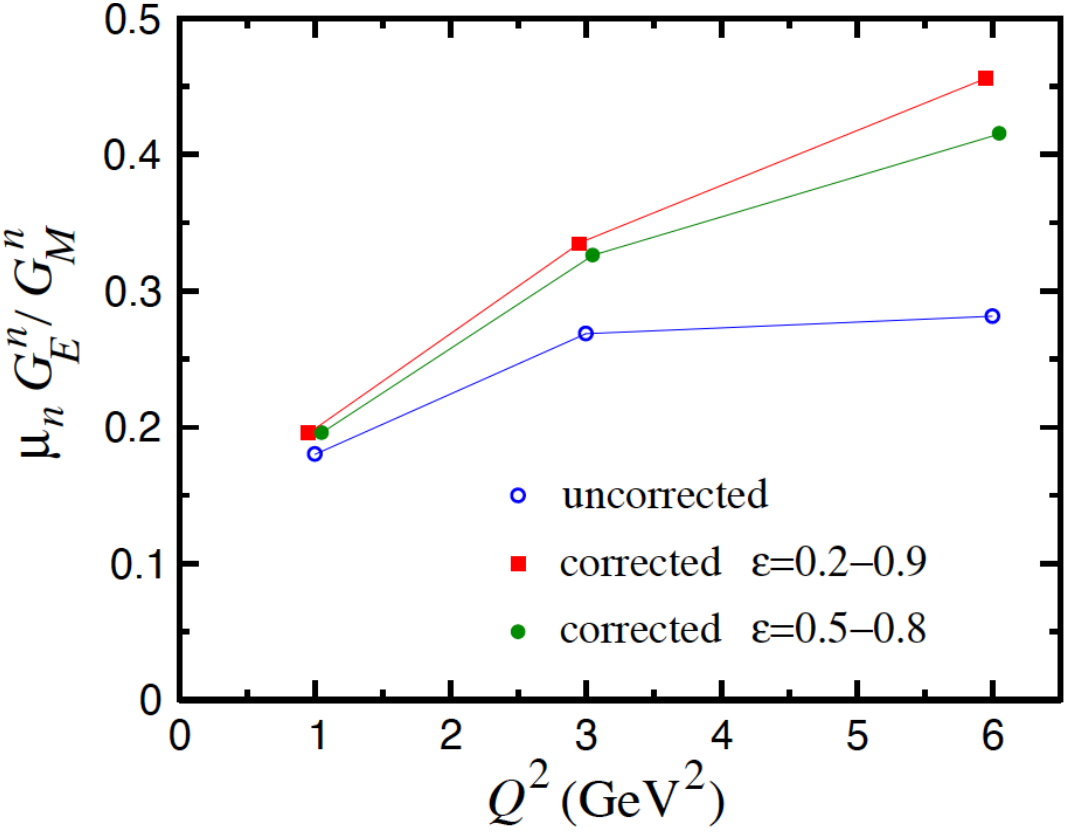

- Accounting for the ϵ dependence, the correction is applied to the cross-section, reduced cross-section, and then the FF ratio.
- For $Q^2 = 4.5$ (GeV/c)^2, TPE correcting a Rosenbluth measurement could increase the neutron form factor ratio by 30%

Ref: P. Blunden *et al*, *Two-photon exchange in elastic electron nucleon scattering*

Improved Inelastic Background Systematic

Determination of Inelastic Background

- From MC W^2 distributions of signal and MC inelastic generator events. Select events outside quasi-elastic peak
- Select out-of-time events
- Fit delta x distribution of selected background events
- Use background shape in Systematic uncertainty evaluation

$Q^2 = 13.6\ (GeV/c)^2$

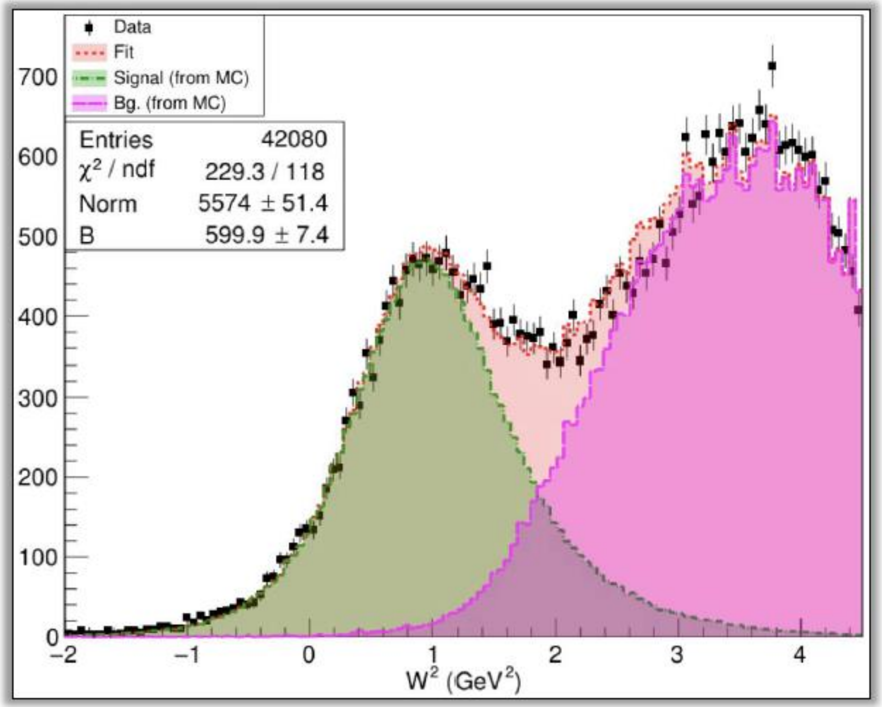

Analysis Credit and Ref: P. Datta APS 2025 Talk

Systematic: Radiative Corrections

Analysis Credit and Ref:
P. Datta

- Radiative corrections (analysis credit: P. Datta, LBNL):
  - SIMC events with the following configurations for radiative effects:
    - (1) - No radiative corrections i.e. none of the tails are radiated
    - (2) - One tail = 0 => All (e, e', and p) tails are radiated
    - (3) - One tail = -3 => All but p tails are radiated
  - SIMC events processed through g4sbs → libsbsdig → SBS-offline;
  - Properly weighted Dx distribution for all types of events with the same selection
  - Extract individual yields and then quantify the correction

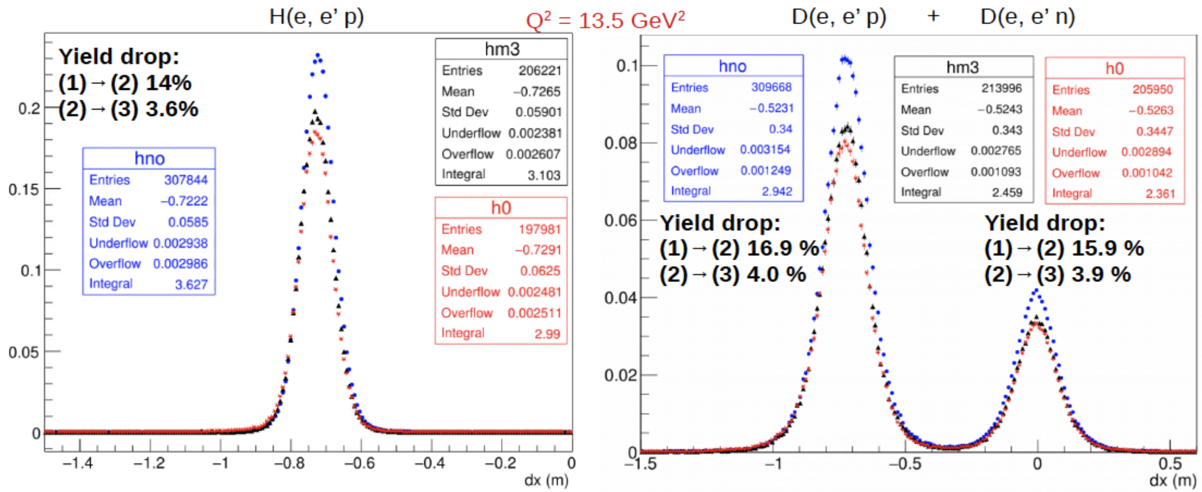

Future TPE Experiments

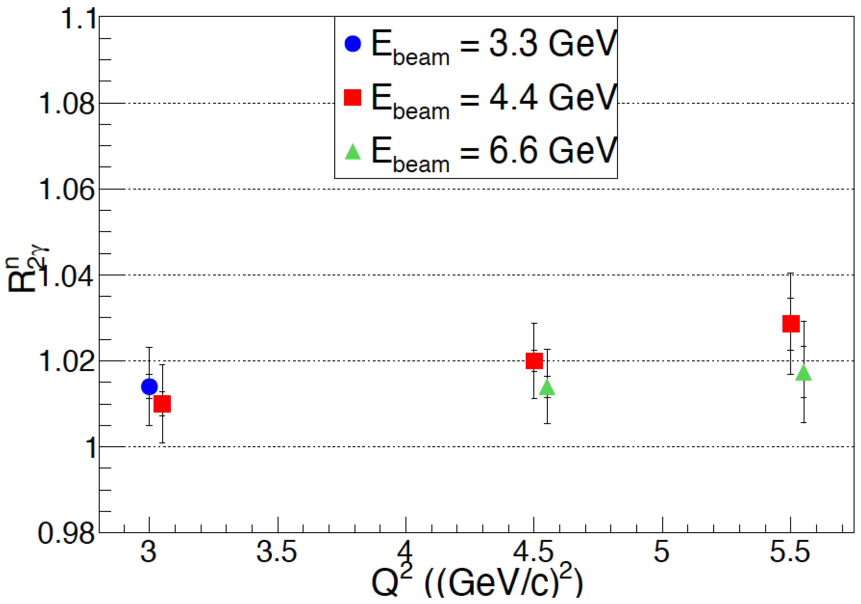

Ref: E. Fuchey *et al*, *Measurement of the Two-Photon Exchange Contribution in the Electron-Neutron and Positron-Neutron Elastic Scattering*

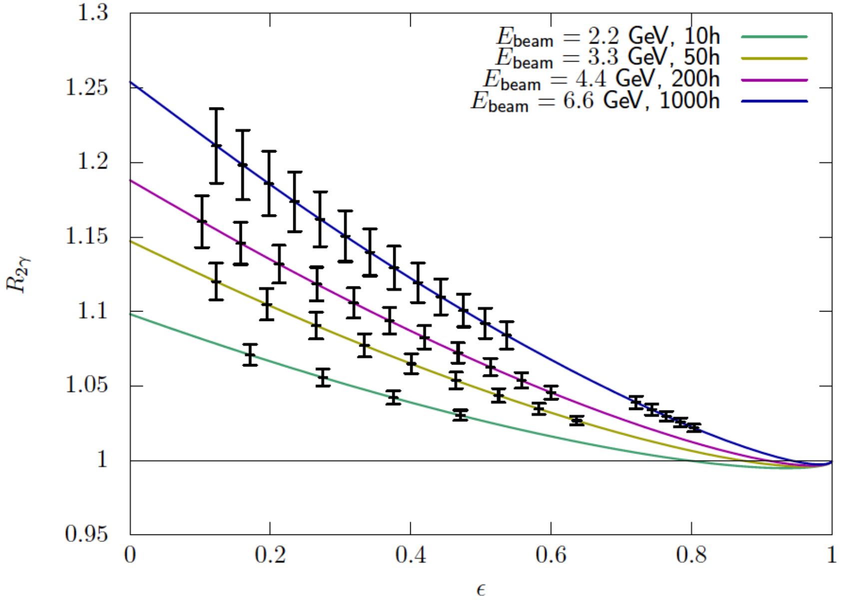

Ref: J. Bernaeur *et al*, *Determination of two-photon exchange via e^+p/e^-p Scattering with CLAS12*

Nucleon Structure

- Hadrons (including protons and neutrons) have an internal structure!
- Not structureless point-like.
- Complex internal structure of valence quarks, gluons, and quark-antiquark pairs.

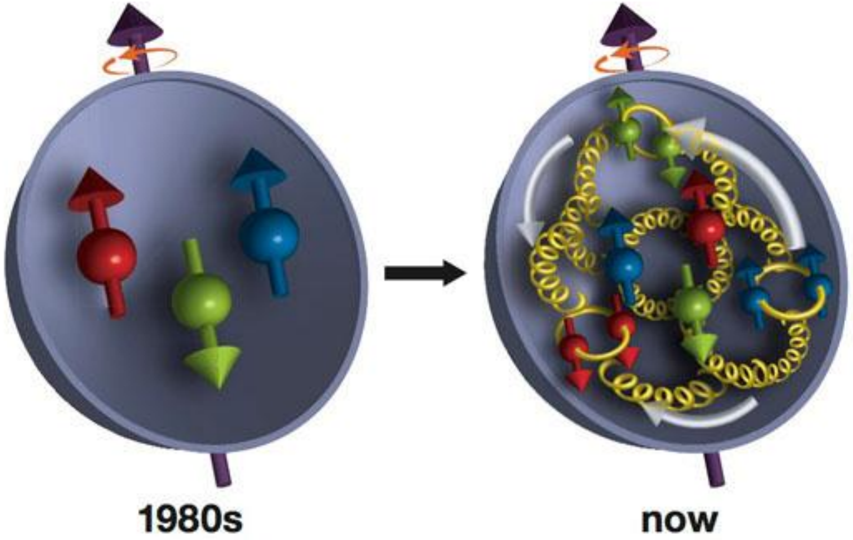

Important Questions:

- How are the charge and magnetization distributed inside a nucleon?
- How do emergent properties of the nucleon arise?
- How does the internal nucleon structure behave at different momentum transfer scales (non-perturbative vs. perturbative regimes)?
- How do the gluon and quark-antiquark pairs contribute?

BigBite Spectrometer (Electron Arm)

BigBite Dipole Magnet:

- 1.2 T · m
- 53 msr, 1.6 m from target

Tracking:

Gas Electron Multiplier

Cherenkov Detector:

GRINCH

Scintillator Array:

Timing Hodoscope

Electron Calorimeter:

BigBite Calorimeter (Preshower + Shower)

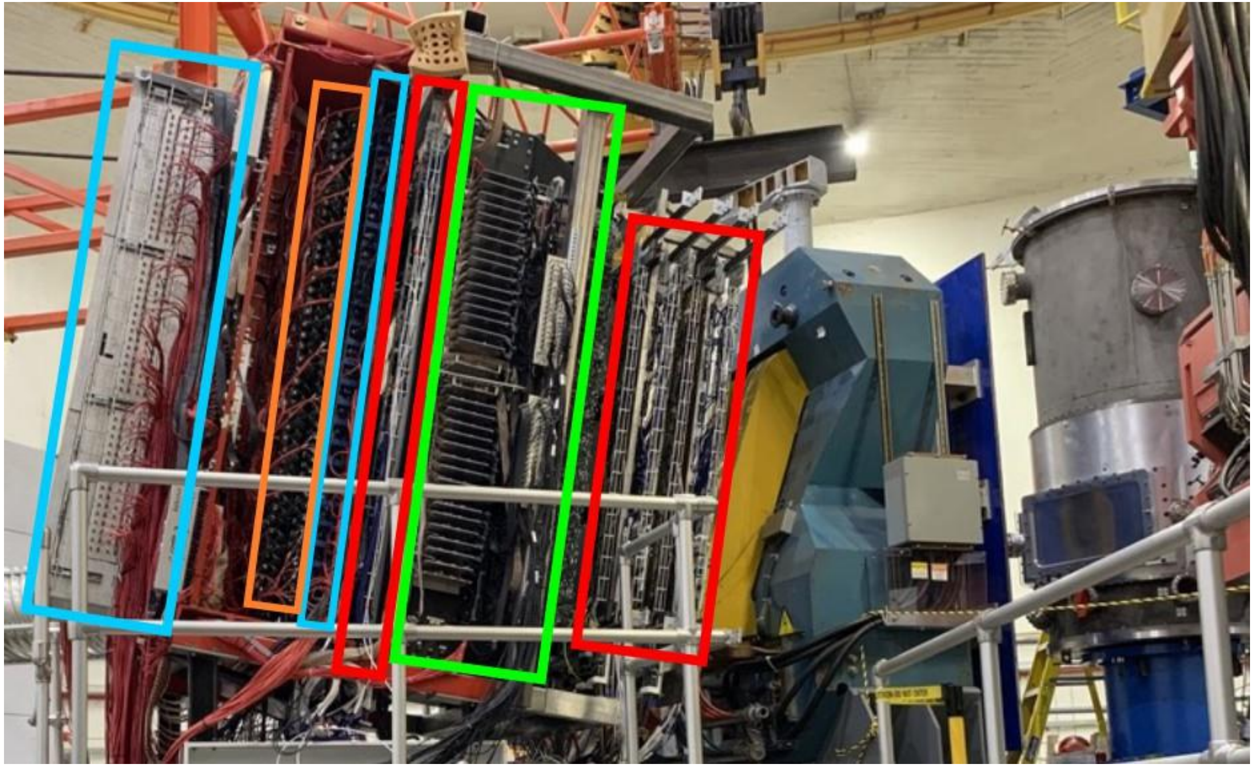

Hadron Calorimeter (HCal)

- SBS magnet is a large dipole magnet
- One module consists of 40 layers of iron absorber and 40 layers scintillator.
- Hadronic showers are created in the iron absorbers and the energy is sampled by scintillators and guided to the PMTs
- 3-4 cm spatial resolution
- 30% energy resolution

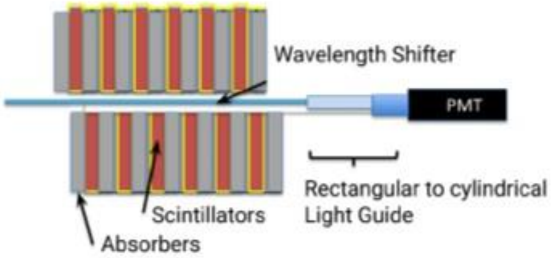

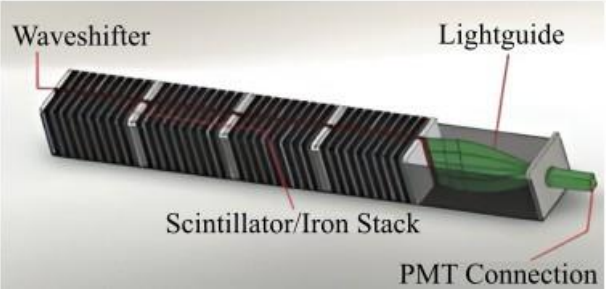

Interior of an HCal module

A side view of HCal in Hall A

Quasi-Elastic Scattering

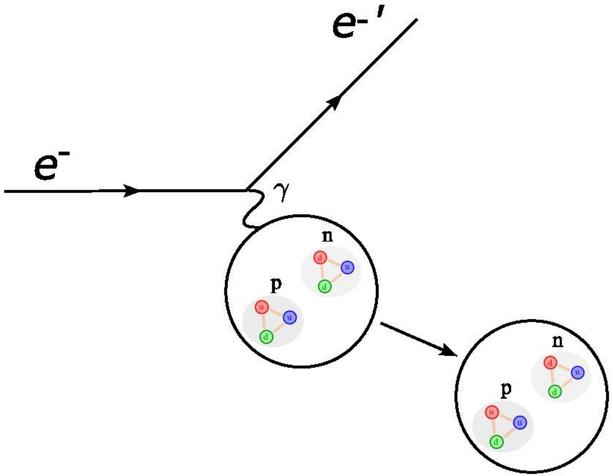

Elastic Scattering on Deuterium
$W = M_T$

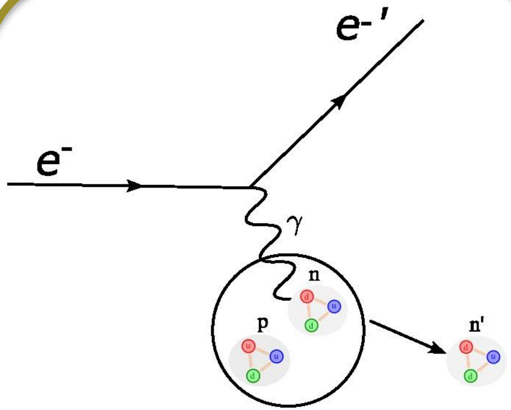

Quasi-Elastic Scattering on Deuterium
$W = M_N$

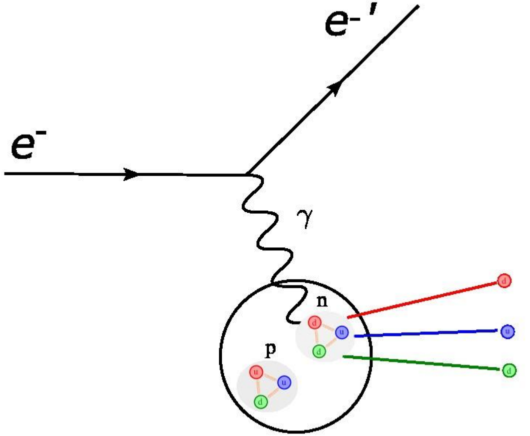

Inelastic Scattering on Deuterium
$W > M_N$

- SBS nucleon physics program focuses on quasi-elastic scattering.
- M_T is mass of the target (deuterium)
- M_N is mass of the nucleon

Quasi-Elastic Scattering

- GMn, $Q^2 = 3.0 - 13.5\ (GeV/c)^2$
- nTPE, $Q^2 = 4.5\ (GeV/c)^2$
- Need many statistics and strong cuts on the electron arm to resolve the quasi-elastic peak above the inelastic background.

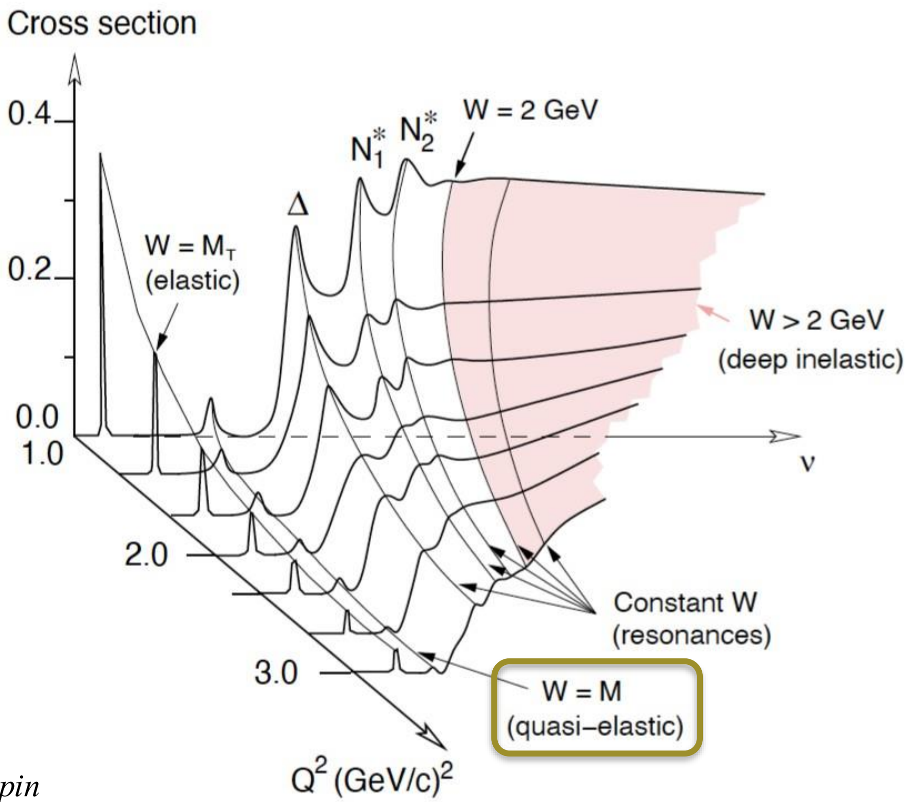

Diagram: Xiaochao Zheng, *Precision Measurement of Neutron Spin Asymmetry A1n at Large* x_{Bj} *Using CEBAF at 5.7 GeV*

Analysis Methods – Introducing HCal Δx and Δy

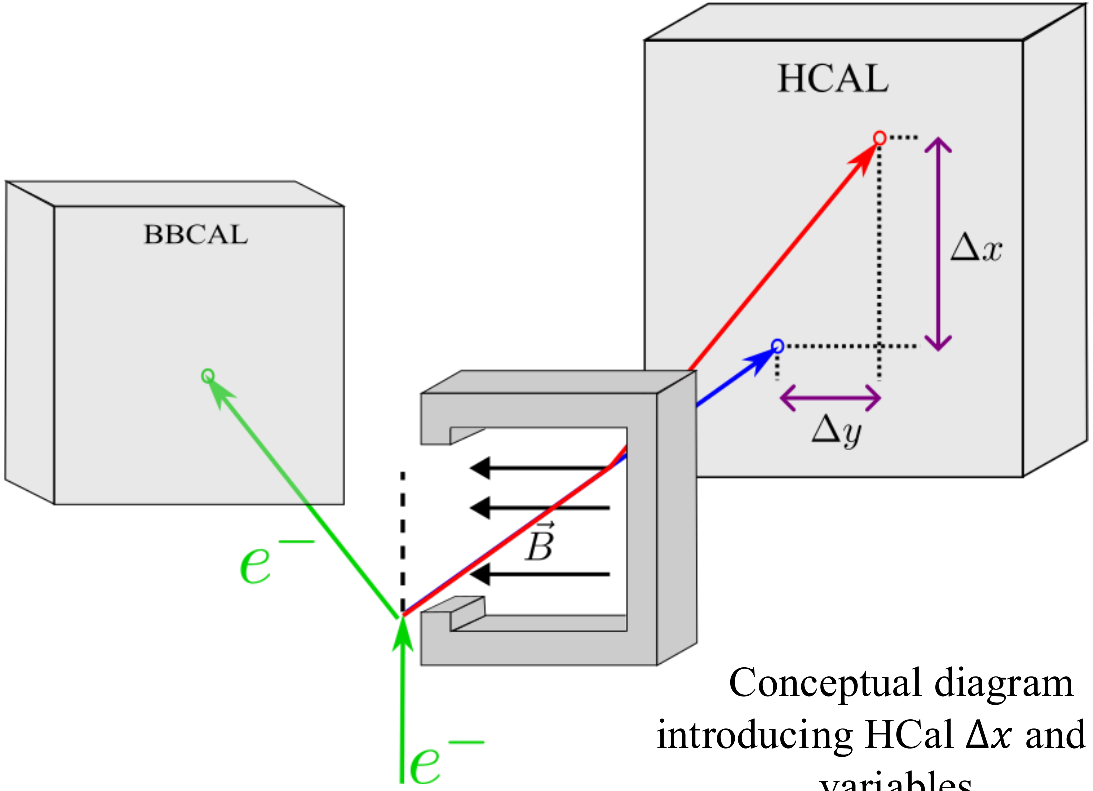

Conceptual diagram introducing HCal Δx and Δy variables.

- Definition of Δx (Δy): The difference between the observed and the expected nucleon (assuming neutron) position on HCal in the dispersive (non-dispersive) direction.
- Used to separate neutrons and protons

Neutron Rosenbluth Slope Technique

- **Goal:** Extract neutron Rosenbluth Slope, $S^n = (G_E^n)^2/\tau_n(G_M^n)^2$
- Consider 2 kinematics with same Q^2-value and with different values of ϵ**.**
- Consider 2 elastic neutron-to-proton cross-section ratios.
- Combine the Ratio Method with a Rosenbluth Technique.

$$R'_{\epsilon_1} = R_{\epsilon_1} \cdot f^{-1}_{nuc,\epsilon_1} f^{-1}_{RC,\epsilon_1} f^{-1}_{Det,\epsilon_1} = \frac{\frac{\tau_{\epsilon_{1,n}} \sigma_{\text{Mott}}}{\epsilon_{1,n}(1+\tau_{\epsilon_{1,n}})}\left(\epsilon_{1,n}\sigma^n_{L,\epsilon_1} + \sigma^n_{T,\epsilon_1}\right)}{\frac{\tau_{\epsilon_{1,p}} \sigma_{\text{Mott}}}{\epsilon_{1,p}(1+\tau_{\epsilon_{1,p}})}\left(\epsilon_{1,p}\sigma^p_{L,\epsilon_1} + \sigma^p_{T,\epsilon_1}\right)}$$

$$R'_{\epsilon_2} = R_{\epsilon_2} \cdot f^{-1}_{nuc,\epsilon_2} f^{-1}_{RC,\epsilon_2} f^{-1}_{Det,\epsilon_2} = \frac{\frac{\tau_{\epsilon_{2,n}} \sigma_{\text{Mott}}}{\epsilon_{2,n}(1+\tau_{\epsilon_{2,n}})}\left(\epsilon_{2,n}\sigma^n_{L,\epsilon_2} + \sigma^n_{T,\epsilon_2}\right)}{\frac{\tau_{\epsilon_{2,p}} \sigma_{\text{Mott}}}{\epsilon_{2,p}(1+\tau_{\epsilon_{2,p}})}\left(\epsilon_{2,p}\sigma^p_{L,\epsilon_2} + \sigma^p_{T,\epsilon_2}\right)}$$

Neutron Rosenbluth Slope Technique

Physics Result:

- Consider 'super-ratio' of R' for two different values of ϵ.
- Define $S^{n(p)} = \left(G_E^{n(p)}\right)^2 / \tau_{n(p)} \left(G_M^{n(p)}\right)^2$ and $\Delta\epsilon = \epsilon_{1,n} - \epsilon_{2,n}$.

Super-Ratio

$$\frac{R'_{\epsilon_1}}{R'_{\epsilon_2}} = B \cdot \frac{1 + \epsilon_{1,n} S^n_{\epsilon_1}}{1 + \epsilon_{2,n} S^n_{\epsilon_2}}$$

From Kinematic Information

$$B = \frac{\dfrac{\tau_{\epsilon_{1,n}}}{\epsilon_{1,n}\left(1+\tau_{\epsilon_{1,n}}\right)} \dfrac{\tau_{\epsilon_{2,p}}}{\epsilon_{2,p}\left(1+\tau_{\epsilon_{2,p}}\right)}}{\dfrac{\tau_{\epsilon_{1,p}}}{\epsilon_{1,p}\left(1+\tau_{\epsilon_{1,p}}\right)} \dfrac{\tau_{\epsilon_{2,n}}}{\epsilon_{2,n}\left(1+\tau_{\epsilon_{2,n}}\right)}} \frac{\left(G_M^n\right)^2_{\epsilon_1}}{\left(G_M^p\right)^2_{\epsilon_1}} \frac{\left(G_M^p\right)^2_{\epsilon_2}}{\left(G_M^n\right)^2_{\epsilon_2}} \frac{1 + \epsilon_{2,p} S^p_{\epsilon_2}}{1 + \epsilon_{1,p} S^p_{\epsilon_1}}$$

From Global Form Factor Analysis.

Neutron Rosenbluth Slope Technique

Physics Result:

- Consider 'super-ratio' of R' for two different values of ϵ.
- Define $S^{n(p)} = \left(G_E^{n(p)}\right)^2 / \tau_{n(p)} \left(G_M^{n(p)}\right)^2$ and $\Delta\epsilon = \epsilon_{1,n} - \epsilon_{2,n}$.

Physics Result!

$$S^n = \frac{\left(\frac{R'_{\epsilon_1}}{R'_{\epsilon_2}} - B\right)}{\Delta\epsilon \cdot B} \simeq \frac{(G_E^n)^2}{\tau_n (G_M^n)^2}$$

From Data Extraction

From Kinematic Information

$$B = \frac{\frac{\tau_{\epsilon_{1,n}}}{\epsilon_{1,n}(1+\tau_{\epsilon_{1,n}})} \frac{\tau_{\epsilon_{2,p}}}{\epsilon_{2,p}(1+\tau_{\epsilon_{2,p}})}}{\frac{\tau_{\epsilon_{1,p}}}{\epsilon_{1,p}(1+\tau_{\epsilon_{1,p}})} \frac{\tau_{\epsilon_{2,n}}}{\epsilon_{2,n}(1+\tau_{\epsilon_{2,n}})}} \frac{(G_M^n)^2_{\epsilon_1}}{\left(G_M^p\right)^2_{\epsilon_1}} \frac{\left(G_M^p\right)^2_{\epsilon_2}}{(G_M^n)^2_{\epsilon_2}} \frac{1+\epsilon_{2,p} S^p_{\epsilon_2}}{1+\epsilon_{1,p} S^p_{\epsilon_1}}$$

From Global Form Factor Analysis.

Position-Dependent Efficiency Correction to MC

- Reweight MC events based on data map
- Treat proton and neutron MC events equally
- Relative efficiency correction factor

$$c(x,y) = \frac{\epsilon_{\mathrm{HCal}}^{\mathrm{data}}(x,y)}{\langle \epsilon_{\mathrm{HCal}}^{\mathrm{data}} \rangle}$$

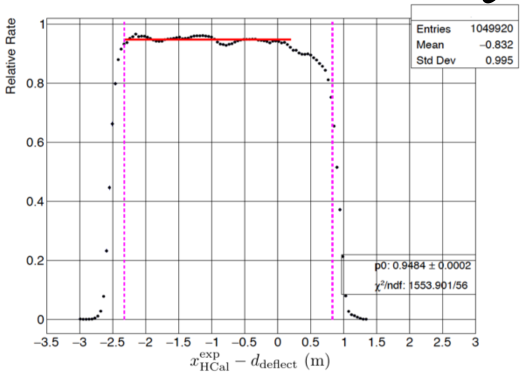

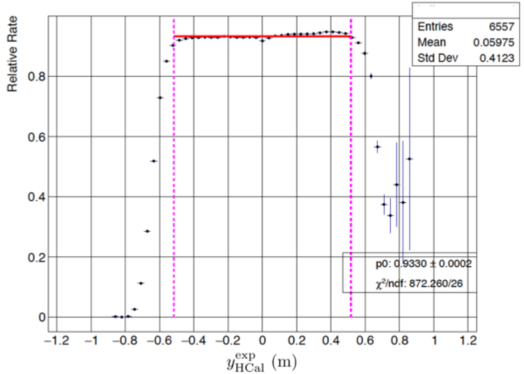

- $\epsilon_{\mathrm{HCal}}^{\mathrm{data}}(x,y)$ is the interpolated position-dependent efficiency value
- $\langle \epsilon_{\mathrm{HCal}}^{\mathrm{data}} \rangle$ is the acceptance-averaged value
- Comparisons of Δx between uncorrected and corrected MC events were used to quantify systematic effects on $R_{sf}^{n/p}$

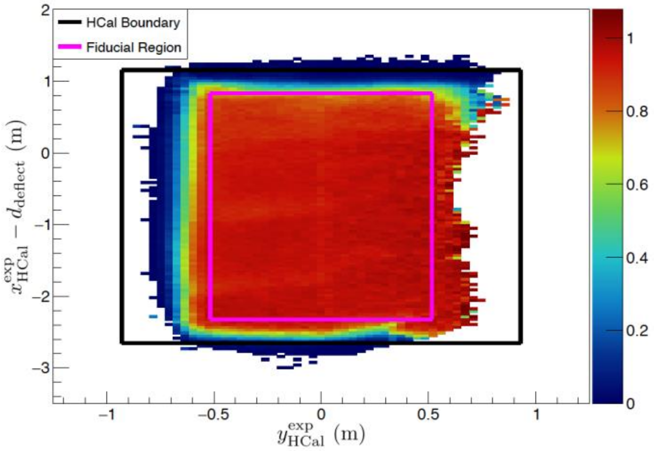

SBS-8, $Q^2 = 4.5\ (\mathrm{GeV/c})^2$

$Q^2 = 4.5\ (GeV/c)^2$

Data-Monte Carlo Comparison

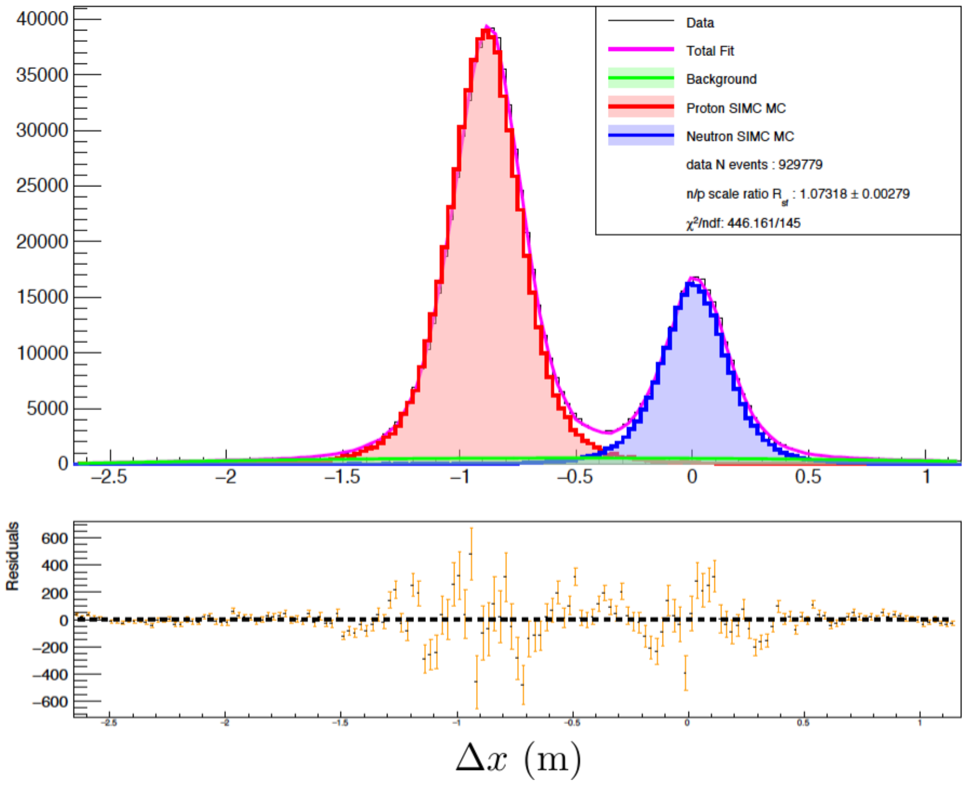

- Fit Equation:

$$f_{total}(x_i) = f_{sf}^{p}\left(R_{sf}^{n/p} h^{n}(x_i - \delta_n) + h^{p}(x_i - \delta_p)\right) + f_{bkgd}(x_i)$$

- Fit Parameters:
  1. f_{sf}^{p} - proton scale factor
  2. $R_{sf}^{n/p}$ - ratio of neutron to proton scale factors
  3. $\delta_{n(p)}$ - neutron (proton) centroid shift parameters
  4. f_{bkgd} - parameters associated with the background

$Q^2 = 4.5\ (GeV/c)^2$

Data-Monte Carlo Comparison

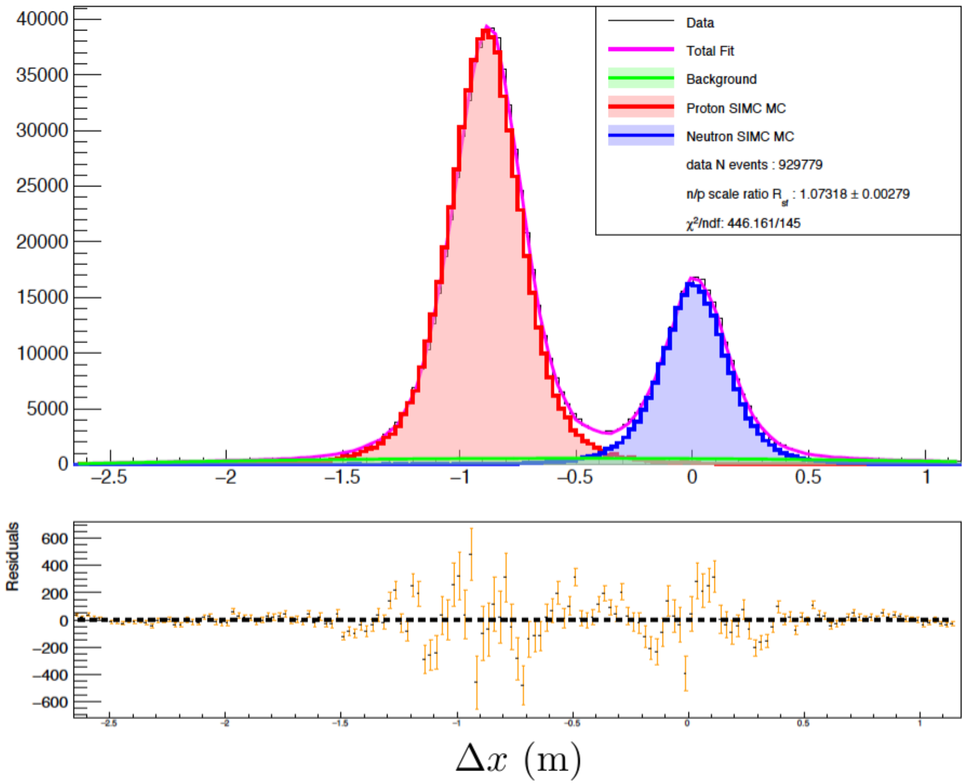

Simulation:

- D(e,e'n) and D(e,e'p) simulated events realistically account for nuclear, radiative, and detector effects that are present in data.
- Calculate the neutron to proton cross-section ratio identically to the MC

$$R'_{sim} = \frac{\left(\frac{d\sigma}{d\Omega}\right)\Big|_{n(e,e'),sim}}{\left(\frac{d\sigma}{d\Omega}\right)\Big|_{p(e,e'),sim}}$$

$$= R_{sim} \cdot f^{-1}_{nuc,sim} f^{-1}_{RC,sim} f^{-1}_{Det,sim}$$

$Q^2 = 4.5\ (\text{GeV}/c)^2$

Data-Monte Carlo Comparison

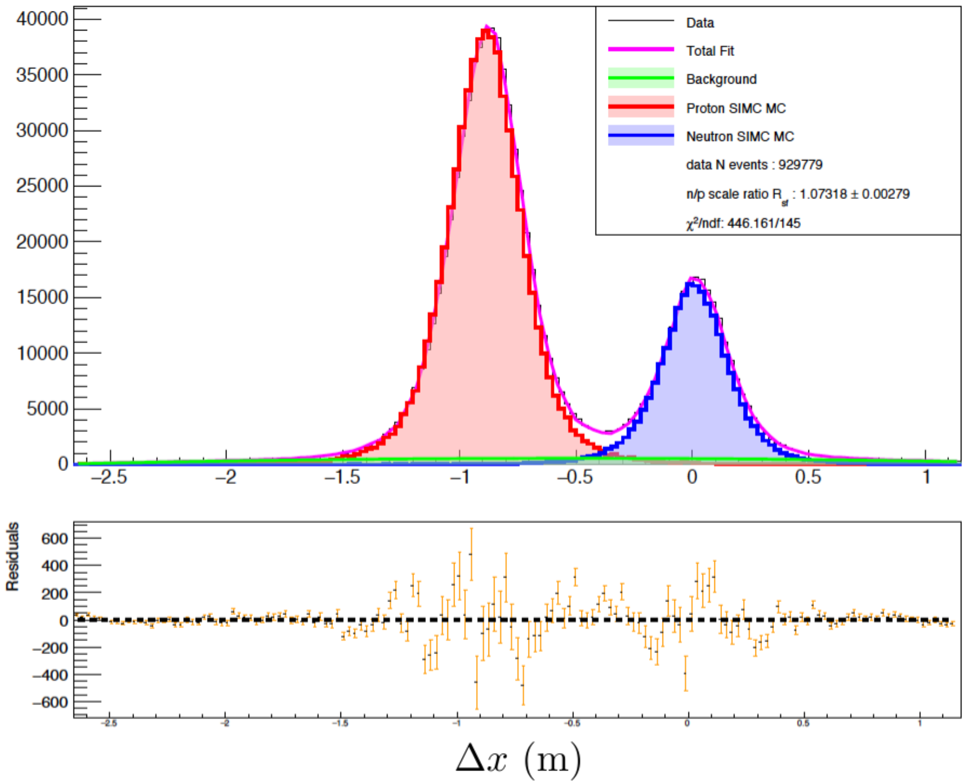

Extraction:

$$R = R' \cdot f_{nuc} f_{RC} f_{det}$$
$$= R_{sf}^{n/p} \cdot R'_{sim} \cdot f_{nuc,sim} f_{RC,sim} f_{det,sim}$$

Claim:

- Simulation consistently replicates nuclear, radiative, and detector effects that are present in the experimental data.

Implication:

$$\frac{f_{nuc}}{f_{nuc,sim}} \sim 1 \qquad \frac{f_{RC}}{f_{RC,sim}} \sim 1 \qquad \frac{f_{det}}{f_{det,sim}} \sim 1$$

$$R' = \frac{\left.\left(\frac{d\sigma}{d\Omega}\right)\right|_{n(e,e')}}{\left.\left(\frac{d\sigma}{d\Omega}\right)\right|_{p(e,e')}} = R_{sf}^{n/p} \cdot R'_{sim}$$

Event Selection Criteria

Good Electron Cuts

1. Track Quality
   - No. of GEM Layers with Hits
   - Track χ^2/ndf
   - Vertex Z position
   - BigBite Optics Validity
2. PID
   - Preshower Energy
   - E_{BBCal}/p

Quasi-Elastic Event Cuts

- HCal Cluster Energy
- Coincidence Time
- W^2
- Δy
- Fiducial

- Cut regions were optimized
- Systematic effects on $R_{sf}^{n/p}$ due to cut sensitivity were quantified

Event Selection Criteria

Good Electron Cuts

1. Track Quality
   - No. of GEM Layers with Hits
   - Track χ^2/ndf
   - Vertex Z position
   - BigBite Optics Validity
2. PID
   - Preshower Energy
   - E_{BBCal}/p

Quasi-Elastic Event Cuts

- HCal Cluster Energy
- Coincidence Time
- W^2
- Δy
- Fiducial

- Cut regions were optimized
- Systematic effects on $R_{sf}^{n/p}$ due to cut sensitivity were quantified

$Q^2 = 4.5\ (GeV/c)^2$

Preshower Energy (PID cut)

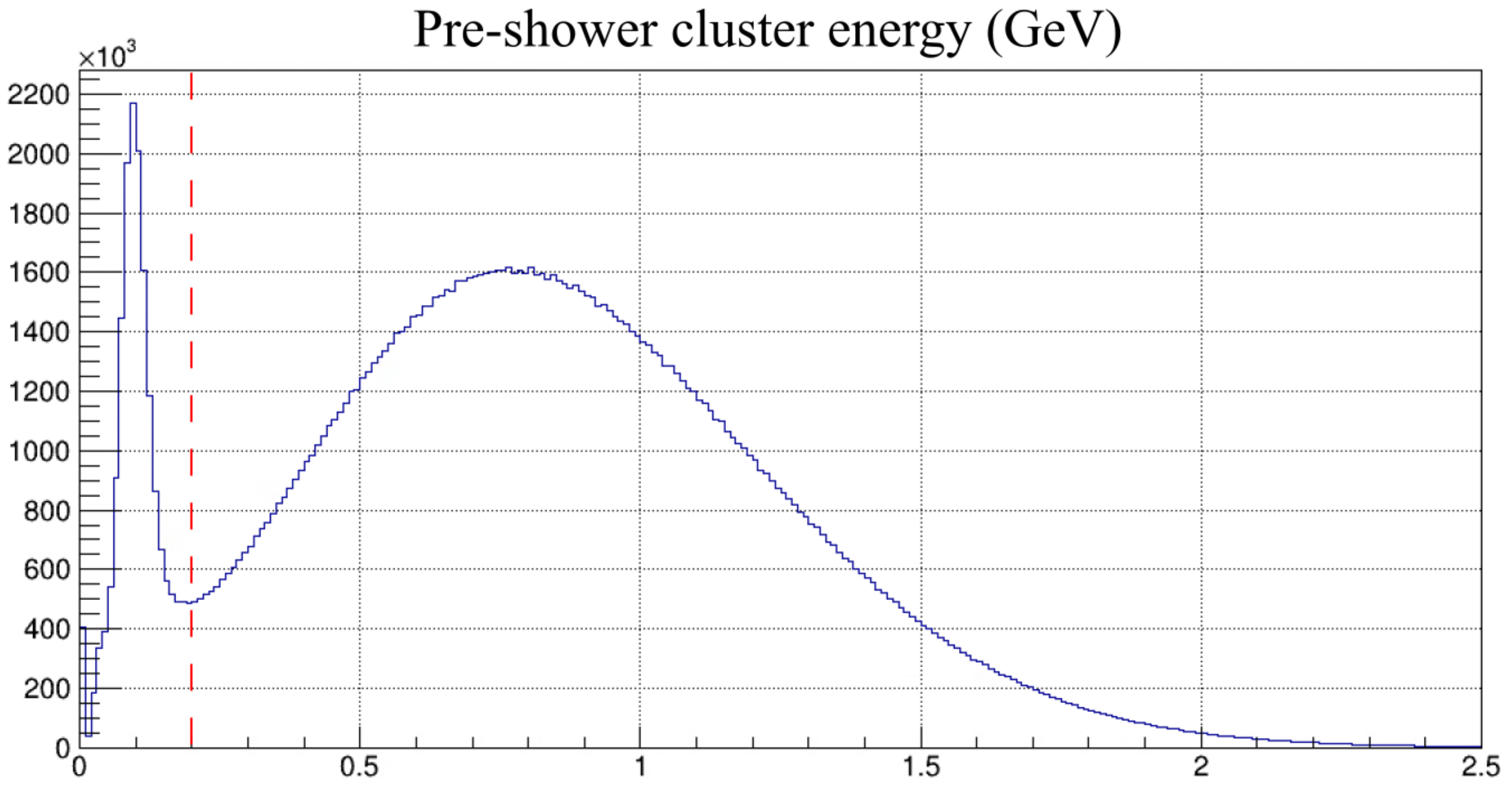

Q^2 = 4.5 (GeV/c)^2

Invariant Mass Squared (W^2)

No Cuts Applied

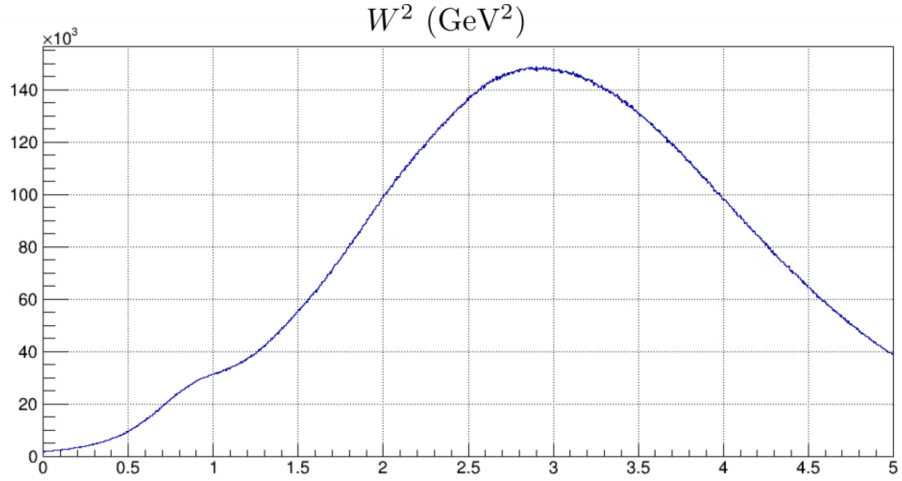

All Other Cuts Applied

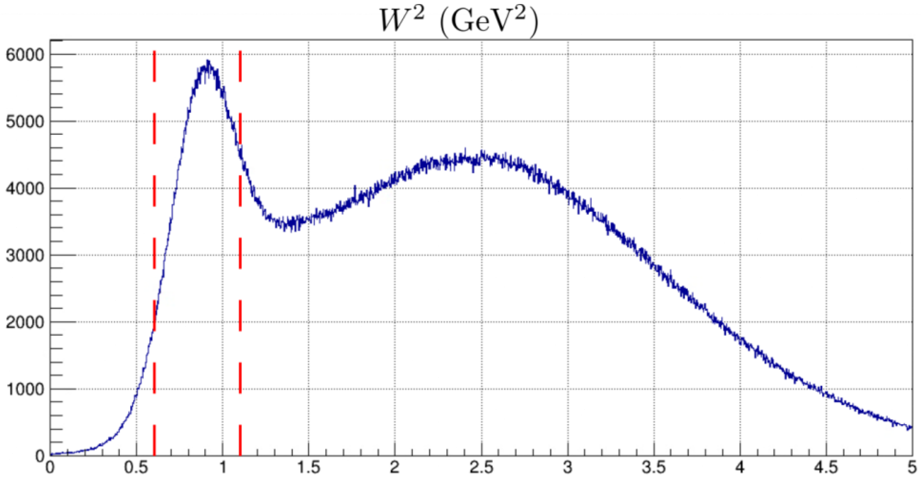

Proton and Neutron Relative-Rate Comparisons

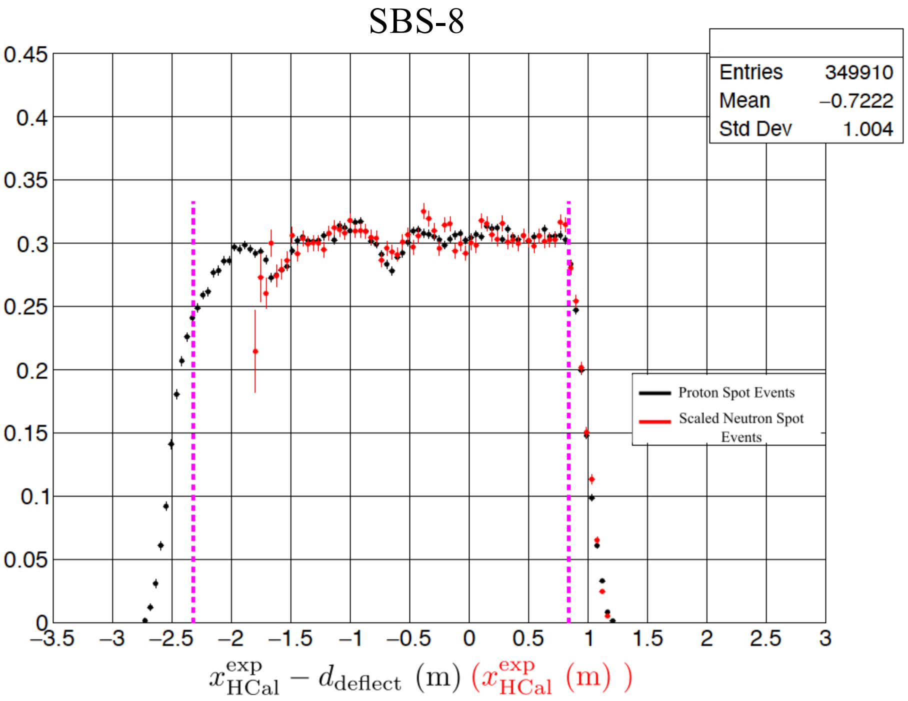

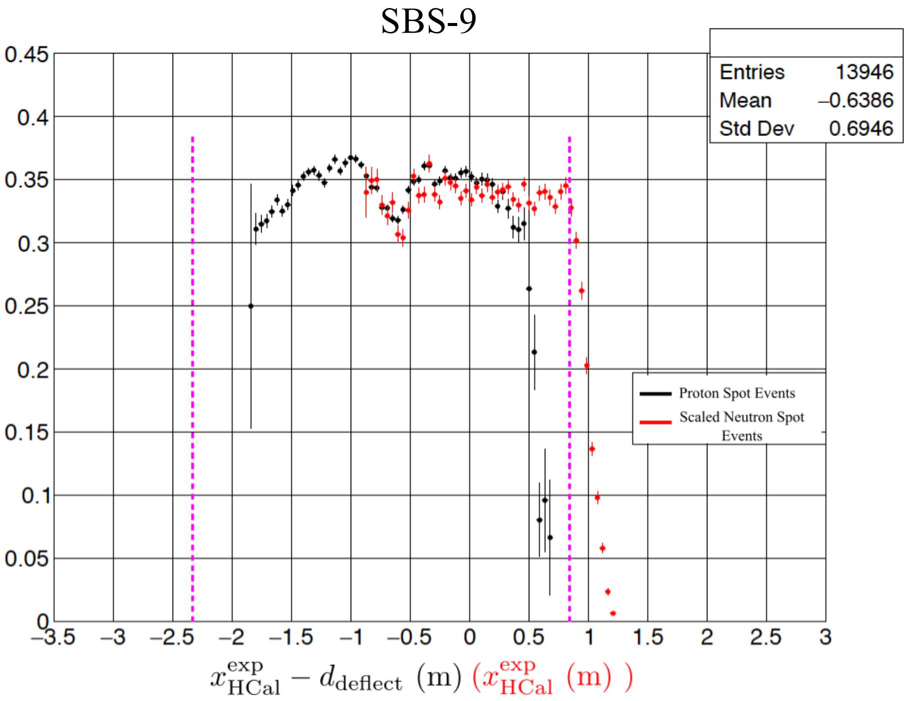

Proton Spot Events

Neutron Spot Events

Extracted $R_{sf}^{n/p}$ Values

Setting	$R_{sf}^{n/p}$	$\Delta\left(R_{sf}^{n/p}\right)_{\text{total}}$	$\Delta\left(R_{sf}^{n/p}\right)_{\text{stat}}$	$\Delta\left(R_{sf}^{n/p}\right)_{\text{sys}}$
SBS-8 50%	1.0787	0.0152	0.0082	0.0128
SBS-8 70%	1.0732	0.0110	0.0028	0.0106
SBS-8 100%	1.0651	0.0133	0.0065	0.0116
SBS-9 70%	1.0648	0.0088	0.0034	0.0081

	Uncertainty Source	Setting			
		SBS-8 50%	SBS-8 70%	SBS-8 100%	SBS-9 70%
$\Delta\left(R_{sf}^{n/p}\right)_{\text{sys}}$	HDENU	0.0003	0.0018	0.0012	0.0053
	Cut S.	0.0078	0.0083	0.0052	0.0054
	Ine. Con.	0.0101	0.0065	0.0103	0.0029
	Total	0.0128	0.0106	0.0116	0.0081

	$\overline{R}_{sf}^{n/p}$	$\Delta\left(\overline{R}_{sf}^{n/p}\right)_{\text{total}}$	$\Delta\left(\overline{R}_{sf}^{n/p}\right)_{\text{uncorr}}$	$\Delta\left(\overline{R}_{sf}^{n/p}\right)_{\text{corr}}$
Value for SBS-8	1.0711	0.0104	0.0054	0.0089

Extracted R' Values

Setting	R'	$\Delta(R')_{total}$	$\Delta(R')_{stat}$	$\Delta(R')_{sys}$
SBS-8 50%	0.3936	0.0055	0.0030	0.0047
SBS-8 70%	0.3916	0.0040	0.0010	0.0039
SBS-8 100%	0.3886	0.0049	0.0024	0.0042
SBS-9 70%	0.3875	0.0032	0.0013	0.0030

	$\overline{R'}$	$\Delta\left(\overline{R'}\right)_{total}$	$\Delta\left(\overline{R'}\right)_{uncorr}$	$\Delta\left(\overline{R'}\right)_{corr}$
Value for SBS-8	0.3908	0.0038	0.0020	0.0032

Rosenbluth Separation Technique

- Fixed Q^2-value
- Vary electron beam energy and scattering angle, to make measurements at different ϵ values
- Reduced cross-section linear dependence in ϵ

$$\sigma_R = \frac{\epsilon(1+\tau)}{\tau}\frac{E}{E'}\frac{d\sigma}{d\Omega}/\sigma_{\text{Mott}}$$
$$= \frac{\epsilon}{\tau}G_E^2(Q^2) + G_M^2(Q^2)$$
$$= (\epsilon\sigma_L + \sigma_T)$$

$$\epsilon = (1 + 2(1+\tau)\tan^2(\theta/2))^{-1}$$

Rosenbluth Slope

$$S = \sigma_L/\sigma_T = G_E^2(Q^2)/\tau G_M^2(Q^2)$$

Rosenbluth Separation Technique

$$\sigma_R = \frac{\epsilon(1+\tau)}{\tau}\frac{E}{E'}\frac{d\sigma}{d\Omega}/\sigma_{\mathrm{Mott}}$$
$$= \frac{\epsilon}{\tau}G_E^2(Q^2) + G_M^2(Q^2)$$
$$= (\epsilon\sigma_L + \sigma_T)$$

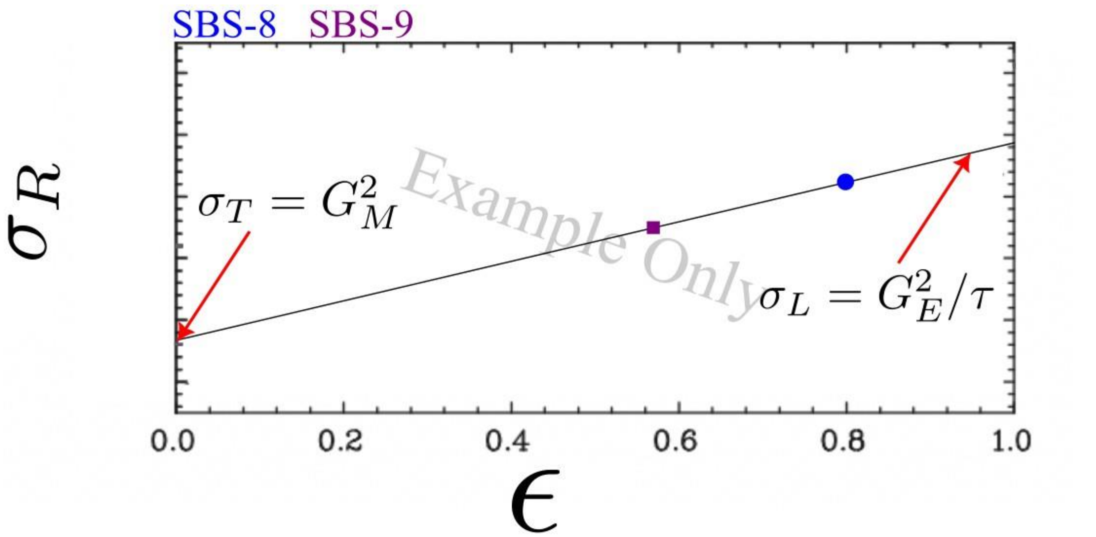

Rosenbluth Slope

$$S = \sigma_L/\sigma_T = G_E^2(Q^2)/\tau G_M^2(Q^2)$$

Targets

Cryogenic Targets:

- Liquid Hydrogen
  - 19 Kelvin
  - Proton Source
  - Used for apparatus calibrations
- Liquid Deuterium
  - 22 Kelvin
  - Proton and Neutron Source
  - Used for production data

Solid Targets:

- Used for calibrations, systematics, and optics studies
- Include dummy, carbon hole, and optics foil targets

Target ladder with cryotarget cells.

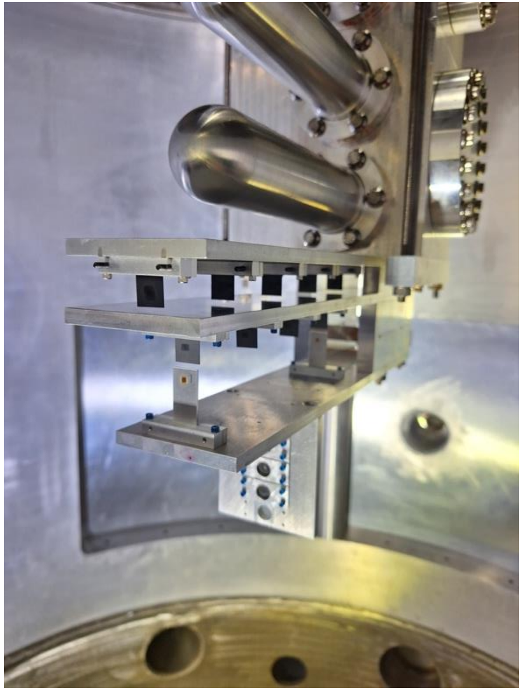

Target ladder showing solid foil targets.

Gas Electron Multiplier (GEM)

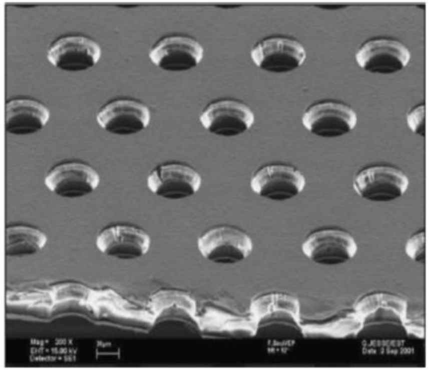

Diagram of a typical GEM electrode

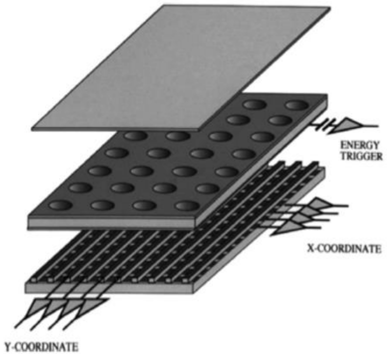

Diagram of a single GEM detector with Cartesian readout

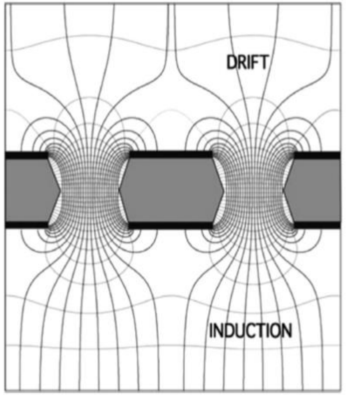

Electric Field in the region of the holes of a GEM electrode

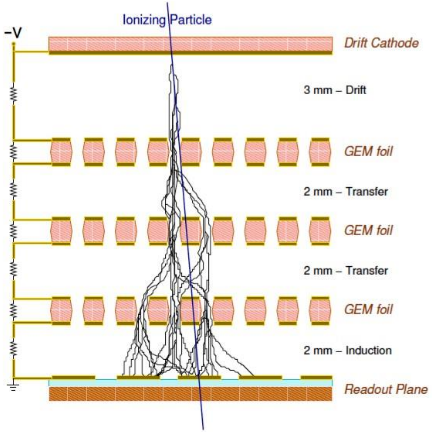

Diagram of a triple GEM detector

- Type of gaseous ionization detector, reliant on electron avalanche and a subclass of detectors known as Micro-Pattern Gas Detectors (MPGDs).
- Used as tracking detectors, preamplification, drift chambers, time projection chambers, radio imaging.
- Triple GEM detector effective gains typically are 10^4 or 10^5 .
- ~100 μm spatial resolution and 100-500 kHz/cm^2 particle rate.

GEM Detectors for SBS Program

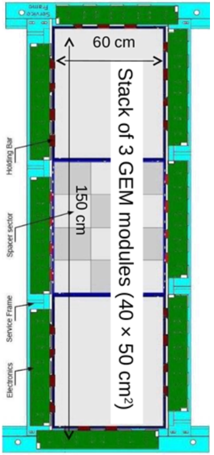

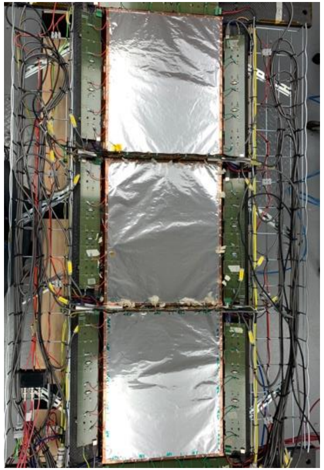

INFN XY-GEM Layer schematic and picture with RF shielding

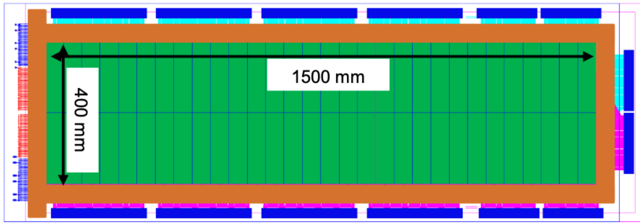

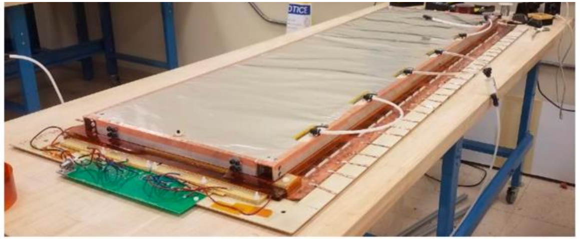

UVA UV-GEM Layer schematic and picture with RF shielding

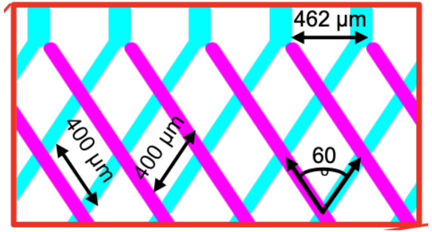

- 4 INFN GEM layers prepared for SBS program
- 4 UVA UV-GEM layers prepared for SBS program
- 11 UVA XY-GEM layers prepared for SBS program
- 2 INFN GEM layers operated during G_M^n
- 2 UVA UV-GEM layers operated during G_M^n
- 2 more UVA UV-GEM layers moved to BigBite during G_M^n

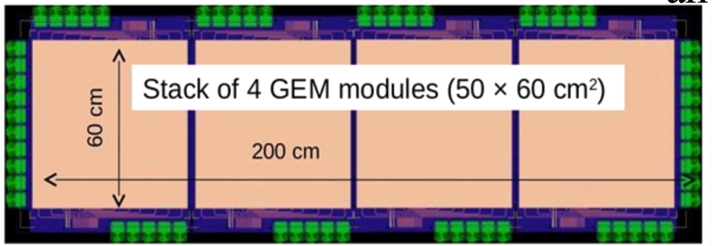

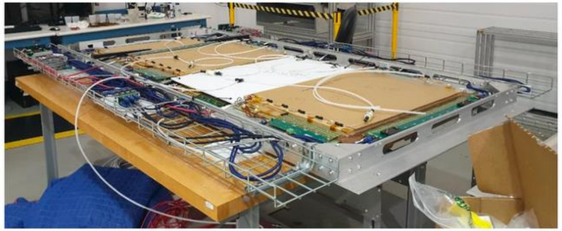

UVA XY-GEM Layer schematic and picture without RF shielding

GEM DAQ Electronics

INFN Analog Pipeline Voltage (APV25) Card

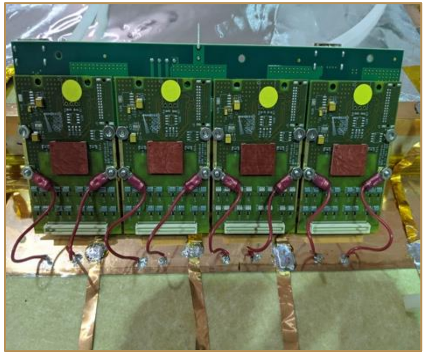

UVA APV25 Card

10 or 20 m HDMI Cables

Multi Purpose Digitizer (MPD)

Long Fiber Optic Cables

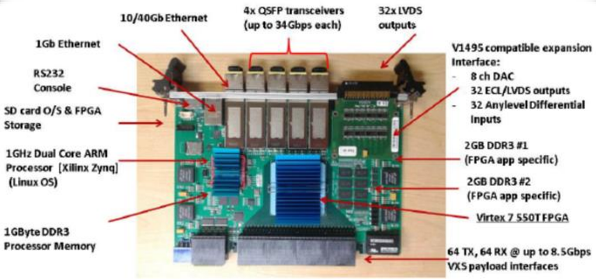

VXS Trigger Processor (VTP)

CODA3 Platform

Gas RINg CHerenkov (GRINCH)

- PID for electrons and pions
- 510 one-inch PMTs in a honeycomb array
- 4 highly reflective cylindrical mirrors
- Filled with heavy gas: C_4F_8
- Pion Threshold of 2.7 GeV
- NINO front-end cards instrumented for data collection in high-background environment

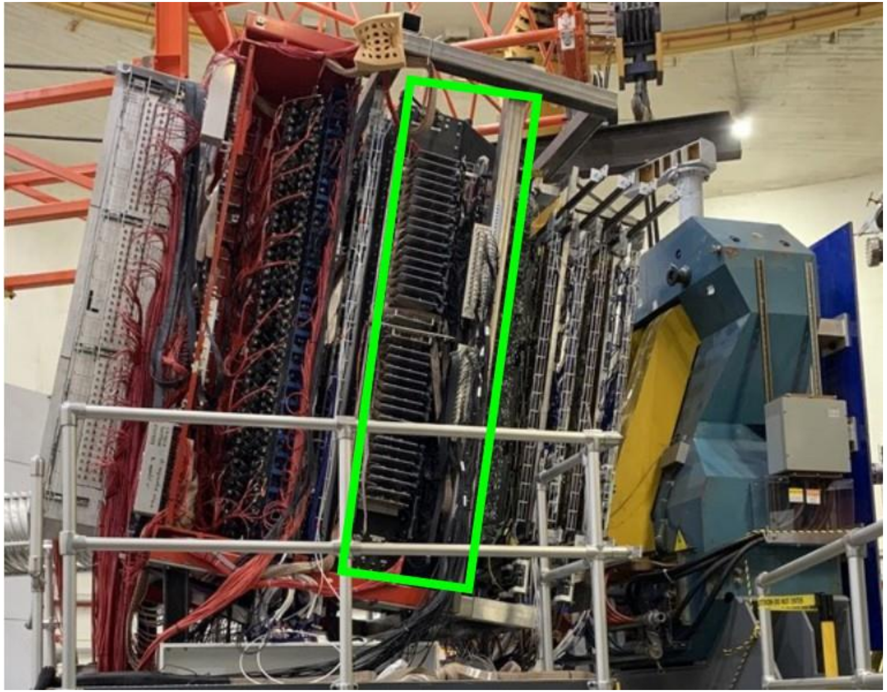

GRINCH in the BigBite Spectrometer in Hall A

Cylindrical Mirrors Inside GRINCH

Timing Hodoscope

- High precision timing reference
- 90 plastic scintillators with light guides and PMTs on each end
- Alternated straight and curved light guides
- Located between Preshower and Shower
- ~60 ps timing resolution
- ~5 cm spatial resolution

Zoom-in of Timing Hodoscope in BigBite Spectrometer

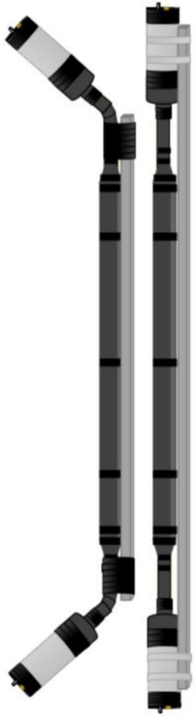

Top-View of Scintillator Bar Types

Diagram: Ralph Marinaro, *Performance and Commissioning of the BigBite Timing Hodoscope for Nucleon Form Factor Measurements at Jefferson Lab.*

BigBite Calorimeter (BBCal)

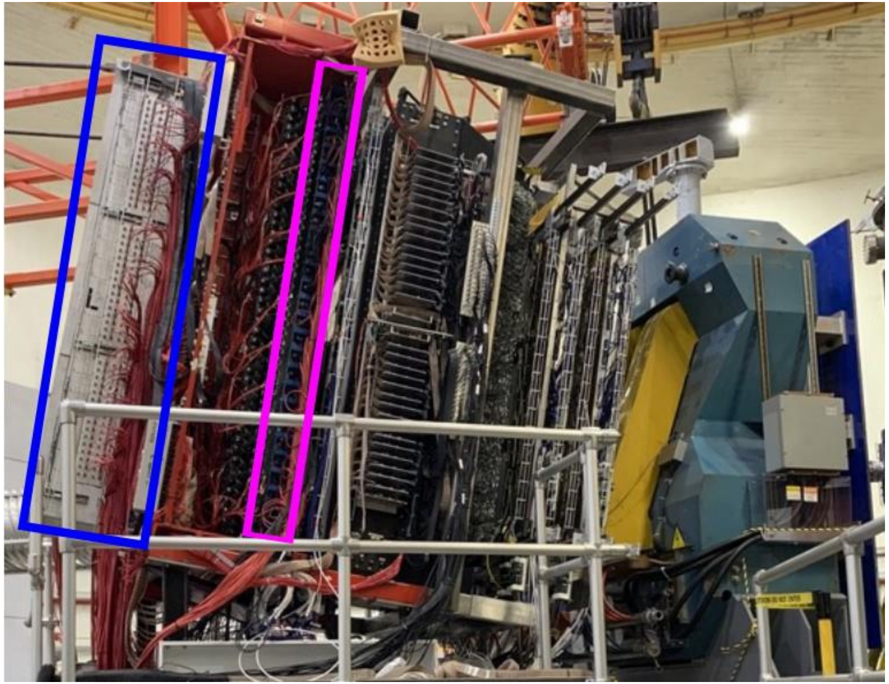

BBCal in BigBite Spectrometer, composed of Preshower and Shower.

- Preshower and Shower together sample the total energy and position of the scattered electron.
- Electron induces electromagnetic shower in the lead-glass blocks. Light is collected with PMTs.
- Preshower
  - 52 lead-glass blocks perpendicular to e' track
  - Pions leave a lower energy signal, ~200 MeV/c^2
- Shower
  - 189 lead-glass blocks parallel to e' track
  - Electrons deposit remaining energy
- Provides single-arm trigger.
- Allows for energy measurement, constraints on track search region, and pion rejection.

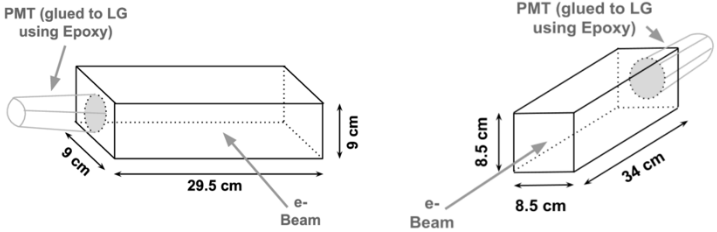

Super BigBite Magnet

Side View of SBS Magnet

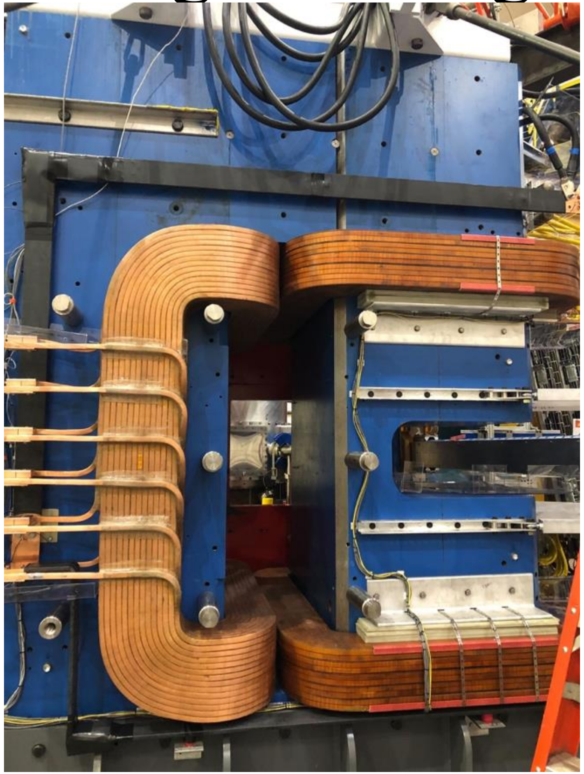

Downstream View of SBS Magnet

- Dipole magnet
- Deflects positively charged particles, differentiating between scattered protons and neutrons.
- 100 tons
- $1.3\ T \cdot m$
- 2.1 kA excitation current
- 35 msr, 2.25 m from target

Theta Scattered Electron Distributions (after all cuts)

For Extraction Theta Scattered Electron values SBS-8: 0.4619 , SBS-9: 0.8506

SBS-8 70%

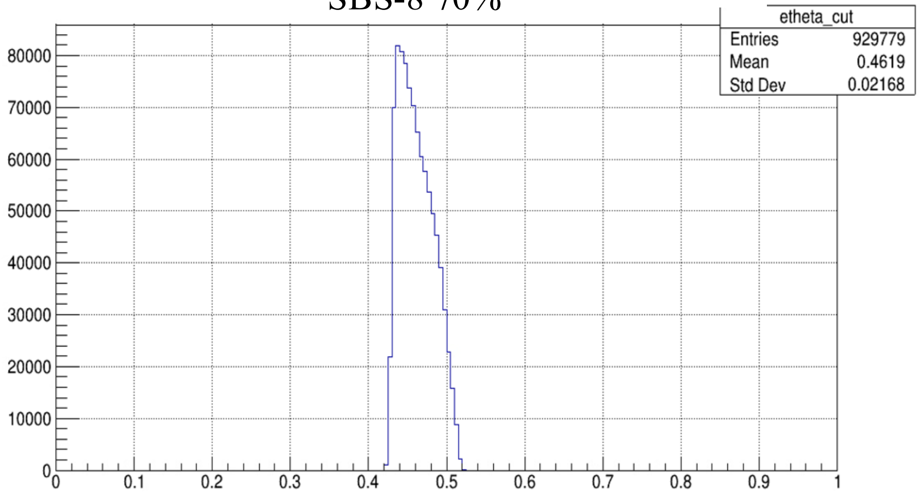

SBS-9 70%

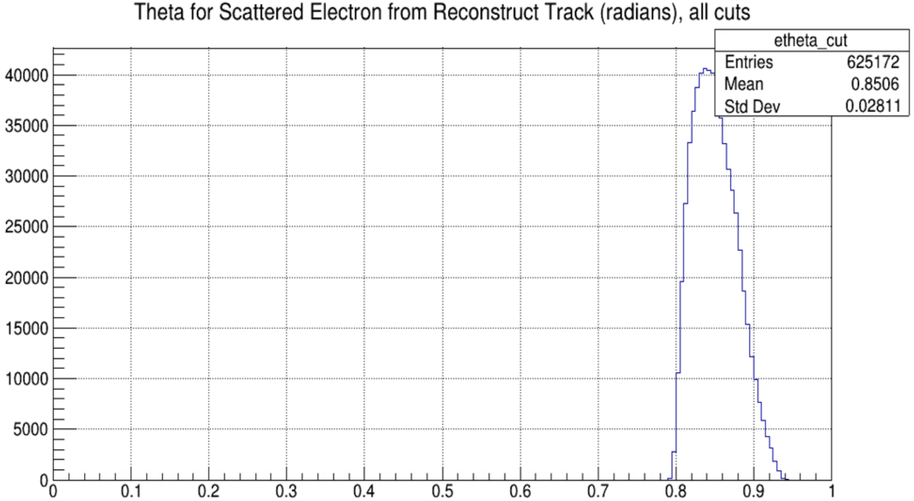

Q^2 Distributions (after all cuts)

For Extraction Q^2 values SBS-8: 4.48, SBS-9: 4.476

SBS-8 70%

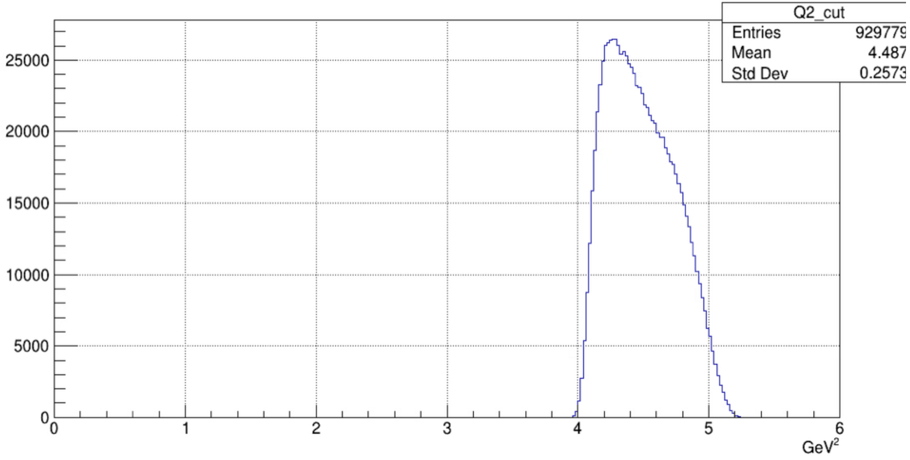

SBS-9 70%

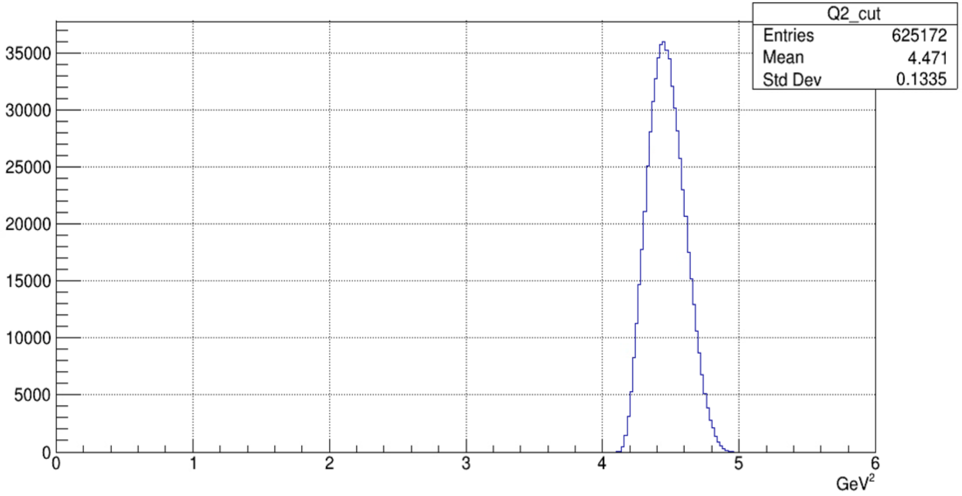

Scattered Nucleon Momentum Distributions (after all cuts)

For Extraction Scattered Nucleon Momentum values SBS-8: 3.19 , SBS-9: 3.19

SBS-8 70%

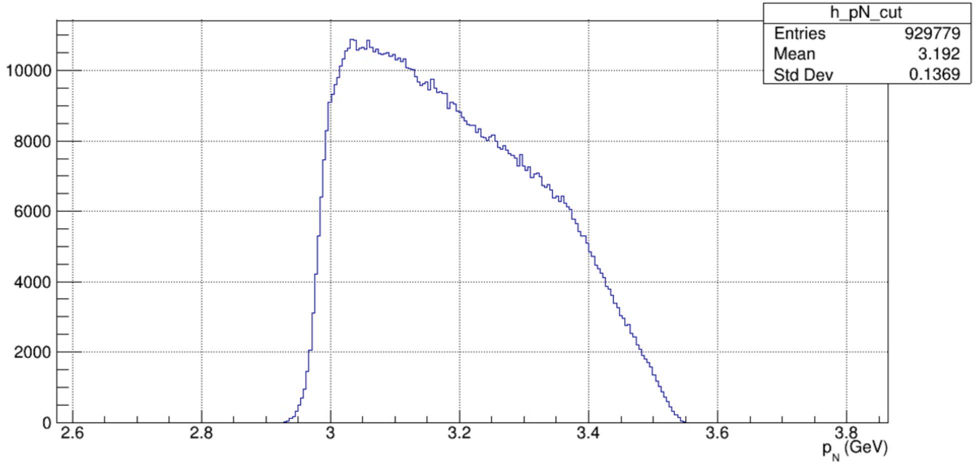

SBS-9 70%

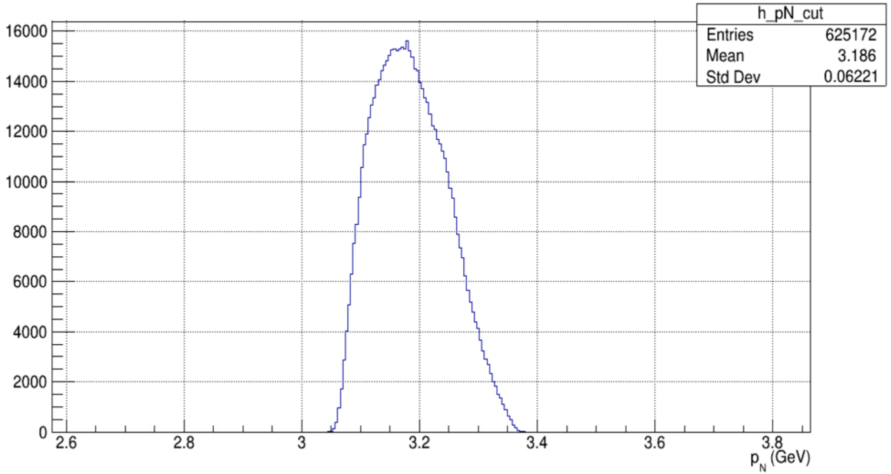

ϵ Distributions (after all cuts)

For Extraction ϵ values (neutrons) SBS-8: 0.79925 , SBS-9: 0.51802

SBS-8 70%

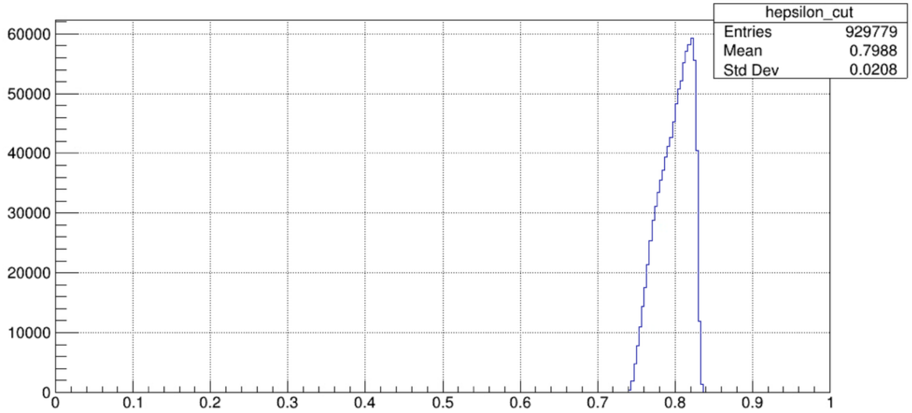

SBS-9 70%

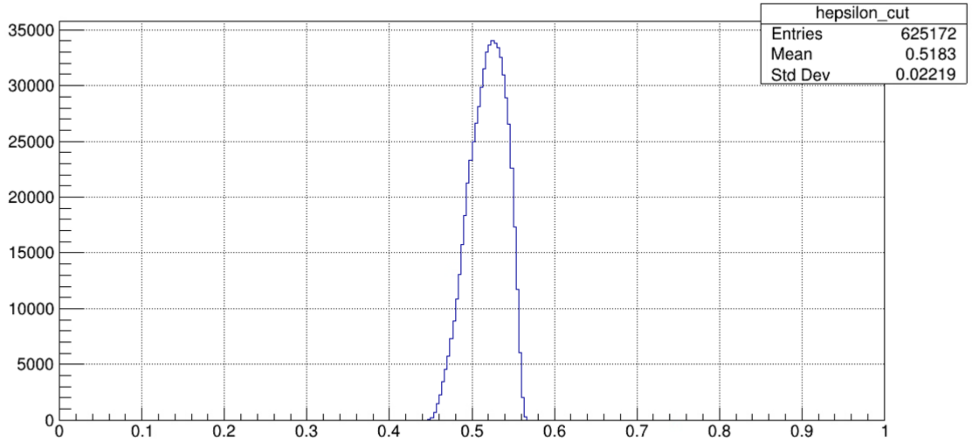

Analysis Methods – Introducing HCal Δx and Δy

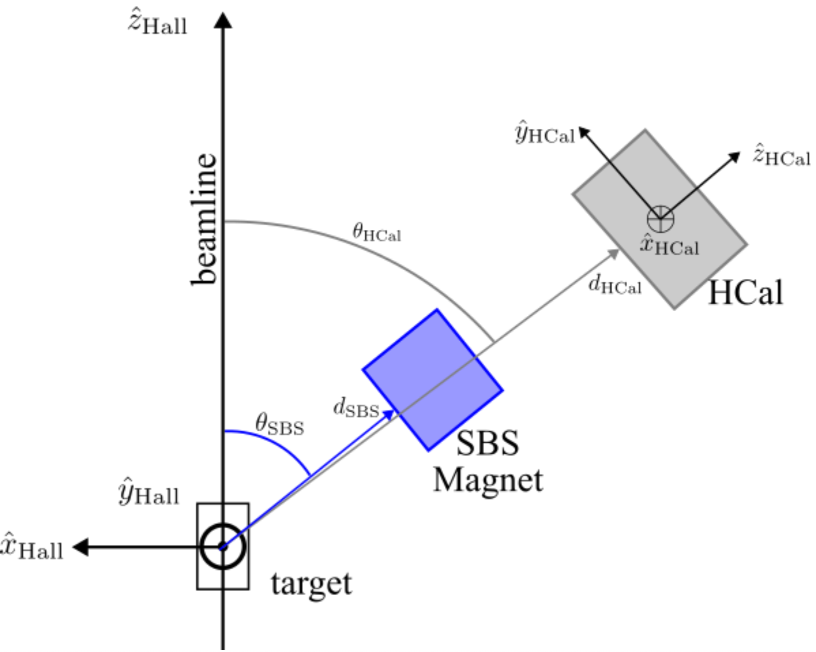

$$\Delta x = x^{\rm obs}_{\rm HCal} - x^{\rm exp}_{\rm HCal},$$

$$\Delta y = y^{\rm obs}_{\rm HCal} - y^{\rm exp}_{\rm HCal},$$

$$x^{\rm exp}_{\rm HCal} = \left(\vec{h}_{\rm intersect} - \vec{O}_{\rm HCal}\right) \cdot \hat{x}_{\rm HCal},$$

$$y^{\rm exp}_{\rm HCal} = \left(\vec{h}_{\rm intersect} - \vec{O}_{\rm HCal}\right) \cdot \hat{y}_{\rm HCal},$$

$$\vec{h}_{\rm intersect} = \vec{v} + s_{\rm intersect}\hat{p}_{N'}.$$

$$\hat{p}_{N'} = (\sin\theta_{N'}\cos\phi_{N'}, \sin\theta_{N'}\sin\phi_{N'}, cos\theta_{N'})\,.$$

$$s_{\rm intersect} = \frac{\left(\vec{O}_{\rm HCal} - \vec{v}\right) \cdot \hat{z}_{\rm HCal}}{\hat{p}_{N'} \cdot \hat{z}_{\rm HCal}}$$

Analysis Methods – Introducing HCal Δx and Δy

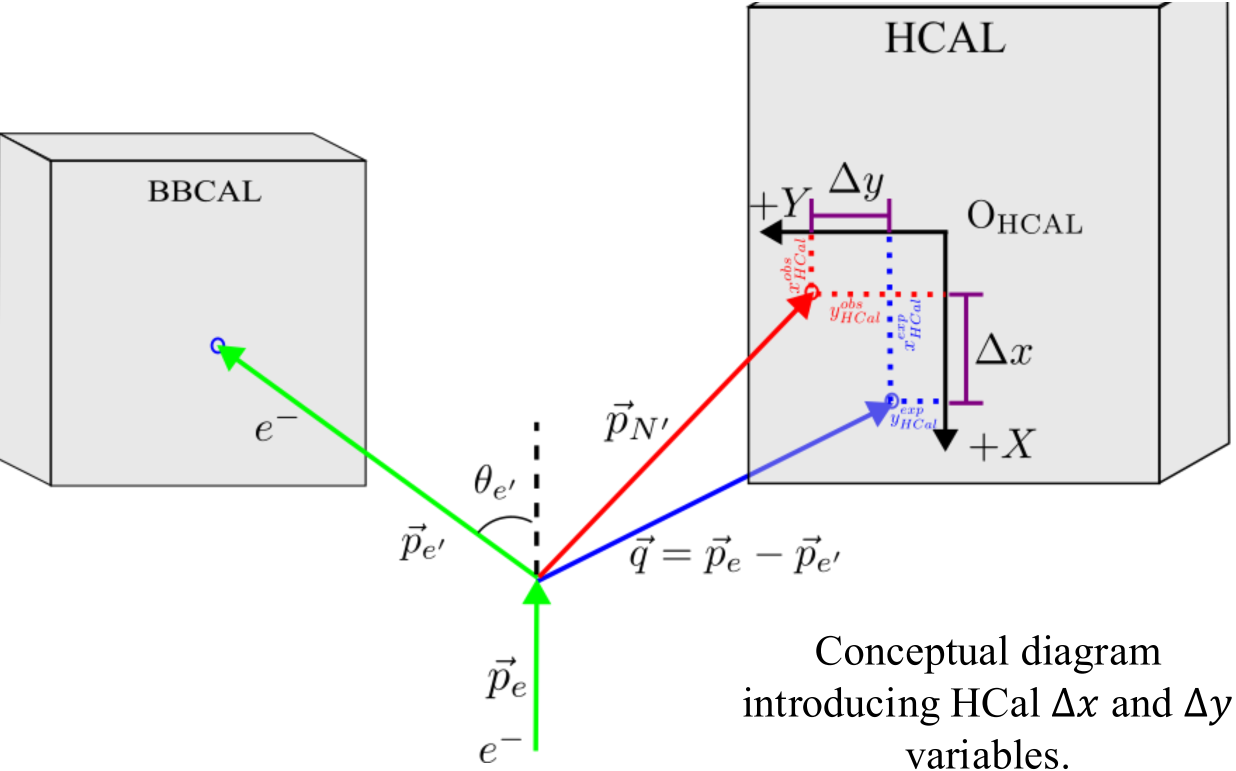

Conceptual diagram introducing HCal Δx and Δy variables.

- Definition of Δx: The difference between the observed (x^{obs}_{HCAL}) and the expected (x^{exp}_{HCAL}) nucleon position on HCal in the vertical (dispersive) direction.

- Definition of Δy: The difference between the observed (y^{obs}_{HCAL}) and the expected (y^{exp}_{HCAL}) nucleon position on HCal in the horizontal (non-dispersive) direction.

$Q^2 = 4.5\ (GeV/c)^2$

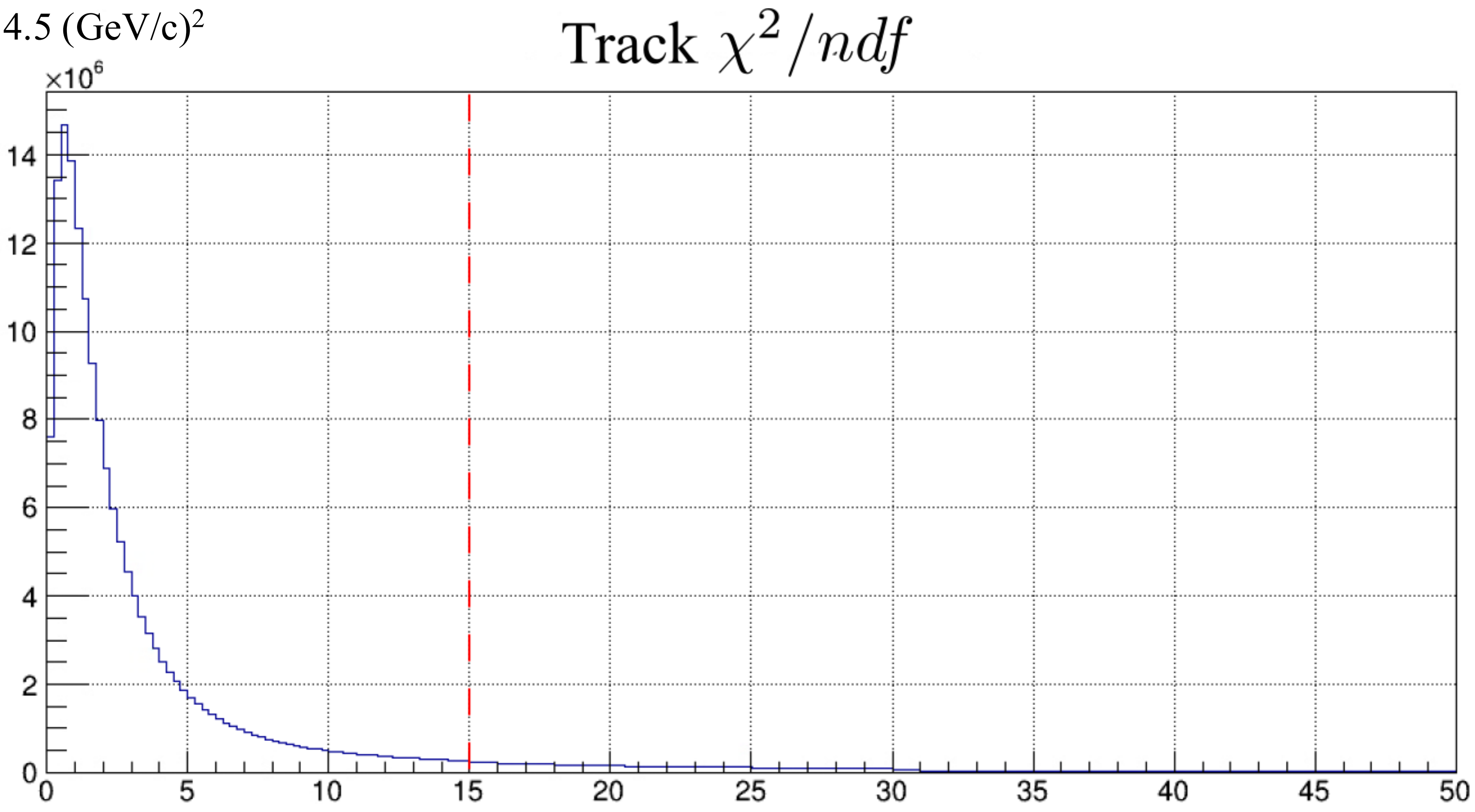

$Q^2 = 4.5\ (GeV/c)^2$

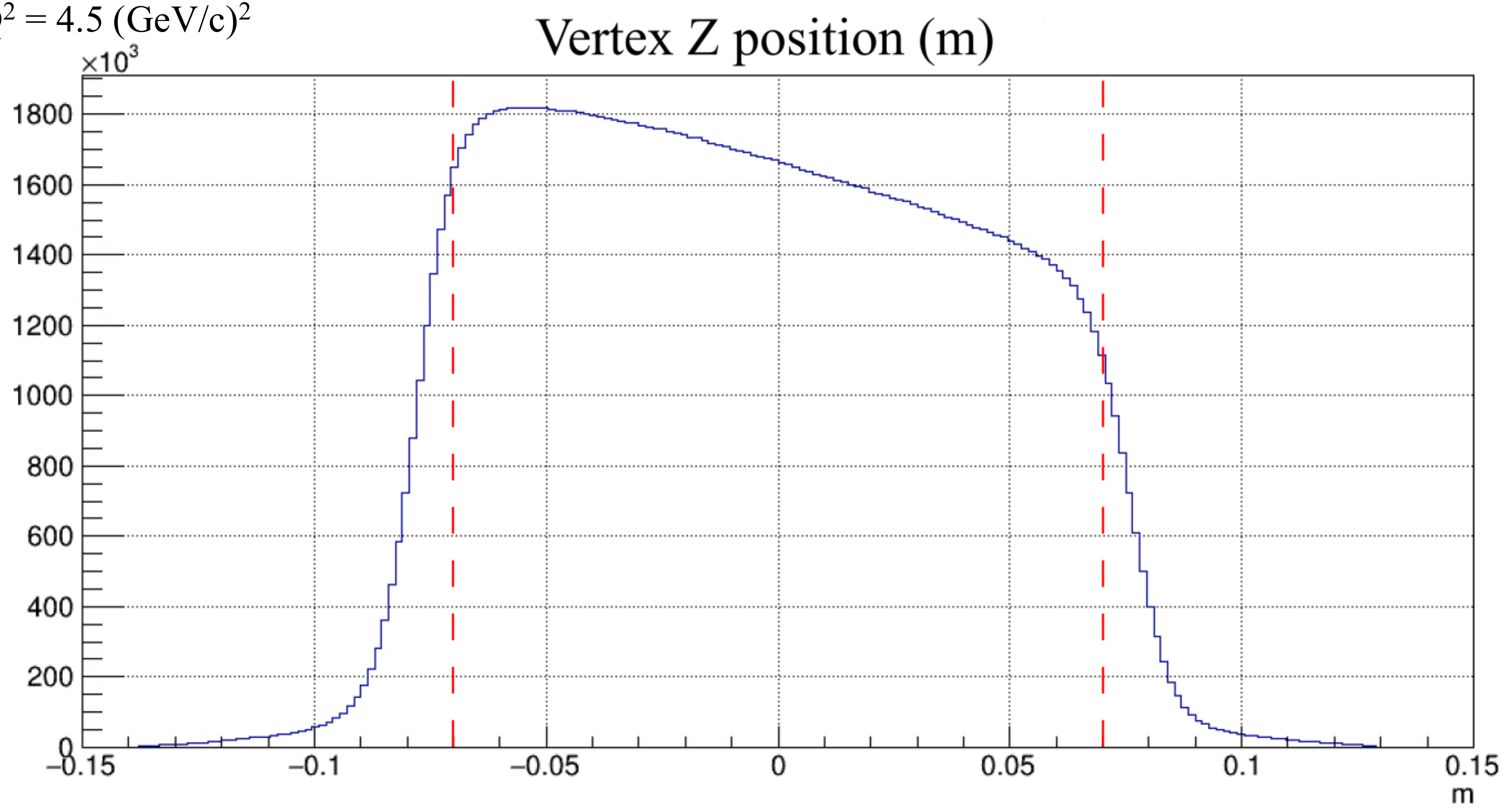

Vertex Z position (m)
×10^3
1800
1600
1400
1200
1000
800
600
400
200
0
−0.15
−0.1
−0.05
0
0.05
0.1
0.15
m

Optics Validity Cuts

$Q^2 = 4.5\ (GeV/c)^2$

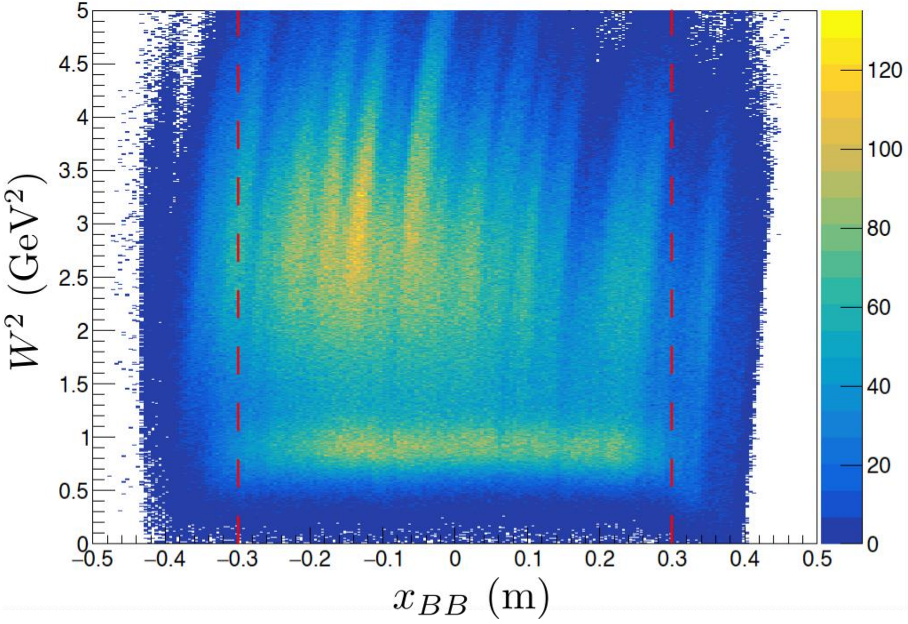

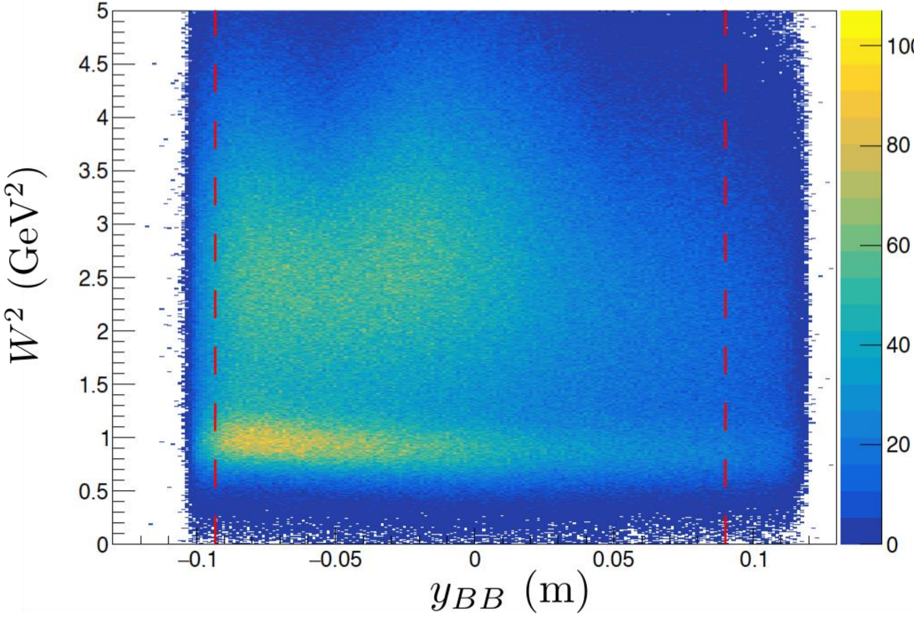

$Q^2 = 4.5\ (GeV/c)^2$

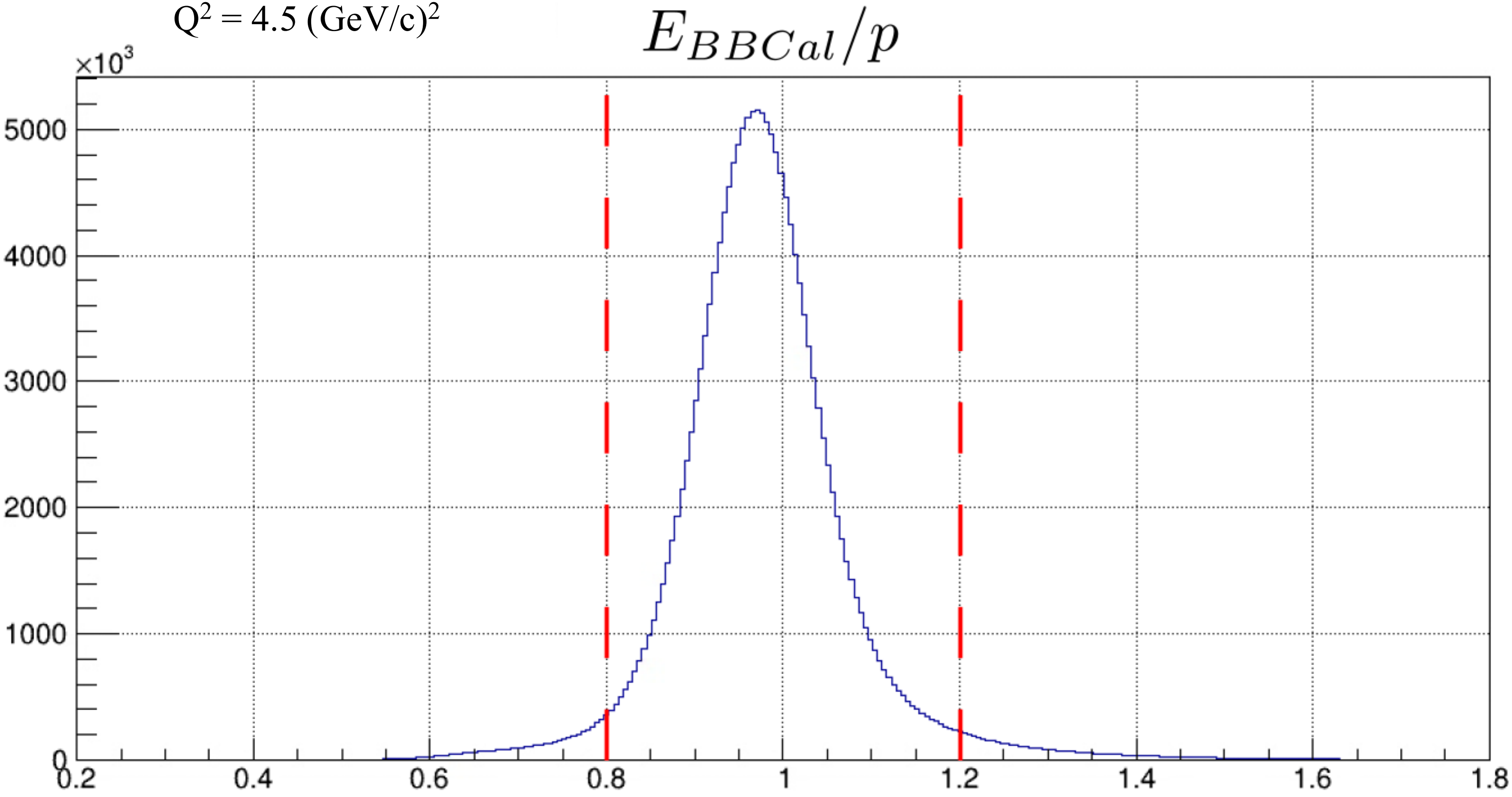

$Q^2 = 4.5\ (GeV/c)^2$

HCal Cluster Energy (GeV)

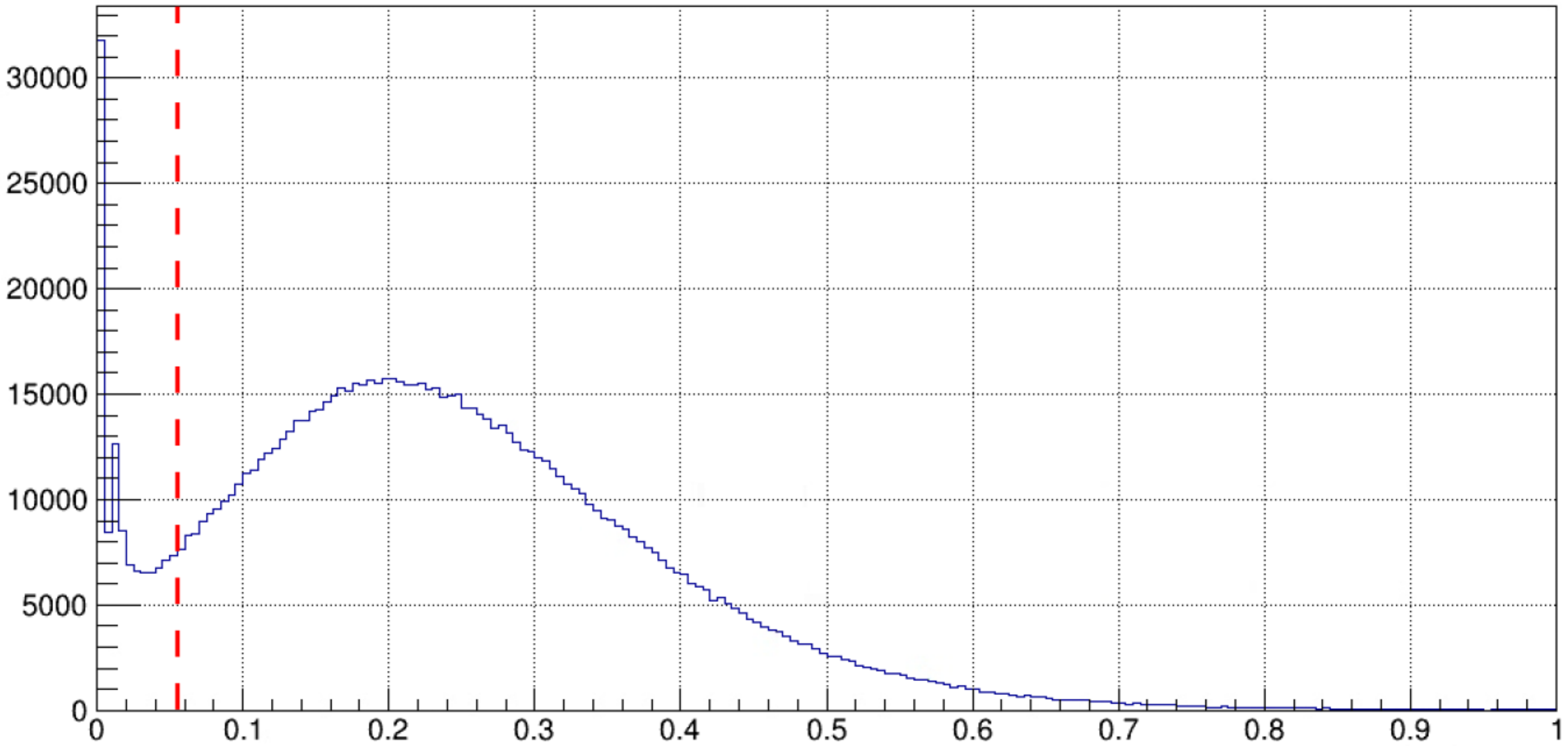

$Q^2 = 4.5\ (GeV/c)^2$

No Cuts Applied

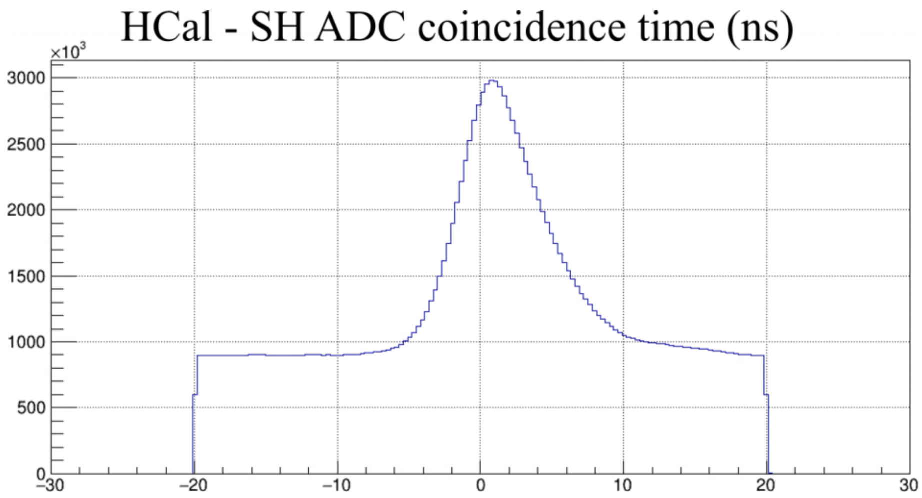

All Other Cuts Applied

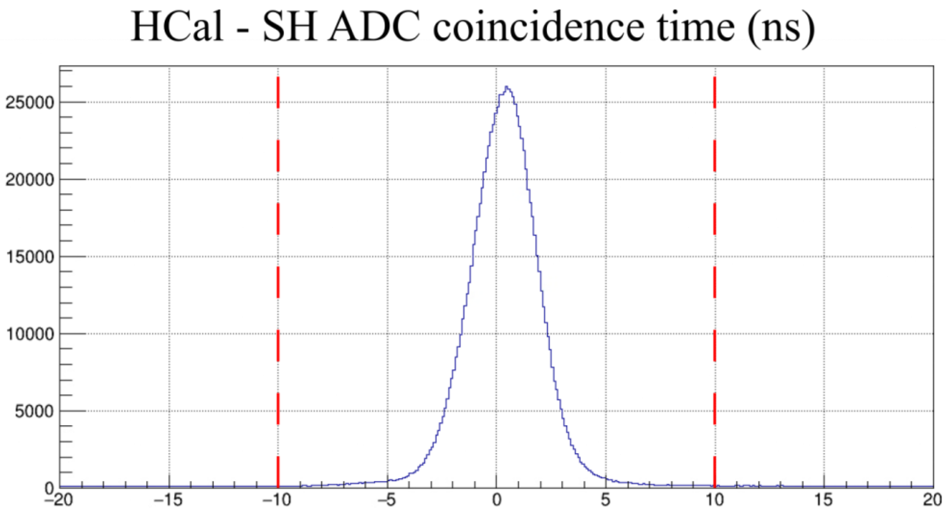

$Q^2 = 4.5\ (GeV/c)^2$

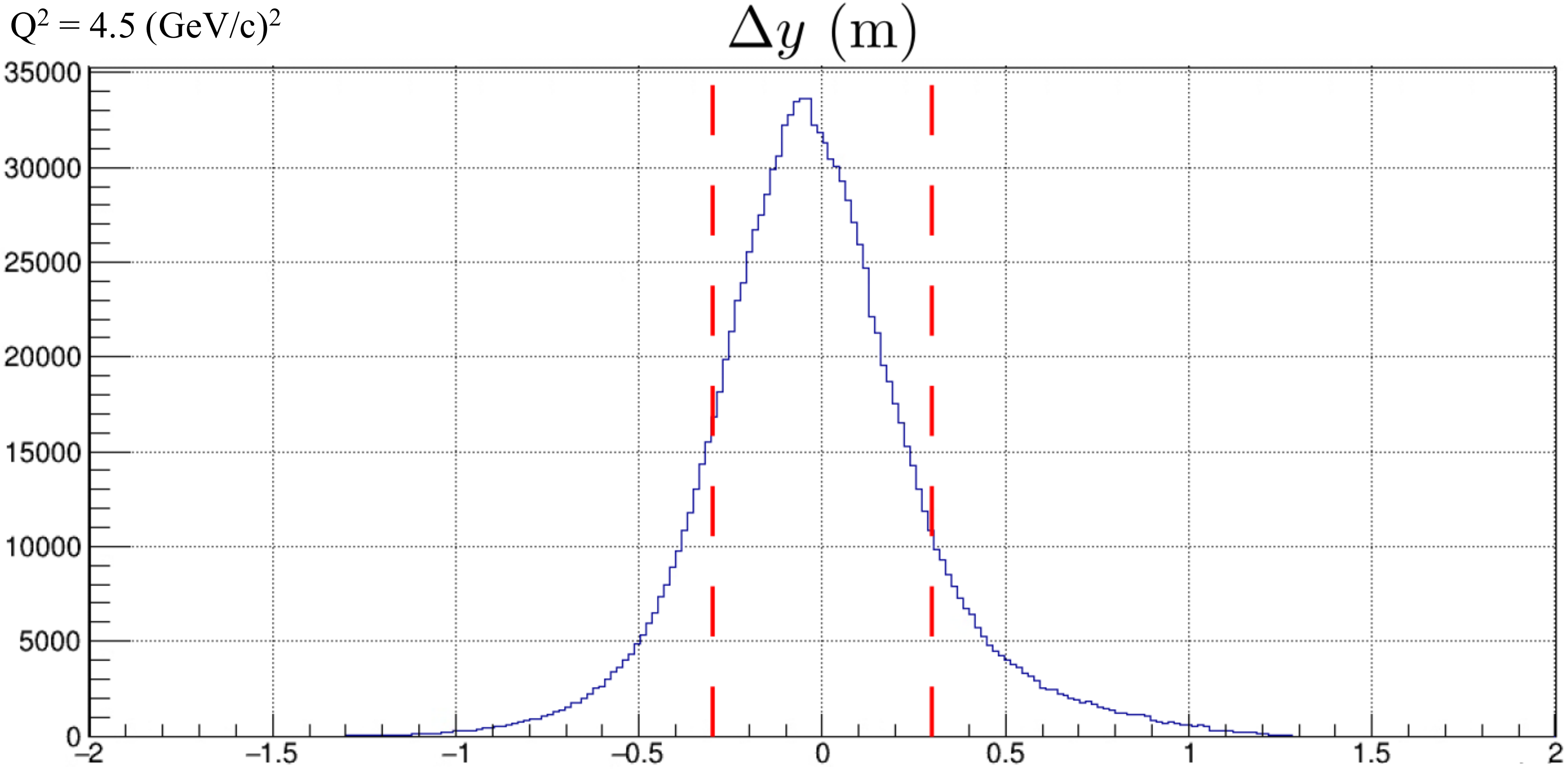

Δy (m)
35000
30000
25000
20000
15000
10000
5000
0
−2
−1.5
−1
−0.5
0
0.5
1
1.5
2

$Q^2 = 4.5\ (GeV/c)^2$

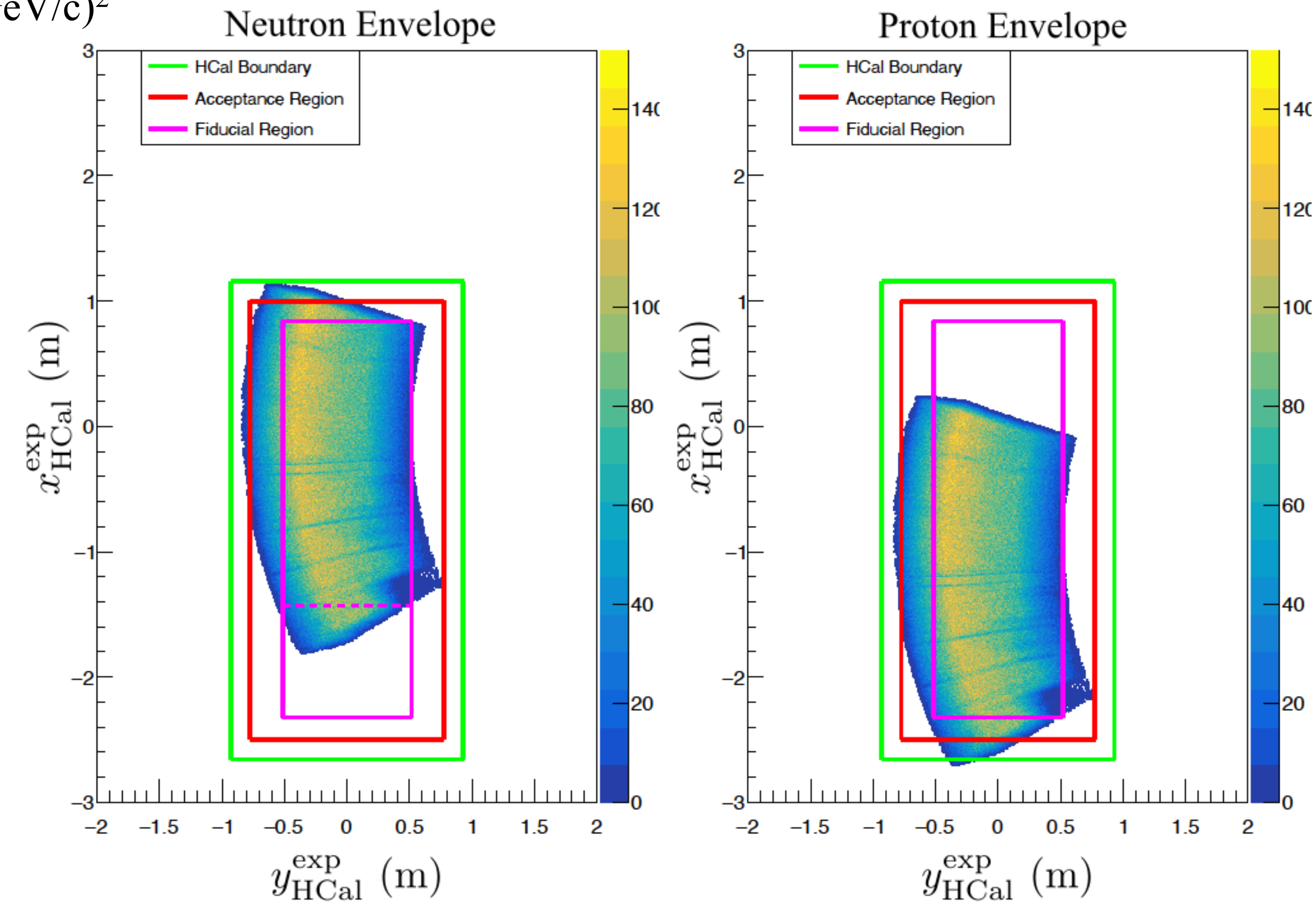

Neutron Envelope
HCal Boundary
Acceptance Region
Fiducial Region
x^{exp}_{HCal} (m)
y^{exp}_{HCal} (m)
Proton Envelope
HCal Boundary
Acceptance Region
Fiducial Region
x^{exp}_{HCal} (m)
y^{exp}_{HCal} (m)

Fiducial Cut

$Q^2 = 4.5\ (GeV/c)^2$

For a given electron event, the Fiducial Cut ensures the event is in the acceptance for both a scattered neutron and proton.

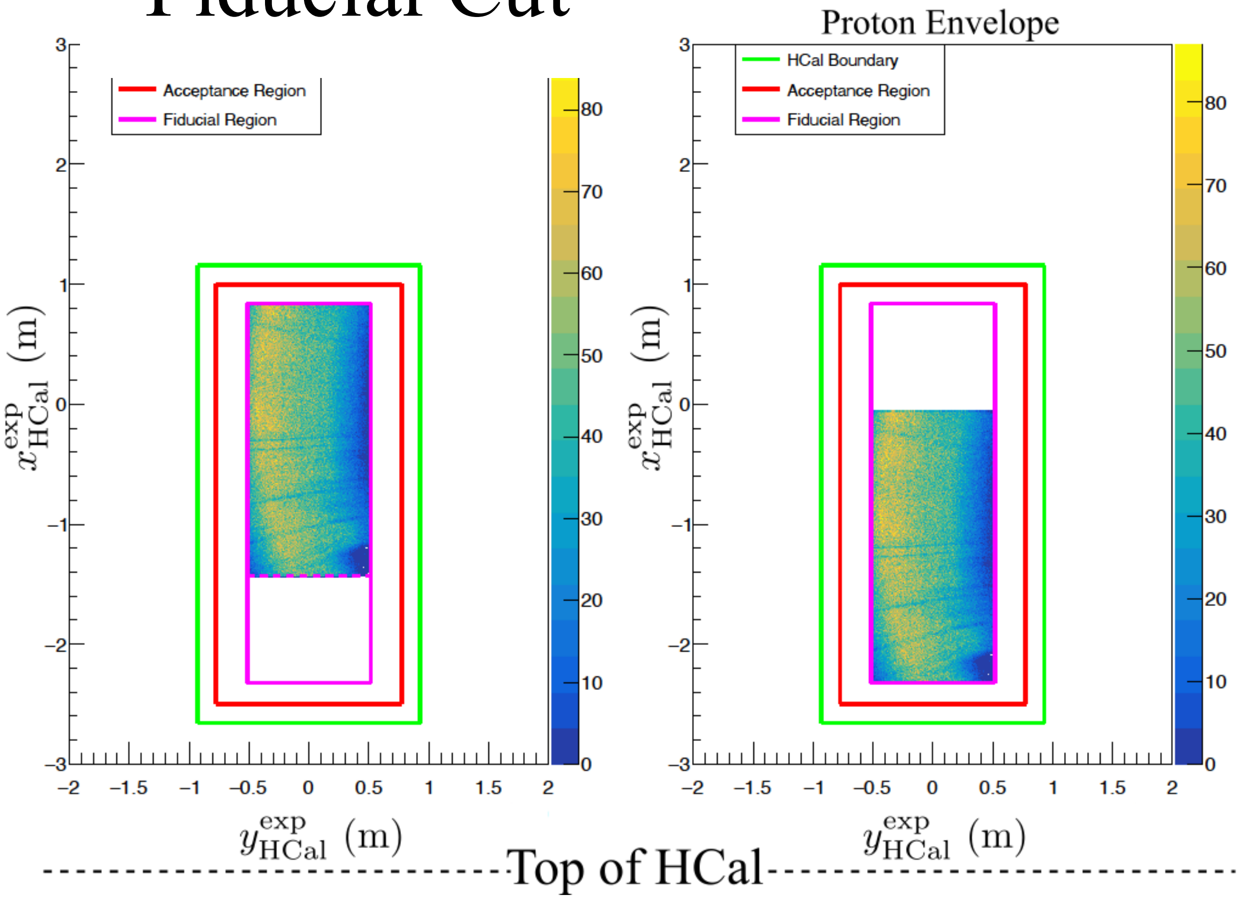

Cut Variable	Optimized Cut Regions			
	SBS-8 50%	SBS-8 70%	SBS-8 100%	SBS-9 70%
N_{GEMhits}	≥ 3	≥ 3	≥ 3	≥ 3
Track χ^2/ndf	≤ 15	≤ 15	≤ 15	≤ 15
v_z (m)	$[-0.07, 0.07]$	$[-0.07, 0.07]$	$[-0.07, 0.07]$	$[-0.07, 0.07]$
x_{BB} (m)	$(-0.15, 0.30)$	$(-0.15, 0.30)$	$(-0.15, 0.20)$	$(-0.15, 0.30)$
y_{BB} (m)	$(-0.09, 0.09)$	$(-0.09, 0.09)$	$(-0.08, 0.08)$	$(-0.09, 0.09)$
E_{PS} (GeV)	> 0.2	> 0.2	> 0.2	> 0.2
E_{BBCal}/p	$(0.8, 1.2)$	$(0.8, 1.2)$	$(0.8, 1.2)$	$(0.8, 1.2)$
E_{HCal} (GeV)	≥ 0.055	≥ 0.055	≥ 0.055	≥ 0.05
Δt (ns)	$[-10, 10]$	$[-10, 10]$	$[-10, 10]$	$[-10, 10]$
W^2 (GeV^2)	$[0.6, 1.1]$	$[0.6, 1.1]$	$[0.6, 1.1]$	$[0.65, 1.1]$
Δy (m)	$[-0.3, 0.3]$	$[-0.3, 0.3]$	$[-0.3, 0.3]$	$[-0.3, 0.3]$
$x^{\text{exp}}_{\text{HCal}}$	$(-2.32, 0.83)$	$(-2.32, 0.83)$	$(-2.32, 0.83)$	$(-2.32, 0.84)$
$y^{\text{exp}}_{\text{HCal}}$	$(-0.51, 0.51)$	$(-0.51, 0.51)$	$(-0.51, 0.51)$	$(-0.5, 0.5)$

Correlated Cut Variables Pt 1

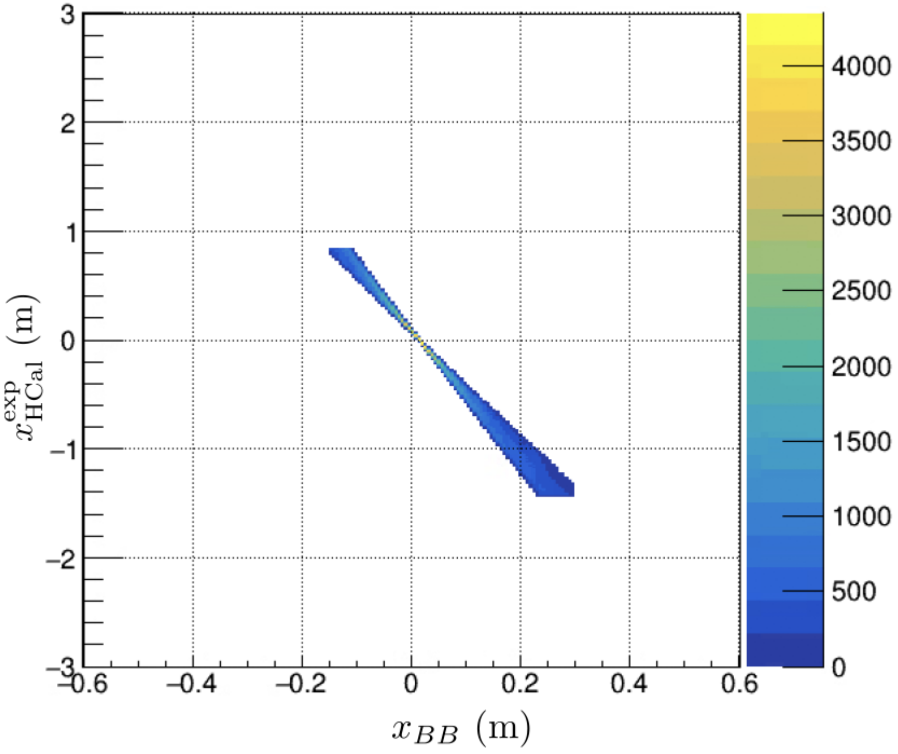

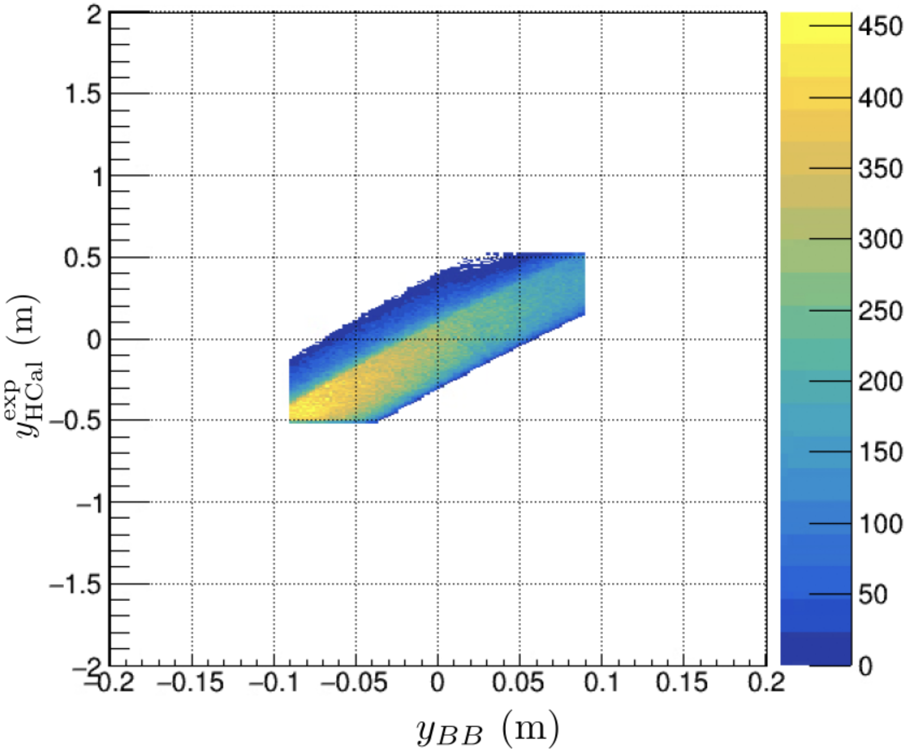

Correlated Cut Variables Pt 2

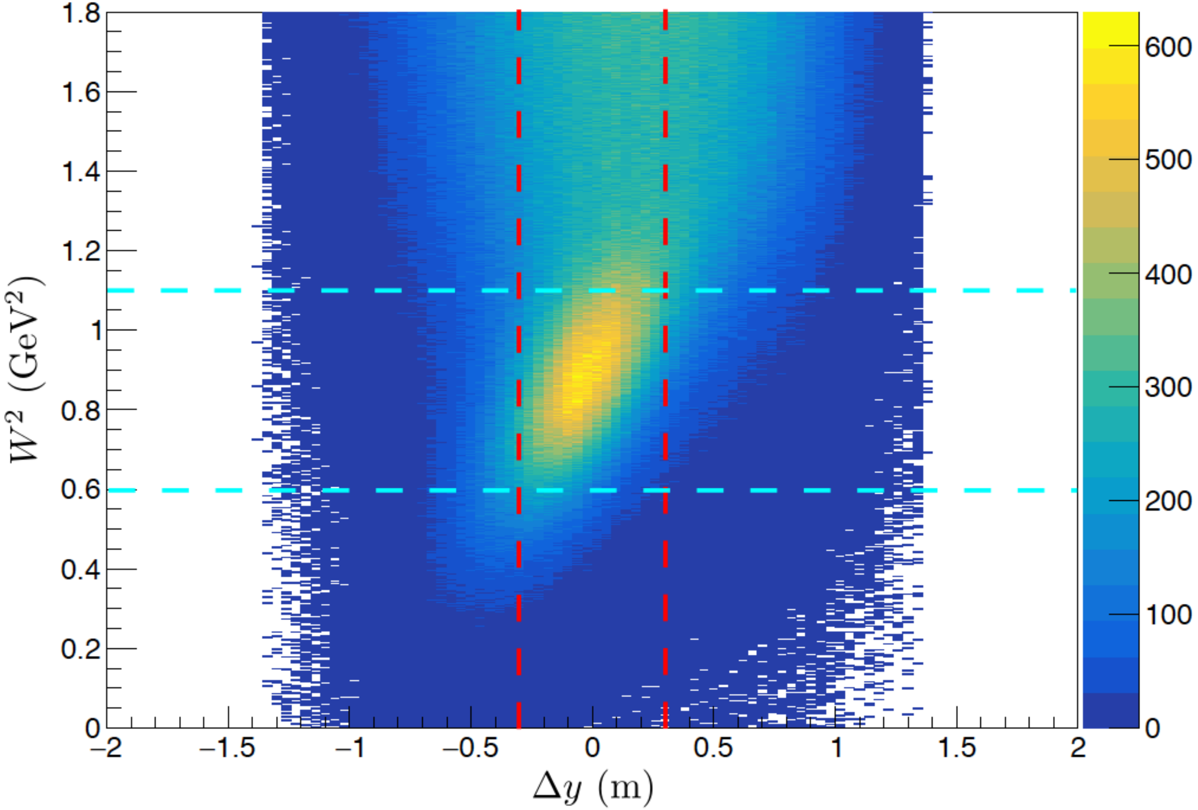

Cut Region Optimization

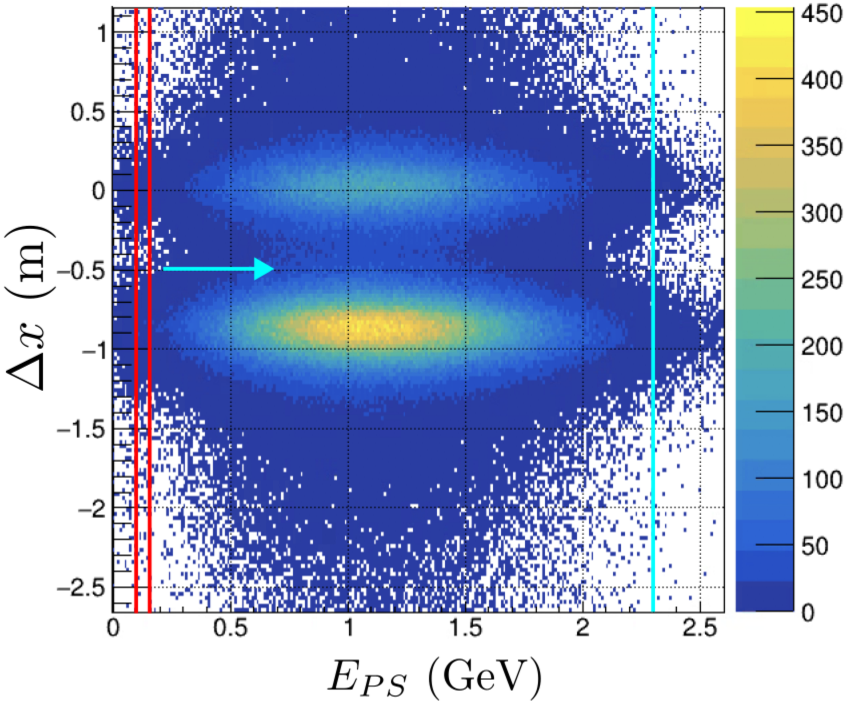

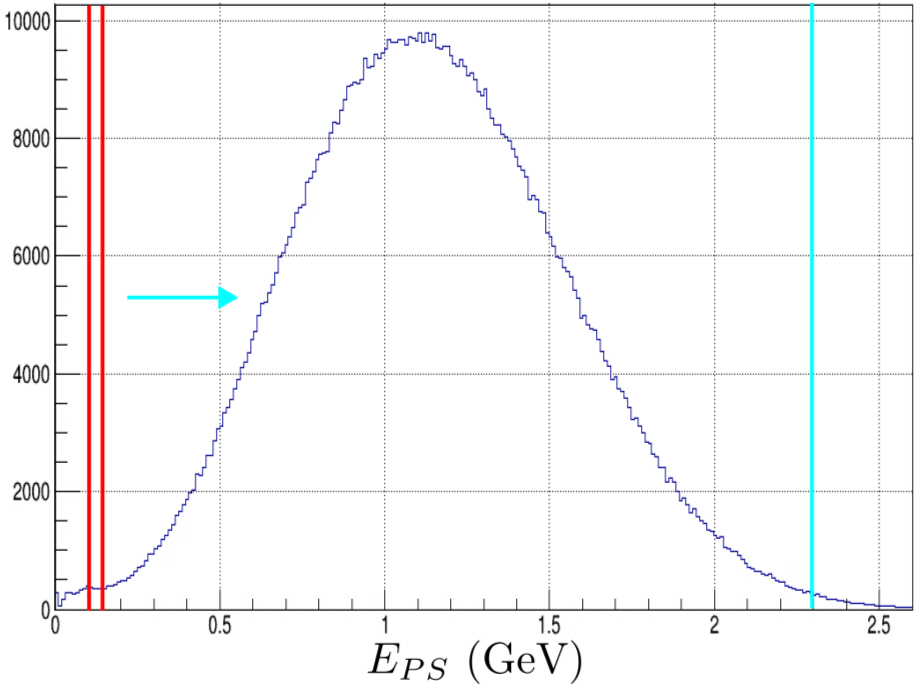

Cut Region Optimization

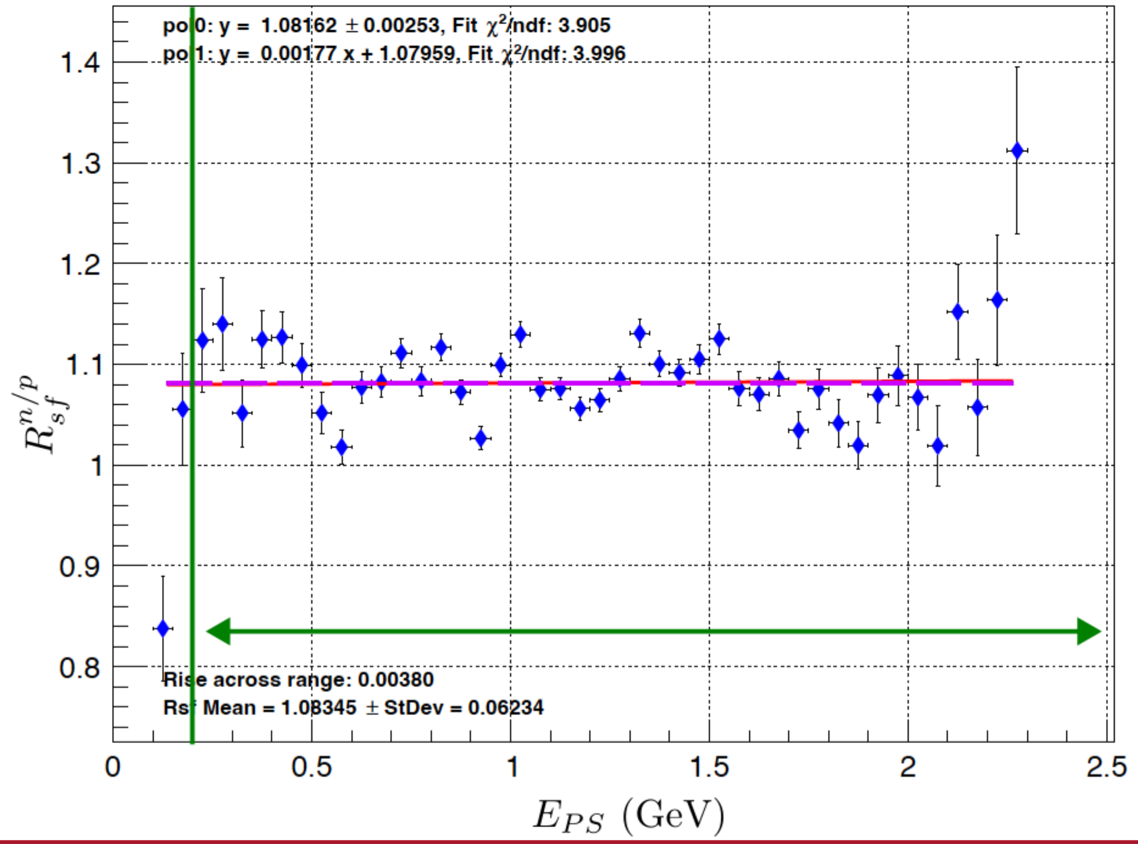

Cut Variable	Systematic Uncertainty Contribution			
	SBS-8 50%	SBS-8 70%	SBS-8 100%	SBS-9 70%
N_{GEMhits}	0.0025	0.0061	0.0029	0.00007
Track χ^2/ndf	0.0005	0.0005	0.0002	0.0014
v_z (m)	0.0017	0.00003	0.0003	0.0009
x_{BB} (m)	0.0012	0.0044	0.0021	0.0019
y_{BB} (m)	0.0014	0.0013	0.0023	0.0007*
E_{PS} (GeV)	0.0002	0.0002	0.0006	0.0005
E_{BBCal}/p	0.0002	0.0007	0.0013	0.0003
E_{HCal} (GeV)	0.0006	0.0002	0.0003	0.0002
Δt (ns)	0.0027	0.0023	0.0022	0.0030
W^2 (GeV^2)	0.0063	0.0007*	0.0012	0.0035
Δy (m)	0.0041*	0.0019	0.0012*	0.0010*
$x^{\text{exp}}_{\text{HCal}}$	0.0006*	0.0002*	0.0006*	0.0008*
$y^{\text{exp}}_{\text{HCal}}$	0.0007*	0.0007*	0.0013*	0.0011
$\Delta\left(R^{n/p}_{sf}\right)_{\text{cuts}}$	0.0078	0.0083	0.0052	0.0054

Cut Systematic One Boundary

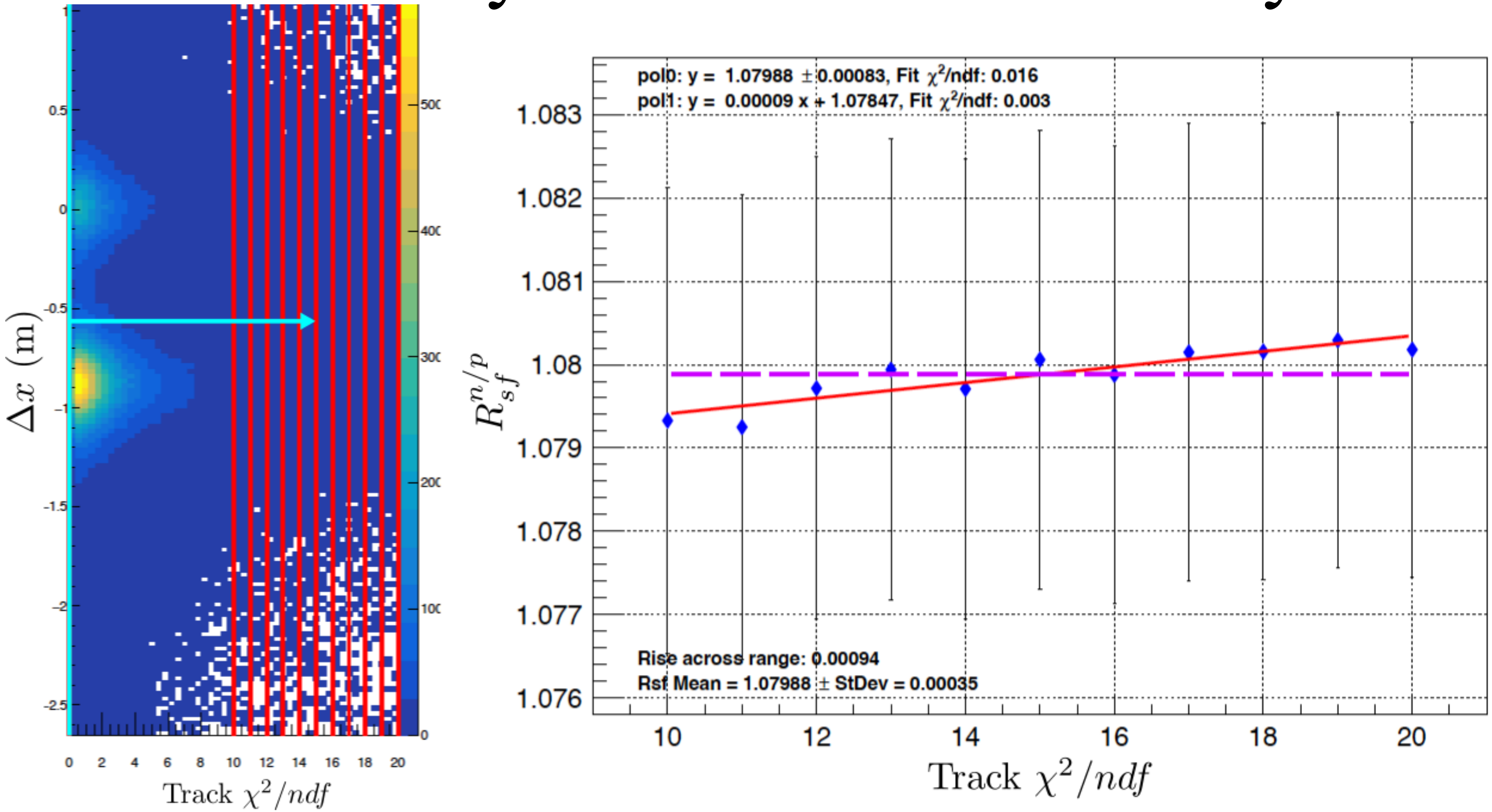

Cut Systematic Two Separate Boundary

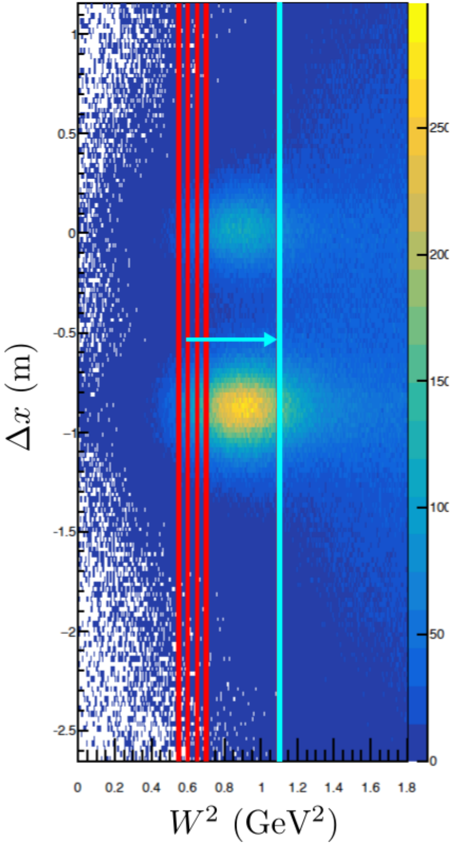

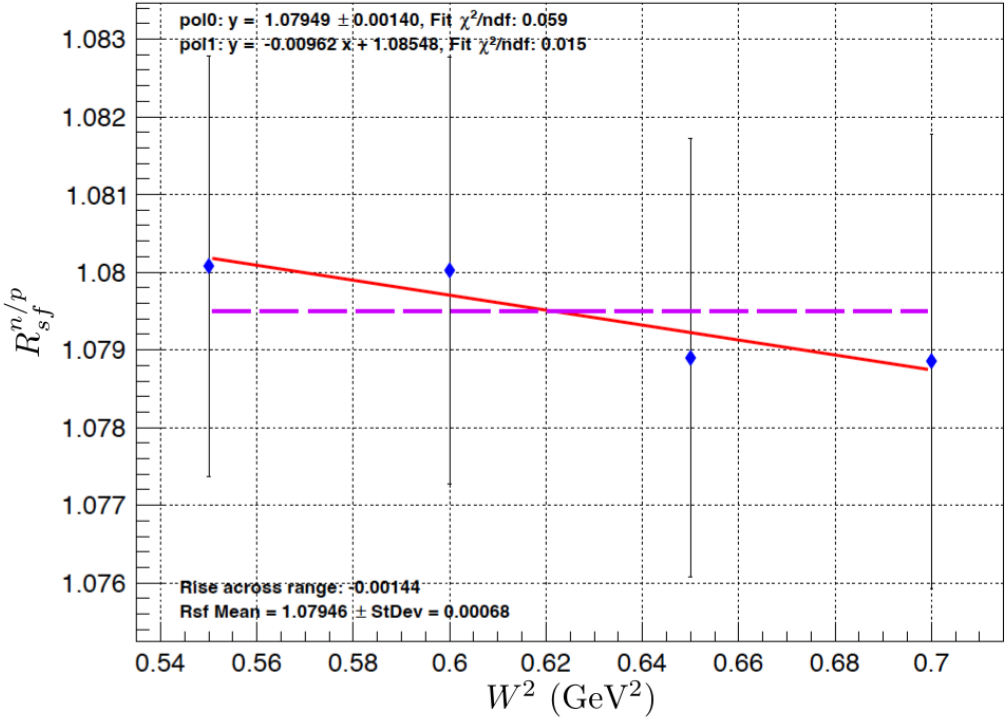

Cut Systematic Two Boundary Symmetric

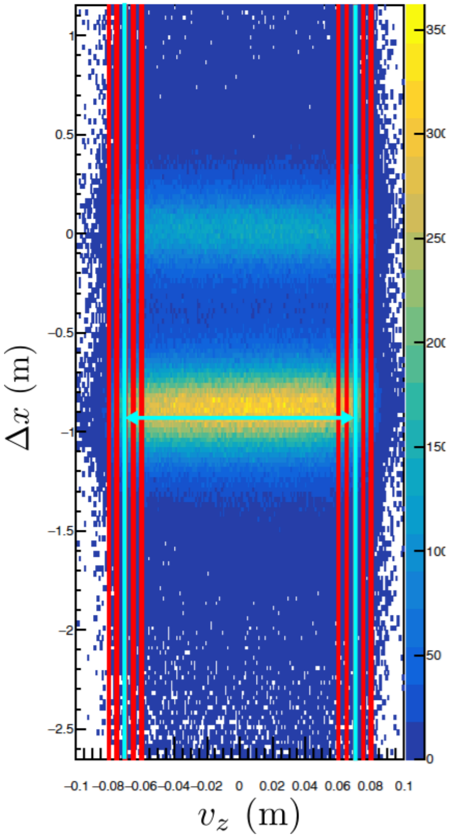

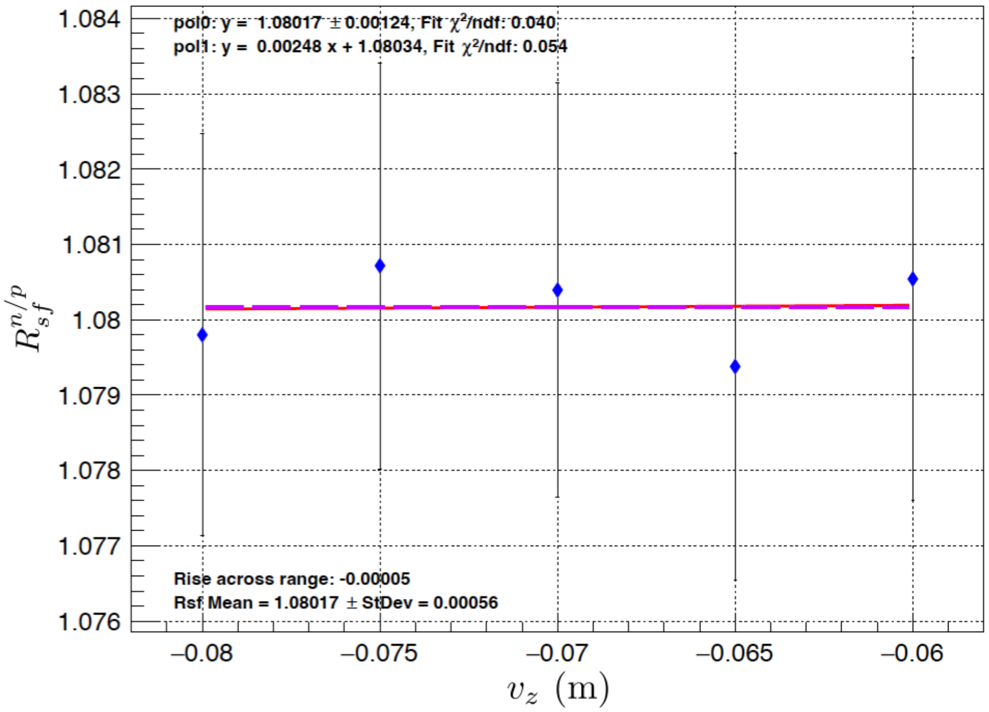

Proton Relative Rate Information

Data

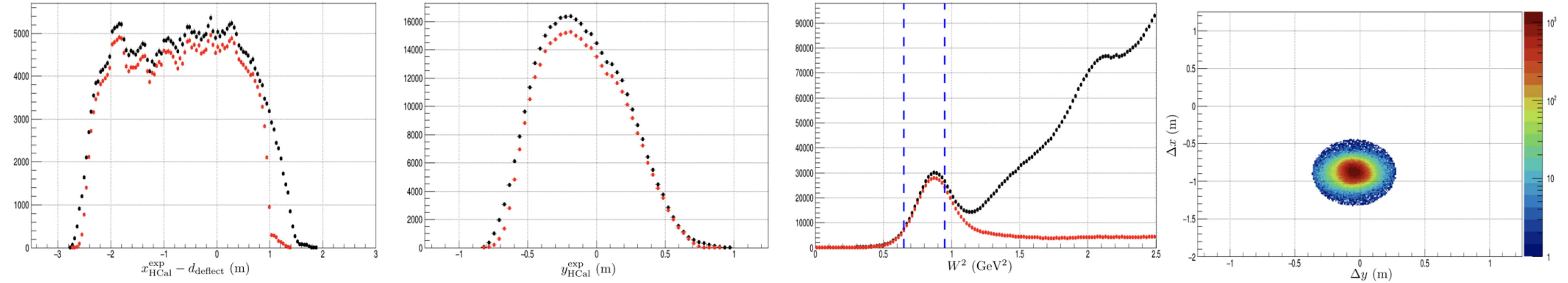

MC

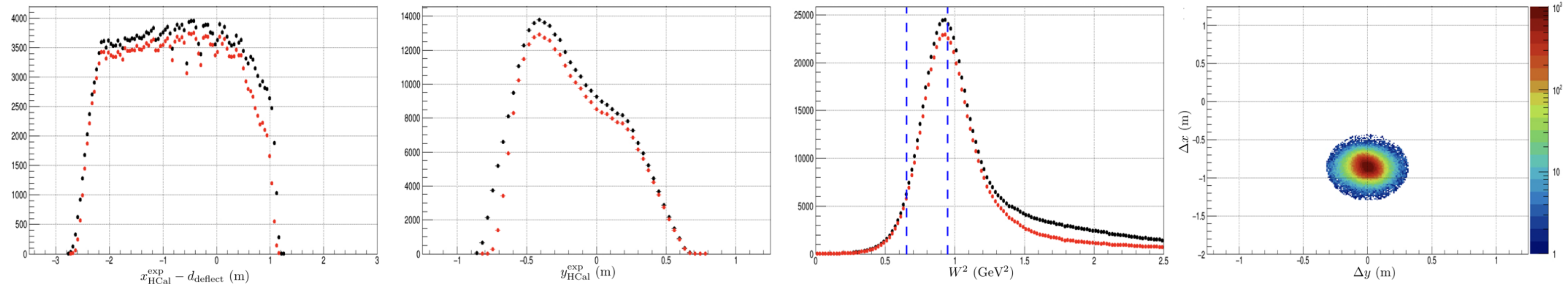

Proton Relative Rate Information

Data Combined

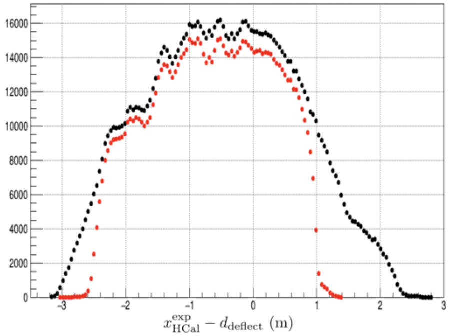

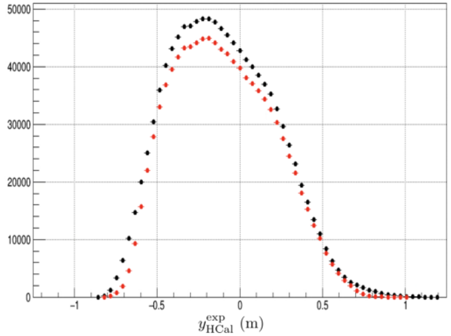

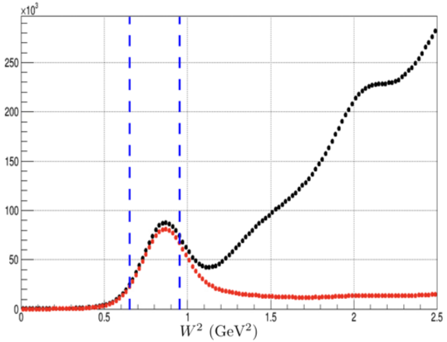

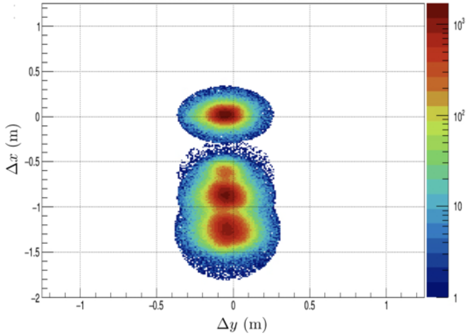

HCal Non-uniformity Systematic

Setting	$R_{sf}^{n/p}$ from Uncorrected MC	$R_{sf}^{n/p}$ from SBS-8 Map Corrected MC	Absolute Difference
SBS-8 50%	1.0842	1.0845	0.0003
SBS-8 70%	1.0782	1.0764	0.0018
SBS-8 100%	1.0678	1.0666	0.0012
SBS-9 70%	1.0876	1.0823	0.0053

Uncorrected MC

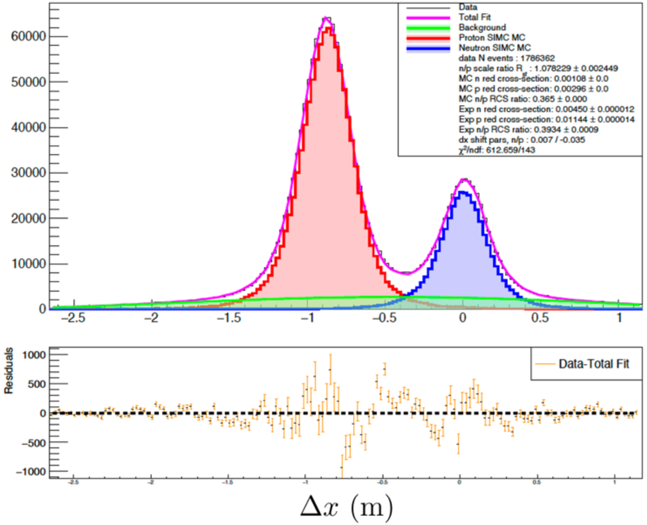

MC Corrected for HCal Non-Uniformity

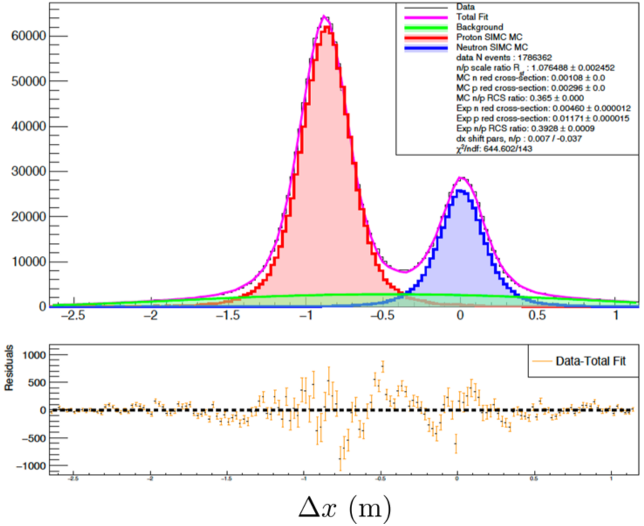

SBS-9 Proton Relative Rate

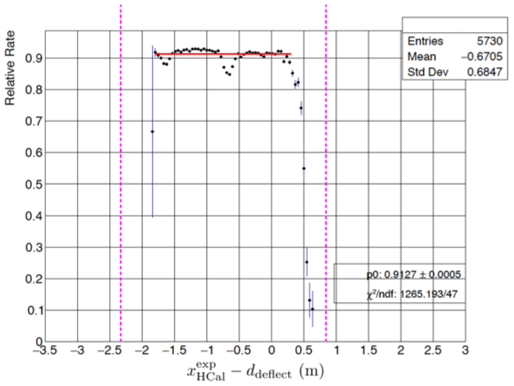

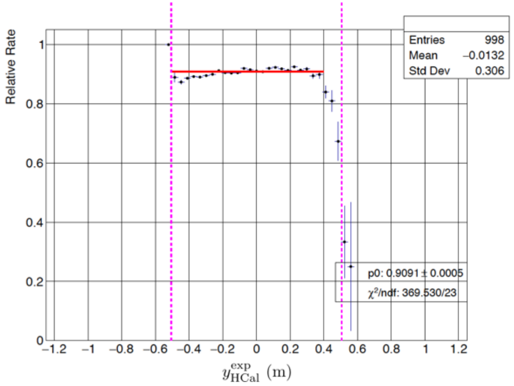

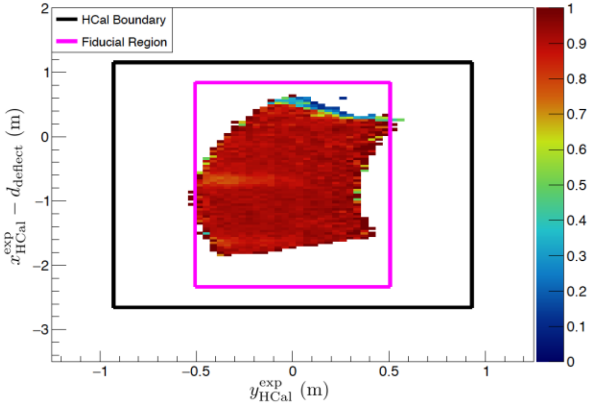

Spot Cuts for HCal Non-uniformity

SBS-8

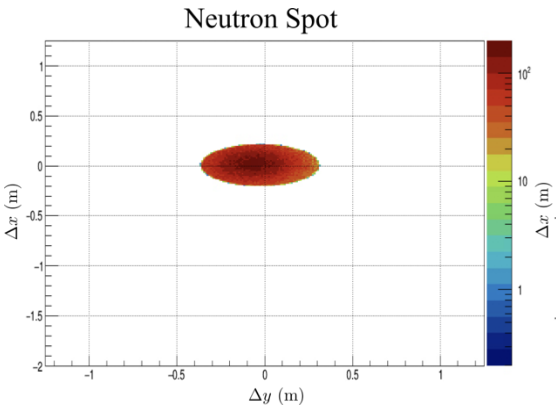

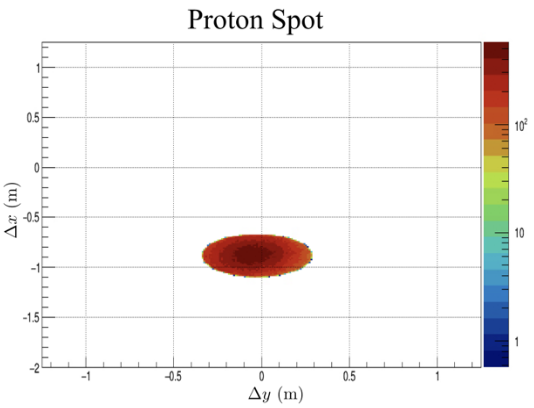

SBS-9

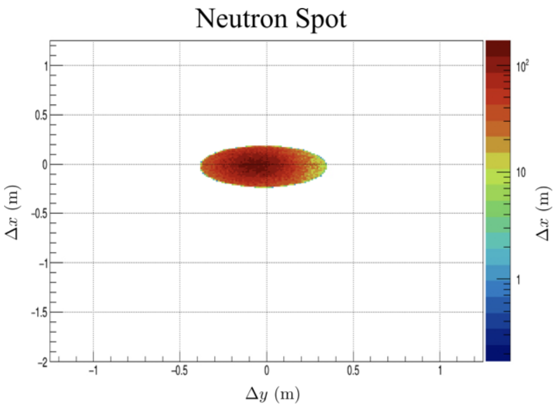

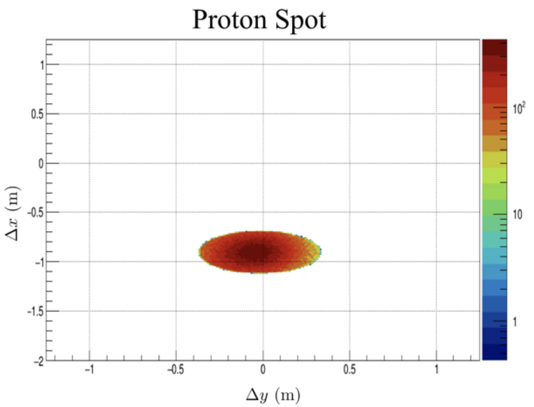

SBS-8 and SBS-9 Comparison

neutron

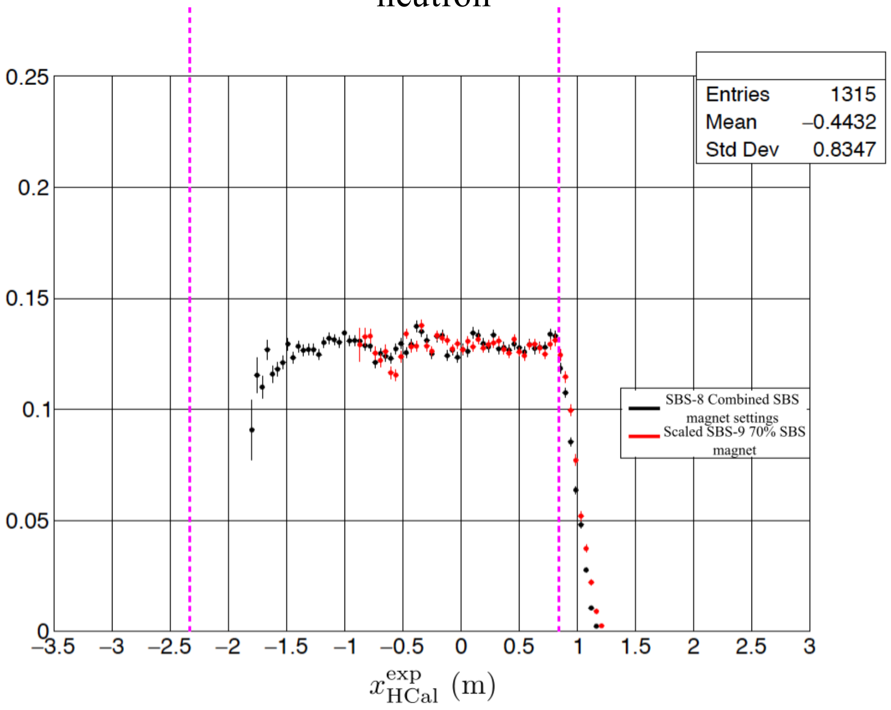

proton

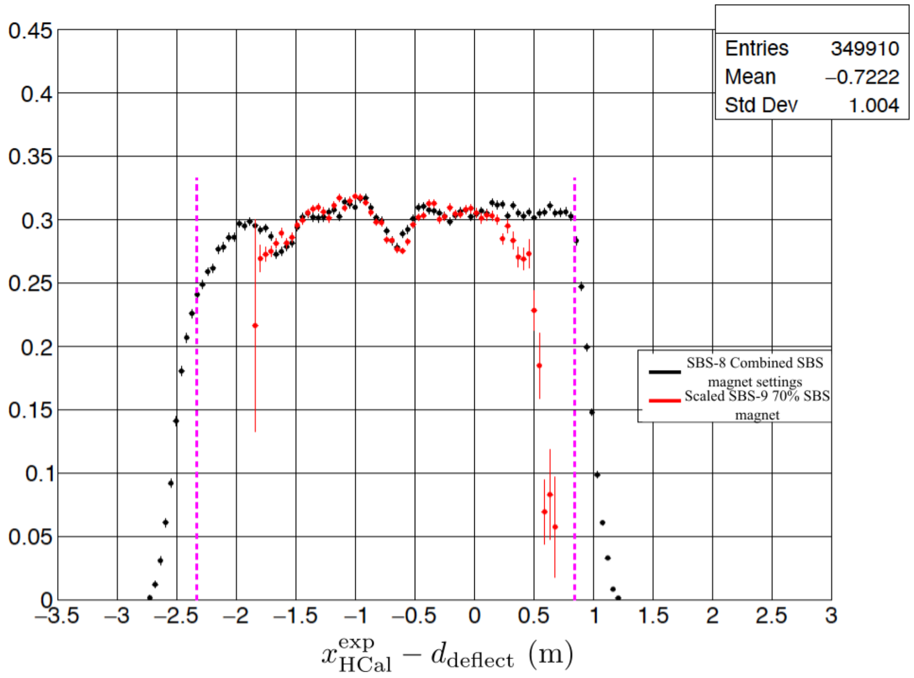

Detection Efficiency (MC)

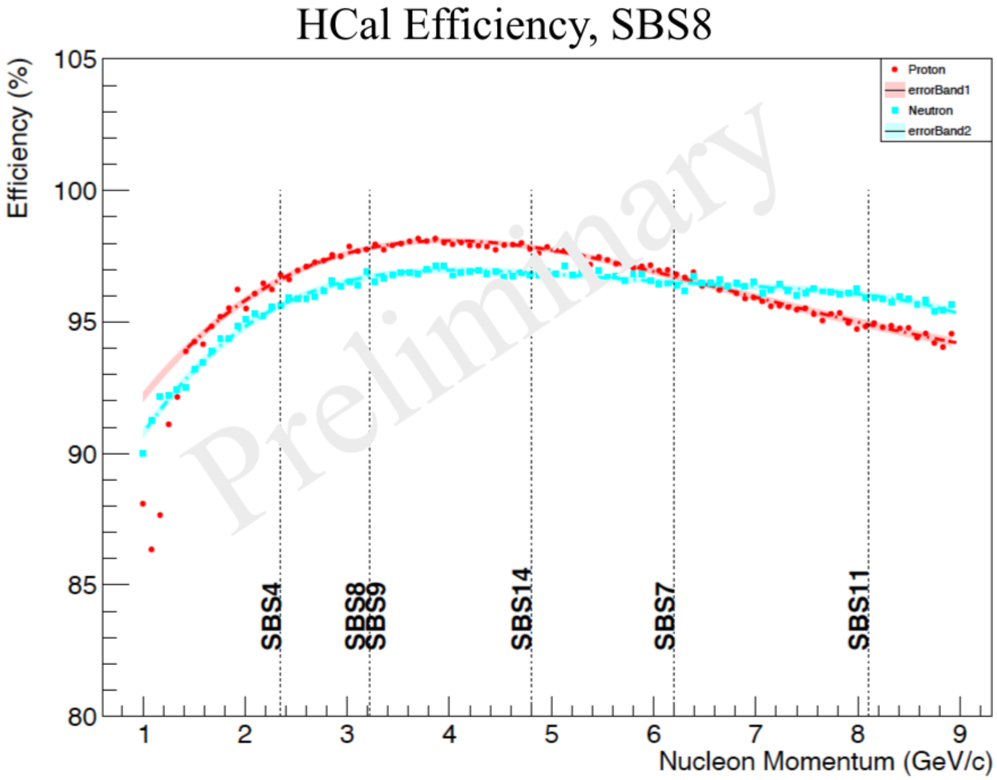

Method:

- Simulate, digitize, replay protons and neutrons separately, with momentum 1-9 GeV. Throw flat and populate 1000 events/channel.
- Get energy spectra vs nucleon momentum. Fit each peak to determine mean E for p bin.
- Total: Populate energy per p bin regardless.
- Pass: Separately populate energy per p bin > $E_{mean}/4$.
- By looping over p bins, evaluate the integral of energy histograms so Efficiency = Pass / Total.

Detection Efficiency (MC)

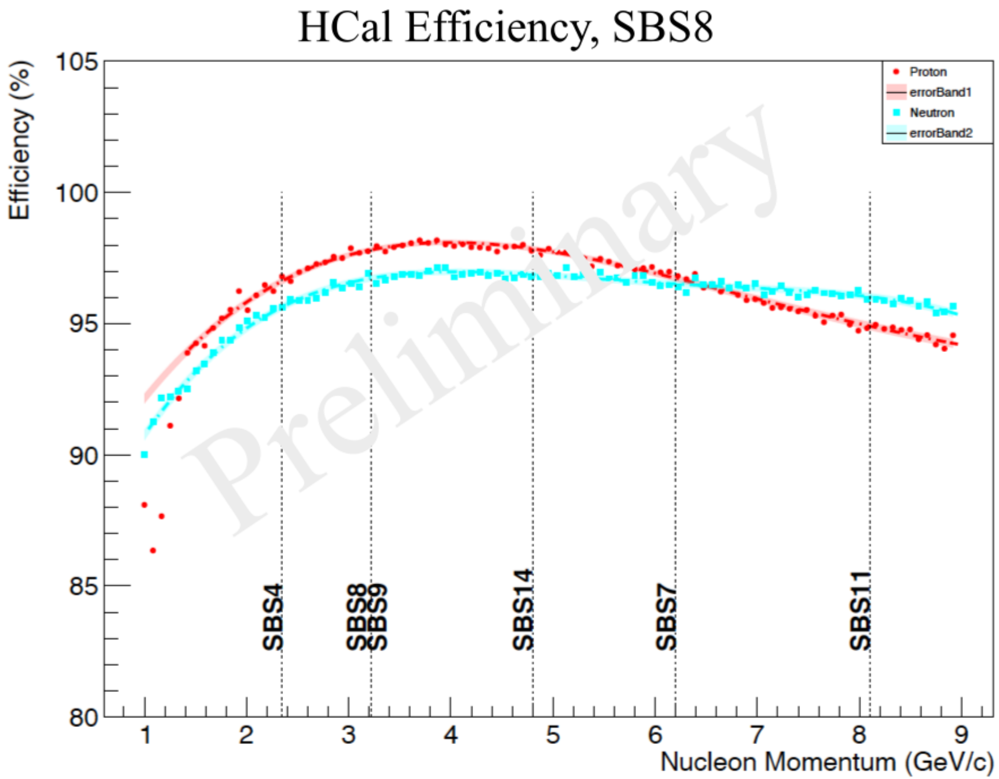

	Proton Efficiency	Neutron Efficiency
SBS4	96.6%	95.6%
SBS8	97.8%	96.7%
SBS9	97.8%	96.7%
SBS14	97.9%	96.9%
SBS7	96.7%	96.5%
SBS11	94.9%	96.0%

Preliminary

Coincidence Time Anti-cut

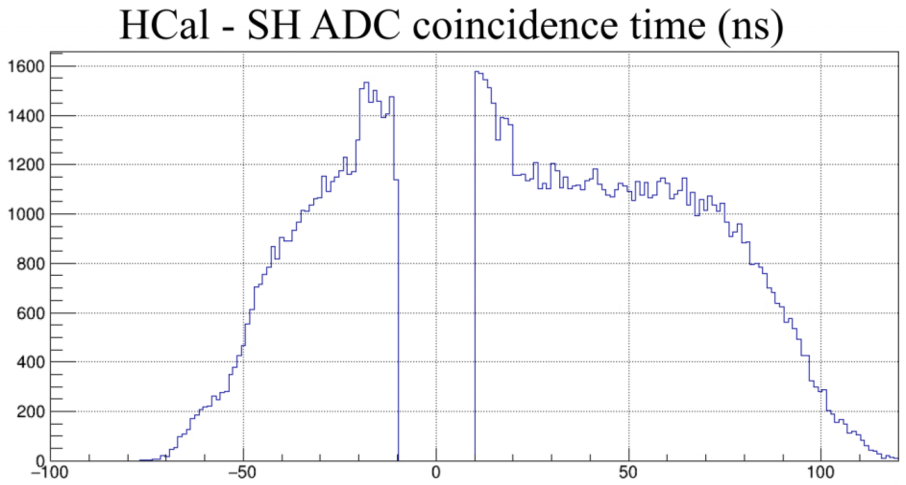

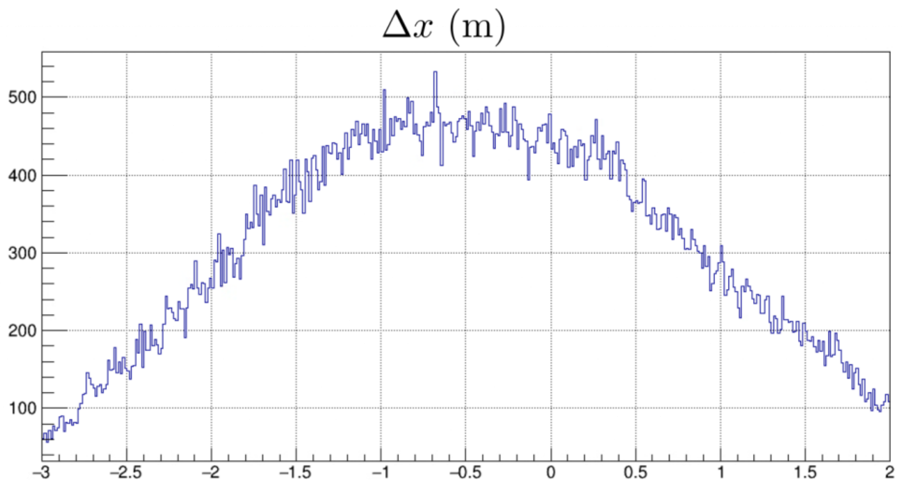

W^2 anti-cut

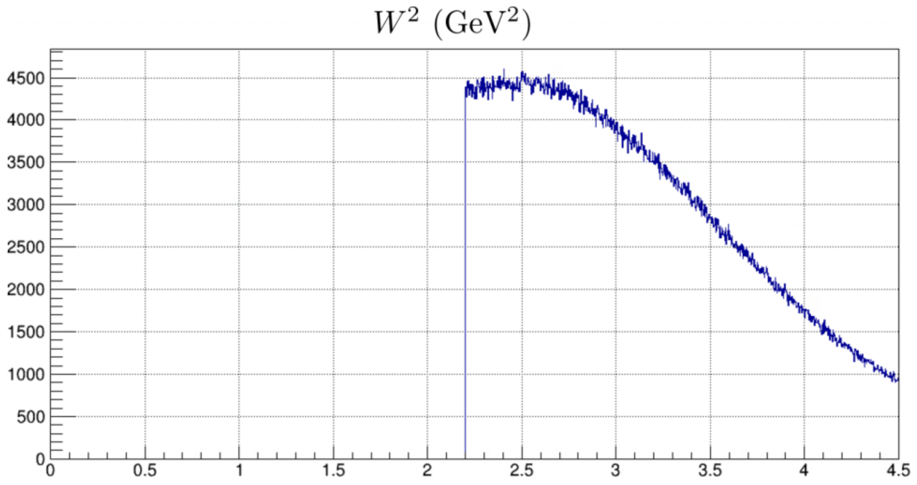

W^2 (GeV^2)
4500
4000
3500
3000
2500
2000
1500
1000
500
0
0
0.5
1
1.5
2
2.5
3
3.5
4
4.5

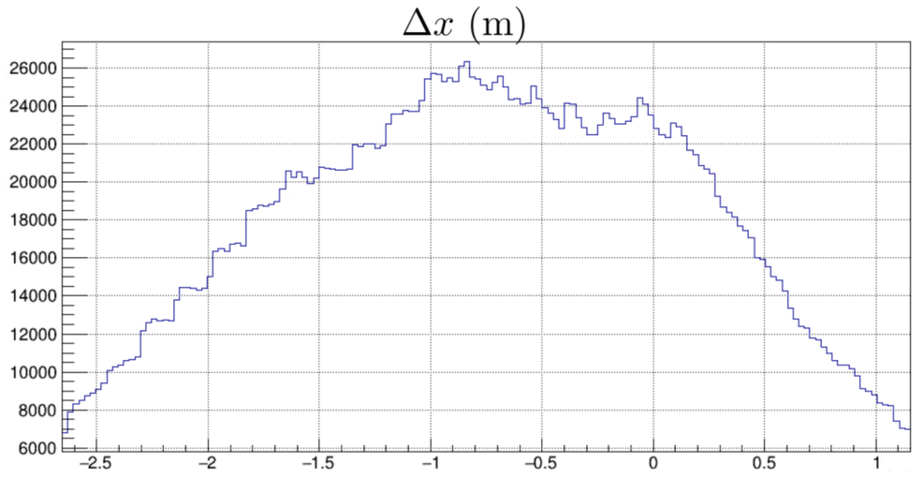

Δx (m)
26000
24000
22000
20000
18000
16000
14000
12000
10000
8000
6000
−2.5
−2
−1.5
−1
−0.5
0
0.5
1

Inelastic Background Systematic

Bkgd Model	$R_{sf}^{n/p}$ value			
	SBS-8 50%	SBS-8 70%	SBS-8 100%	SBS-9 70%
Gaussian	1.0655	1.0658	1.0611	1.0680
Polynomial-2	1.0787	1.0732	1.0651	1.0648
Polynomial-3	1.0639	1.0687	1.0554	1.0692
Δt Anti-Cut	1.0813	1.0762	1.0681	1.0729
W^2 Anti-Cut	1.0869	1.0823	1.0828	1.0681

Weighted Mean SBS-8

Weighted Mean Formula: $\bar{R}_{sf,w} = \frac{\sum_{i=1}^{3} R_{sf,i} w_i}{\sum_{i=1}^{3} w_i}$, where $w_i = \frac{1}{\sigma^2_{uncorr,i}}$

Uncertainty on the weighted mean, for uncorrelated uncertainties: $\sigma^2_{mean,uncorr} = {}^1/_{\sum_{i=1}^{3} w_i}$

Uncertainty on the weighted mean, for correlated uncertainties, procedure:

1. Add the correlated error, $\sigma_{corr,i}$, for a given data set to the scale factor, $R_{sf,i}$: $R^{+1}_{sf,i} = R_{sf,i} + \sigma_{corr,i}$
2. Apply step 1 for every data set
3. Calculate a new weighed mean from the above formula with all $R^{+1}_{sf,i}$s, call it $\bar{R}^{+1}_{sf,w}$
4. The correlated uncertainty on the weighted mean is the absolute value between $\bar{R}^{+1}_{sf,w}$ and $\bar{R}_{sf,w}$:

$\sigma_{mean,corr} = \left|\bar{R}^{+1}_{sf,w} - \bar{R}_{sf,w}\right|$

5. Repeat Steps 1 through 5 but considering $R^{-1}_{sf,i} = R_{sf,i} - \sigma_{corr,i}$. This should obtain the same value for $\sigma_{mean,corr}$

Total Uncertainty on the weighted mean is $\sigma_{mean,total} = \sqrt{\sigma^2_{mean,uncorr} + \sigma^2_{mean,corr}}$

Values for SBS8

$\bar{R}_{sf,w} = 1.07113$

$\sigma_{mean,total} = 0.01036$, or 0.97% $\sigma_{mean,uncorr} = 0.00538$ $\sigma_{mean,corr} = 0.00886$